



D4.3 Railway environment characterization

Project acronym:	STARS
Project full title:	Satellite Technology for Advanced Railway Signalling
EC Contract No.:	(H2020) 687414

Version of the document:	07
Protocol code:	STR-WP4-D-AZD-096-07
Responsible partner:	AZD
Reviewing status:	Final
Delivery date:	22/10/2018
Dissemination level:	PUBLIC

CHANGE RECORDS

Version	Date	Changes	Authors
01	22.12.2017	First draft	P. Kacmarik (AZD), L. Bazant (AZD), H. Mocek (AZD), M. Bohac (AZD)
02	30.12.2017	Language changes, References added, quality check	B. Stamm (SIE)
03	22.5.2018	Appendix 2 added.	H. Mocek (AZD)
04	6.6.2018	Composition of MPL and RIL, explanation of SVF calculation, analysis of selected cases, evaluation and conclusion added, Appendix 2 removed.	L. Bazant (AZD)
05	15.8.2018	Changes based on comments in partners' reviews were included	L. Bazant (AZD)
06	7.9.2018	SV number and speed profiles figures included	L. Bazant (AZD)
07	16.10.2018	Corrections resulting from review on TMT level	L. Bazant (AZD)
08	22.10.2018	Quality Check	K. Ceka (RINA)

TABLE OF CONTENTS

CHANGE RECORDS	2
1 INTRODUCTION	10
1.1 Executive summary	10
1.2 Definitions and acronyms	10
2 DATA PROCESSING TOWARDS ENVIRONMENT CHARACTERIZATION	13
2.1.1 <i>Techniques for negative phenomenon detection or quantification</i>	14
2.1.2 <i>Techniques classifications</i>	15
2.1.3 <i>Evaluation Symptom (ES) and Analyzed Parameter Value (APV)</i>	15
2.1.4 <i>Combined APV</i>	15
2.2 Environment characterization based on technique outputs	17
2.2.1 <i>Correlation in time domain</i>	17
2.2.2 <i>Correlation in position domain</i>	18
3 RAILWAY ENVIRONMENT CHARACTERIZATION FROM GNSS SIGNAL RECEPTION PERSPECTIVE	20
3.1 Environment Characteristics	20
3.1.1 <i>Sky Visibility Factor - SVF</i>	20
3.1.2 <i>Multipath Level - MPL</i>	23
3.1.3 <i>RF Interference Level - RIL</i>	23
3.1.4 <i>Composition and determination of environment characteristics</i>	24
4 EVALUATION OF NEGATIVE PHENOMENA AND IMPACT ON GNSS PERFORMANCE	27
4.1 WP4.3 outputs of preparatory sub-tasks	27
4.2 Railway environment characterization – Data processing, output specification	27
4.3 Railway environment characterization – Analysis of specific scenarios	28
4.3.1 <i>Case of clear sky view</i>	31
4.3.2 <i>Case of clear sky view in a station</i>	39
4.3.3 <i>Case of test track in vicinity of a military airport</i>	47
4.3.4 <i>Case of test track in mountain range</i>	55
4.3.5 <i>Case of train acceleration from a station</i>	61
4.3.6 <i>Case of forest (normal case)</i>	67
4.3.7 <i>Case of forest (extreme case)</i>	75
4.3.8 <i>Case of panoramic camera measurement_1</i>	83
4.3.9 <i>Case of panoramic camera measurement_2</i>	90
4.3.10 <i>Case of panoramic camera measurement_3</i>	96
4.3.11 <i>Case of panoramic camera measurement_4</i>	103
4.4 Railway environment characterization – Evaluation of results	110
4.4.1 <i>Higher multipath in a forest</i>	110
4.4.2 <i>High multipath during standstill in a station</i>	110

4.4.3	<i>RF interference</i>	110
4.4.4	<i>Lower value of HNSE from GPS L1 position solution compared to EGNOS position solution</i>	111
4.4.5	<i>High detection efficiency of panoramic camera</i>	111
4.4.6	<i>HNSE, MPL and RIL dependency</i>	111
4.4.7	<i>Reference position error</i>	112
4.4.8	<i>Software tools for analysis</i>	112
4.4.9	<i>Receivers for railway environment characterization</i>	112
4.4.10	<i>Necessity of measurement</i>	113
5	RELATION OF CHARACTERISTICS TO THE POSITION OF MEASUREMENT	114
5.1	Position dependency of environment characteristics	114
5.2	Virtual Balise placement	115
6	RECOMMENDED FUTURE ACTIVITIES	116
7	SUMMARY	117
8	REFERENCES	118
9	APPENDIX 1 – DESCRIPTION OF SELECTED TECHNIQUES FOR NEGATIVE PHENOMENA EVALUATION	119
9.1	Analysis based on comparison of antenna position from pseudorange solution and reference antenna position based on GT (Task 4.3.2.1)	119
9.2	Analysis based on comparison of antenna position from pseudorange solution and reference antenna position from PPK (Task 4.3.2.2)	121
9.3	Analysis based on comparison of antenna position from corrected pseudorange solution and reference antenna position based on GT (Task 4.3.2.3)	124
9.4	Analysis based on comparison of antenna position from corrected pseudorange solution and reference antenna position from PPK (Task 4.3.2.4)	126
9.5	Data analysis based on comparison of position solutions from different satellite subsets (Task 4.3.2.5)	129
9.6	Data analysis based on deviation of pseudoranges in time (Task 4.3.3.1)	131
9.7	Data analysis based on comparison of measured pseudorange and distance between SV and reference antenna position (Task 4.3.3.2)	133
9.8	C/N ₀ based data analysis (Task 4.3.3.3)	135
9.9	Code minus carrier based analysis (Task 4.3.3.4)	137
9.10	SSE based analysis (Task 4.3.3.5)	141
9.11	Analysis based on multipath detection algorithm built-in receivers (Task 4.3.3.6)	143
9.12	Analysis based on RF interference detection and mitigation algorithm built-in receiver (Task 4.3.3.7)	145
9.13	Analysis based on AGC level evaluation (Task 4.3.3.8)	147
9.14	Data analysis based on sw receiver implementation (Task 4.3.4.1)	149
9.15	Data analysis based on evaluation of RF sample histogram (Task 4.3.4.2)	151
9.16	Analysis based on power spectral density evaluation (Task 4.3.4.3)	153
9.17	Analysis based on measured power spectrum density (Task 4.3.4.4)	155

9.18	Evaluation of impact of different constellation on GNSS signal availability (Task 4.3.5.0)	156
9.19	Sky visibility mask evaluation (Task 4.3.A.0).....	158

LIST OF FIGURES

Figure 1: Workflow diagram of WP4.3	13
Figure 2: Principle of correlation in time domain	18
Figure 3: Principle of correlation in position domain.....	19
Figure 4: Hemisphere (left) and transformed hemisphere (right).....	21
Figure 5: Principle of processing of figures from panoramic camera.....	22
Figure 6: Principle of assignment of ES value	22
Figure 7: Explanation of RIL	24
Figure 8: Principle of composition of MPL and RIL parameters	24
Figure 9: Case of clear sky view (ASTS test track at Sardinia)	31
Figure 10: Case of clear sky view - HNSE values.....	32
Figure 11: Case of clear sky view - Number of satellites.....	32
Figure 12: Case of clear sky view – Train speed profile.....	33
Figure 13: Case of clear sky view – MPL_GPS_L1 (10Hz output rate).....	33
Figure 14: Case of clear sky view – MPL_GPS_L1 (1Hz output rate)	34
Figure 15: Case of clear sky view – MPL_GAL_E1 (10Hz output rate).....	34
Figure 16: Case of clear sky view – MPL_GAL_E1 (1Hz output rate).....	35
Figure 17: Case of clear sky view – MPL_GPS_L1+GAL_E1 (10Hz output rate).....	35
Figure 18: Case of clear sky view – MPL_GPS_L1+GAL_E1 (1Hz output rate).....	36
Figure 19: Case of clear sky view – MPL_GPS_L5 (10Hz output rate)	36
Figure 20: Case of clear sky view – MPL_GAL_E5 (10Hz output rate).....	37
Figure 21: Case of clear sky view – RIL_ L1/E1 (1Hz output rate).....	37
Figure 22: Case of clear sky view – RIL_ L5/E5 (1Hz output rate).....	38
Figure 23: Case of clear sky view in a station (ASTS test track at Sardinia)	39
Figure 24: Case of clear sky view in a station - HNSE values.....	40
Figure 25: Case of clear sky view in a station - Number of satellites.....	40
Figure 26: Case of clear sky view in a station – Train speed profile.....	41
Figure 27: Case of clear sky view in a station – MPL_GPS_L1 (10Hz output rate).....	41
Figure 28: Case of clear sky view in a station – MPL_GPS_L1 (1Hz output rate).....	42
Figure 29: Case of clear sky view in a station – MPL_GAL_E1 (10Hz output rate).....	42
Figure 30: Case of clear sky view in a station – MPL_GAL_E1 (1Hz output rate).....	43

Figure 31: Case of clear sky view in a station – MPL_GPS_L1+GAL_E1 (10Hz output rate).....	43
Figure 32: Case of clear sky view in a station – MPL_GPS_L1+GAL_E1 (1Hz output rate).....	44
Figure 33: Case of clear sky view in a station – MPL_GPS_L5 (10Hz output rate).....	45
Figure 34: Case of clear sky view in a station – MPL_GAL_E5 (10Hz output rate).....	45
Figure 35: Case of clear sky view in a station – RIL_L1/E1 (1Hz output rate).....	46
Figure 36: Case of clear sky view in a station – RIL_L5/E5 (1Hz output rate).....	46
Figure 37: Case of test track in vicinity of a military airport (ASTS test track at Sardinia).....	47
Figure 38: Case of test track in vicinity of military airport – HNSE values	48
Figure 39: Case of test track in vicinity of military airport – Number of satellites	48
Figure 40: Case of test track in vicinity of military airport – Train speed profile	49
Figure 41: Case of test track in vicinity of military airport – MPL_GPS_L1 (10Hz output rate)	49
Figure 42: Case of test track in vicinity of military airport – MPL_GPS_L1 (1Hz output rate)	50
Figure 43: Case of test track in vicinity of military airport – MPL_GAL_E1 (10Hz output rate)	50
Figure 44: Case of test track in vicinity of military airport – MPL_GAL_E1 (1Hz output rate)	51
Figure 45: Case of test track in vicinity of military airport – MPL_GPS_L1+GAL_E1 (10Hz output rate).....	51
Figure 46: Case of test track in vicinity of military airport – MPL_GPS_L1+GAL_E1 (1Hz output rate)	52
Figure 47: Case of test track in vicinity of military airport – MPL_GPS_L5 (10Hz output rate)	53
Figure 48: Case of test track in vicinity of military airport – MPL_GAL_E5 (10Hz output rate)	53
Figure 49: Case of test track in vicinity of military airport – RIL_L1/E1 (1Hz output rate)	54
Figure 50: Case of test track in vicinity of military airport – RIL_L5/E5 (1Hz output rate)	54
Figure 51: Case of test track in mountain range (SIE test track at Switzerland)	55
Figure 52: Case of test track in mountain range - HNSE values	56
Figure 53: Case of test track in mountain range - number of satellites.....	56
Figure 54: Case of test track in mountain range – Train speed profile	57
Figure 55: Case of test track in mountain range – MPL_GPS_L1 (1Hz output rate)	57
Figure 56: Case of test track in mountain range – MPL_GAL_E1 (1Hz output rate)	58
Figure 57: Case of test track in mountain range – MPL_GPS_L1+GAL_E1 (1Hz output rate)	58
Figure 58: Case of test track in mountain range – MPL_GPS_L5 (1Hz output rate)	59
Figure 59: Case of test track in mountain range – MPL_GAL_E5 (1Hz output rate)	59
Figure 60: Case of test track in mountain range – RIL_L1/E1 (1Hz output rate)	60
Figure 61: Case of test track in mountain range – RIL_L5/E5 (1Hz output rate)	60
Figure 62: Case of train acceleration from a station (SIE test track at Switzerland)	61
Figure 63: Case of train acceleration from a station – HNSE values.....	62
Figure 64: Case of train acceleration from a station – Number of satellites.....	62
Figure 65: Case of train acceleration from a station – Train speed profile.....	63

Figure 66: Case of train acceleration from a station – MPL_GPS_L1 (1Hz output rate).....	63
Figure 67: Case of train acceleration from a station – MPL_GAL_E1 (1Hz output rate).....	64
Figure 68: Case of train acceleration from a station – MPL_GPS_L1+GAL_E1 (1Hz output rate) .	64
Figure 69: Case of train acceleration from a station – MPL_GPS_L5 (1Hz output rate).....	65
Figure 70: Case of train acceleration from a station – MPL_GAL_E5 (1Hz output rate).....	65
Figure 71: Case of train acceleration from a station – RIL_L1/E1 (1Hz output rate).....	66
Figure 72: Case of train acceleration from a station – RIL_L5/E5 (1Hz output rate).....	66
Figure 73: Case of nominal forest (AZD test track at the South Bohemia)	67
Figure 74: Case of nominal forest – HNSE values (10Hz output rate)	68
Figure 75: Case of nominal forest – Number of satellites.....	68
Figure 76: Case of nominal forest – Train speed profile.....	69
Figure 77: Case of nominal forest – MPL_GPS_L1 (10Hz output rate).....	69
Figure 78: Case of nominal forest – MPL_GPS_L1 (1Hz output rate).....	70
Figure 79: Case of nominal forest – MPL_GAL_E1 (10Hz output rate).....	70
Figure 80: Case of nominal forest – MPL_GAL_E1 (1Hz output rate).....	71
Figure 81: Case of nominal forest – MPL_GPS_L1+GAL_E1 (10Hz output rate)	71
Figure 82: Case of nominal forest – MPL_GPS_L1+GAL_E1 (1Hz output rate)	72
Figure 83: Case of nominal forest – MPL_GPS_L5 (10Hz output rate).....	72
Figure 84: Case of nominal forest – MPL_GAL_E5 (10Hz output rate).....	73
Figure 85: Case of nominal forest – RIL_L1/E1 (1Hz output rate).....	73
Figure 86: Case of nominal forest – RIL_L5/E5 (1Hz output rate).....	74
Figure 87: Case of extreme forest (AZD test track at the South Bohemia).....	75
Figure 88: Case of extreme forest HNSE values	76
Figure 89: Case of extreme forest – Number of satellites	76
Figure 90: Case of extreme forest – Train speed profile	77
Figure 91: Case of extreme forest – MPL_GPS_L1 (10Hz output rate)	77
Figure 92: Case of extreme forest – MPL_GPS_L1 (1Hz output rate)	78
Figure 93: Case of extreme forest – MPL_GAL_E1 (10Hz output rate)	78
Figure 94: Case of extreme forest – MPL_GAL_E1 (1Hz output rate)	79
Figure 95: Case of extreme forest – MPL_GPS_L1+GAL_E1 (10Hz output rate)	79
Figure 96: Case of extreme forest – MPL_GPS_L1+GAL_E1 (1Hz output rate)	80
Figure 97: Case of extreme forest – MPL_GPS_L5 (10Hz output rate)	81
Figure 98: Case of extreme forest – MPL_GAL_E5 (10Hz output rate)	81
Figure 99: Case of extreme forest – RIL_L1/E1 (1Hz output rate)	82
Figure 100: Case of extreme forest – RIL_L5/E5 (1Hz output rate)	82
Figure 101: Case of panoramic camera measurement 1 (AZD test track at the South Bohemia)...	83
Figure 102: Case of camera measurement 1 – HNSE EGNOS values (10Hz output rate).....	84

Figure 103: Case of camera measurement 1 – HNSE GPSL1 values (10Hz output rate)	84
Figure 104: Case of camera measurement 1 – Number of satellites (EGNOS solution)	85
Figure 105: Case of camera measurement 1 – Number of satellites (GPS L1 solution).....	85
Figure 106: Case of camera measurement 1 – Train speed profile	86
Figure 107: Case of camera measurement 1 – PDOP (10 Hz output rate)	86
Figure 108: Case of camera measurement 1 – MPL_GPS_L1 (10Hz output rate).....	87
Figure 109: Case of camera measurement 1 – SVF _{APV} (1Hz output rate)	87
Figure 110: Case of camera measurement 1 – SVF _{ES} (1Hz output rate)	88
Figure 111: Case of camera measurement 1 – RIL_L1/E1 (1Hz output rate).....	89
Figure 112: Case of camera measurement 1 – RIL_L5/E5 (1Hz output rate).....	89
Figure 113: Case of panoramic camera measurement 2 (AZD test track at the South Bohemia)...	90
Figure 114: Case of camera measurement 2 – HNSE EGNOS values (10Hz output rate).....	91
Figure 115: Case of camera measurement 2 – HNSE GPSL1 values (10Hz output rate)	91
Figure 116: Case of camera measurement 2 – Number of satellites (EGNOS solution)	92
Figure 117: Case of camera measurement 2 – Number of satellites (GPS L1 solution).....	92
Figure 118: Case of camera measurement 2 – Train speed profile	93
Figure 119: Case of camera measurement 2 – PDOP (10 Hz output rate)	93
Figure 120: Case of camera measurement 2 – MPL_GPS_L1 (10Hz output rate).....	94
Figure 121: Case of camera measurement 2 – SVF _{APV} (1Hz output rate)	94
Figure 122: Case of camera measurement 2 – RIL_L1/E1 (1Hz output rate).....	95
Figure 123: Case of camera measurement 2 – RIL_L5/E5 (1Hz output rate).....	95
Figure 124: Case of panoramic camera measurement 3 (AZD test track at the South Bohemia)...	96
Figure 125: Case of camera measurement 3 – HNSE EGNOS values (10Hz output rate).....	97
Figure 126: Case of camera measurement 3 – HNSE GPSL1 values (10Hz output rate)	97
Figure 127: Case of camera measurement 3 – Number of satellites (EGNOS solution)	98
Figure 128: Case of camera measurement 3 – Number of satellites (GPS solution).....	98
Figure 129: Case of camera measurement 3 – Train speed profile	99
Figure 130: Case of camera measurement 3 – PDOP (10 Hz output rate)	99
Figure 131: Case of camera measurement 3 – MPL_GPS_L1 (10Hz output rate).....	100
Figure 132: Case of camera measurement 3 – SVF _{APV} (1Hz output rate)	101
Figure 133: Case of camera measurement 3 – RIL_L1/E1 (1Hz output rate).....	101
Figure 134: Case of camera measurement 3 – RIL_L5/E5 (1Hz output rate).....	102
Figure 135: Case of panoramic camera measurement 4 (AZD test track at the South Bohemia).	103
Figure 136: Case of camera measurement 4 - HNSE EGNOS values (10Hz output rate)	104
Figure 137: Case of camera measurement 4 - HNSE GPSL1 values (10Hz output rate).....	104
Figure 138: Case of camera measurement 4 – Number of satellites (EGNOS solution)	105
Figure 139: Case of camera measurement 4 – Number of satellites (GPS L1 solution).....	105

Figure 140: Case of camera measurement 4 – Train speed profile	106
Figure 141: Case of camera measurement 4 – PDOP (10 Hz output rate)	106
Figure 142: Case of camera measurement 4 – MPL_GPS_L1 (10Hz output rate).....	107
Figure 143: Case of camera measurement 4 – SVF _{APV} (1Hz output rate).....	107
Figure 144: Case of camera measurement 4 – RIL_L1/E1 (1Hz output rate).....	108
Figure 145: Case of camera measurement 4 – RIL_L5/E5 (1Hz output rate).....	109
Figure 146: “Defocusing” the characteristic position dependency	114
Figure 147: Relation of regions VBE and VBP	115

1 INTRODUCTION

1.1 EXECUTIVE SUMMARY

If GNSS shall be used in safety critical railway applications then the impacts of the environment on the performance of GNSS must be known. Such impacts can reduce the accuracy and availability, but also the safety of the system, and can be caused by multi path signals, by a limited visibility of satellites, by RF interferences, weather etc.

The purpose of this document is to characterize the railway environment in regards to phenomena reducing GNSS performance.

This document consists of several parts. The first one (Section 2) describes the methodology which has been developed to perform the characterization of the railway environment. It includes theoretical background on phenomena which can negatively influence GNSS performance, and a classification of appropriate techniques which can be used for the detection of such phenomena.

Subsequently, the chosen approach is described in Section 3, which enables the transformation of all outputs coming from different techniques into one set of parameters suitable for a railway environment characterization.

Section 4 is focused on the overall analysis and evaluation of the results of the environment factors. The presented results were achieved by applying the proposed process described in this document to recorded data from measurements carried out at different test sites located in three countries. The description of selected techniques is described in Appendix 1 of this document.

Section 5 provides consideration of the use of GNSS in railway applications, depending on the position of measurement.

Section 6 contains proposals for future activities, Section 7 the overall conclusions.

The document utilizes outputs of all tasks performed in a frame of WP4. A list of suitable techniques for detection of presence of negative phenomena was elaborated in a frame of WP4.1 and it can be found in [1]. A repository and basic conception of the reference data set, which includes preprocessed raw data, GNSS support data, configurations of devices, SW codes and output data, has been established also in a frame of WP4.1. The above mentioned input and output data has been generated and uploaded to the reference data set in the frame of WP3.3, WP4.2 and WP4.3. The basic description of reference data set has been done in [2], but there are also a few important documents [3], [4], which are related to the description of the reference data set conception.

1.2 DEFINITIONS AND ACRONYMS

Acronym	Meaning
APV	Analyzed Parameter Value: An APV is a scalar value which provides quantification of the impact of a specific Evaluation Symptom on GNSS performance.
ASTS	Ansaldo STS
AZD	AZD Praha s.r.o.
AGC	Automatic Gain Control
BAG	Biasca – Airolo – Göschenen Line in Switzerland

BDP	Biel/Bienne – Delémont – Porrentruy Line in Switzerland
CPD	Correlation in Position Domain
CTD	Correlation in Time Domain
CVO	Číčenice – Volary Line in the Czech Republic
EDAS	EGNOS Data Access Service
EGNOS	European Geostationary Navigation Overlay Service
EMC	Electromagnetic Compatibility
EMI	Electromagnetic Interference
EMS	EGNOS Message Server
ES	Evaluation Symptom: A specific symptom which indicates a degradation of GNSS performance.
GNSS	Global Navigation Satellite System
GPS	Global Positioning System
GPST	GPS Time
GT	Ground Truth: GNSS independently derived position of a train
HNSE	Horizontal Navigation System Error: Difference between processed receiver position and ground truth position projected in horizontal plane.
IGS	International Earth Rotation and Reference Frames Service
IMU	Inertial Measurement Unit
LHCP	Left Hand Circular Polarization
LOS	Line of Sight
MEMS	MicroElectroMechanical Systems
MPL	Multi Path Level
NLOS	None Line of Sight
PPK	Post Processing Kinematic (PPK used within this document means the use of reference position based on GNSS PPK solution)
PVT	Position Velocity Time
RAIM	Receiver Autonomous Integrity Monitoring
RF	Radio Frequency

RHCP	Right Hand Circular Polarization
RIL	RF Interference Level
RPO	Reference Position (RPO used within this document means the use of Ground Truth based reference position)
RPS	Record and Playback System
SIE	Siemens
STARS	Satellite Technology for Advanced Railway Signalling
SV	Space Vehicle
SVF	Sky Visibility Factor
VB	Virtual Balise
VBE	Virtual Balise Environment
VBP	Pre-Virtual Balise Environment
WP	Work Package

2 DATA PROCESSING TOWARDS ENVIRONMENT CHARACTERIZATION

This section describes the WP4.3 workflow, which consists of the following steps:

- the selection of raw data in the Reference data set, where raw data were collected and uploaded in a frame of WP3
- preprocessing of raw data based on the techniques selected in WP4.1, i. e. data format conversion, check of data inconsistency, supporting PVT calculations etc.)
- processing of preprocessed raw data as defined in WP4.3 sub-tasks
- the calculation of values of the parameters suitable for railway environment characterization.

This is a bottom up approach, meaning that the environment characterization is built entirely from the available WP4.3 sub-task outputs.

This workflow is also presented in Figure 1.

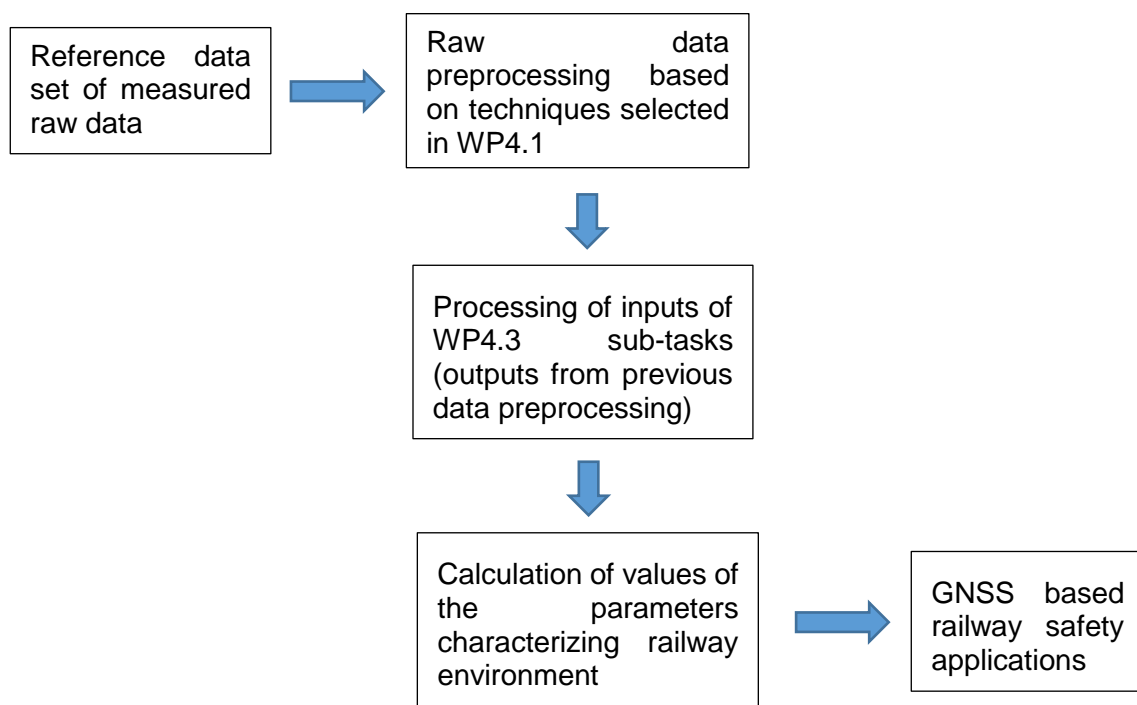


Figure 1: Workflow diagram of WP4.3

Measured data is pre-processed in the frame of WP4.2, stored in the Reference data set and then analyzed in the frame of WP4.3. The data analysis is carried out in parallel in the different WP4.3 sub-tasks. Each sub-task implements a different method which was proposed with the aim to detect or even quantify local phenomena with negative impact on GNSS signal reception and thus on GNSS performance.

The techniques were proposed with a focus on the following negative phenomena:

- Restricted satellite visibility (includes also signal attenuation due to e.g. obstacles, foliage etc.)
- Multipath effects (includes both multipath with and without presence of line-of-sight signal)
- RF interference (includes onboard generated interferences as well as interferences from stationary and non-stationary external sources along the track)

Some of the techniques only have a capability to indicate that something is wrong, but don't provide information on which negative phenomenon is causing interference, while other techniques are directly coupled to one of the listed negative phenomenon, and thus serve as a good indicator for this particular phenomenon.

Note: Some of these techniques might form the basis for future receiver functions which detect interferences in real time.

2.1.1 **Techniques for negative phenomenon detection or quantification**

The following list contains a short description of techniques applied in the different WP4.3 sub-tasks:

- T4.3.2: comparison in position domain: This sub-task includes several techniques, each one based on a comparison of different GNSS receiver positions and a reference positions. The output of the comparison is an estimation of the position error. The GNSS receiver position is computed from receiver code phase measurements in post-processing mode, the reference antenna position is obtained from either transformed ground truth position, or from positions computed from receiver carrier phase measurement using the PPK method. The estimated position error provides a simple scalar value which is proportional to negative phenomena impact but without the possibility to distinguish the particular phenomenon (poor satellite visibility, multipath environment, RF interference or others).
- T4.3.3: raw data analysis and analysis of specific receiver outputs: This sub-task covers several techniques which utilize either measured observables (code or phase measurements, Doppler measurement, signal quality indicator) or specific receiver outputs (monitored receiver internal parameters or outputs of detection or mitigation algorithms built into the receivers). Analysis of observables can indicate either unspecified negative phenomenon (e.g. technique based on time analysis of observables) or can be focused on particular one (e.g. code minus carrier technique indicates multipath error). Receiver internal parameters (e.g. AGC level) or outputs of internal mitigation algorithms are utilized in techniques which provide information regarding specific negative phenomenon (in most cases regarding multipath or RF interference).
- T4.3.4: analysis of recorded RF I/Q samples: The techniques in this subtask are mostly focused on RF interference detection (utilizing of estimated power spectra density, histogram evaluation). Beside this, a SW GNSS receiver with tailored DLL detectors is utilized to analyze multipath error on pseudoranges.
- T4.3.5: evaluation of impact of multiple frequencies and multiple constellations on GNSS signal availability: This sub-task contains only one technique focused on different PVT solution availability. Different PVT types (e.g. single-frequency GPS L1, multi-frequency GPS L1/L5, RAIM PVT on GPS L1, etc.) have different requirements on number of specific observables. Based on prepared assumptions for particular PVT algorithms and real measured data (type and number observables) the availability of particular PVT solution is determined.
- Sky visibility assessment based on panoramic figures: this technique is outside of the main STARS stream due to both installation restrictions (a panoramic camera is installed only on the test train equipped by AZD) and consortium processing capability (the processing of panoramic figures was not planned in the frame of WP4.3). However, it is supposed that panoramic figures can provide valuable information with respect of sky visibility. At least, the AZD measurement set has been collecting such data, and AZD has been trying to implement a simple processing algorithm which can quantify the area of unblocked sky from pictures taken by the panoramic camera.

2.1.2 Techniques classifications

The techniques listed above can be split into four groups according to local phenomenon which can be detected or quantified by each technique. These groups are:

- (G) General: techniques without a capability to indicate specific phenomenon;
- (V) Visibility: techniques with the capability to indicate poor sky visibility,
- (M) Multipath: techniques with the capability to indicate multipath environment,
- (I) Interference: techniques with the capability to indicate RF interference.

Each group (G, V, M, I) is using more than one technique. This redundancy can be utilized to gain the credibility of detected phenomenon as well as to decide, which technique is the most suitable for the phenomenon detection or even for its quantification (from perspective of measurement and processing demands, sensitivity, availability, etc.) for future data analysis.

2.1.3 Evaluation Symptom (ES) and Analyzed Parameter Value (APV)

A unified output format for data processed in frame of WP4.3 sub-tasks has been defined within the STARS project, which is documented in [5]. The purpose of this format is to simplify the further evaluation of the outputs generated by different techniques. Output files are organized into columns, the first three columns are mandatory: GPS System Time (GPST), Evaluation Symptom (ES), and Analyzed Parameter Value (APV).

The APV is a scalar value which provides the quantification of the phenomenon impact based on the technique. The ES parameter represents a roughly quantized APV and mostly achieves values of 0, 1, and 2. Some techniques can provide less or more values of ES.

The purpose of the ES is to have a simple scalar value (a symptom) for the indication of negative phenomenon. There are however techniques which only detect phenomenon without a possibility of phenomenon quantification. In such cases, the APV is filled with NaN and only ES has reasonable values (an example of this case can be a technique in sub-task 4.3.3.7, see Table 1).

The ES has direct relationship to APV and is usually given by two thresholds. It is a responsibility of a partner implementing the technique and doing the processing to determine these thresholds. This approach should ensure that the thresholds are correctly determined with respect to possible range of all APV values obtained during the processing.

2.1.4 Combined APV

There are techniques that naturally provide one scalar value which is proportional to the impact of the environment on GNSS signal reception and position estimation. Such scalar values are then taken as an APV. An example of such cases are sub-tasks from 4.3.2.1 to 4.3.2.4 (see Table 1), where the position error is taken as an APV.

However, there are also techniques which analyze individual satellite signals (on individual observables). The standard output would be a set of values for one measurement epoch, where each value corresponds to one analyzed satellite signal. This form of output is however not suitable from the perspective of future output processing (cross correlation with the outputs of other techniques, see below). Therefore a method, how to combine several values to one reasonable scalar number has been defined. This method should ensure that the values related to satellites on lower elevations are penalized with respect to values coming from satellites on higher elevations. The reason for that is the fact that the data of poor quality is normally received from satellites on low elevations (it is quite common that for low elevation satellite e.g. the signal quality indicator C/No is low and multipath error is high and thus such values should not be taken into account significantly for environment evaluation purpose). In the selected method, the analyzed property is multiplied with a correction factor. The correction factor was proposed to be $\sin(El_i)$, where El_i is the elevation of particular satellite. The function $\sin(\cdot)$ was selected due to the simplicity, another (more appropriate)

function might however be selected in the future depending on results from the various analysis sub-tasks.

The combined APV value is determined according the following equations:

$$APV = \max\{X_1 \sin(El_1), X_2 \sin(El_2), \dots, X_{N_{SV}} \sin(El_{N_{SV}})\},$$

for values X_i where higher value represents the poorer environment (e.g. in case of multipath error [m] estimated on measured satellite signal) or

$$APV = \min\{X_1 \sin(El_1), X_2 \sin(El_2), \dots, X_{N_{SV}} \sin(El_{N_{SV}})\},$$

for values X_i where lower value represents the poorer environment (e.g. in case of signal quality indicator C/N₀ [dB-Hz]). Selecting an extreme from the set endorses a conservative approach which is necessary if the environment description should be used for minimal performance guarantee.

Table 1 lists the techniques and their parameters used in the different sub-tasks. The techniques which utilize a combined APV are marked with C in the ComAPV column.

Task No.	Resp. partner	Group	Output	Com. APV	Task name
4.3.2	Identification of factors disturbing GNSS signal and positioning solution based on comparison in position domain				
4.3.2.1	BT	G	APV,ES		Data analysis based on comparison of pseudorange based receiver antenna position estimation and GT based reference antenna position
4.3.2.2	CAF	G	APV, ES		Data analysis based on comparison of pseudorange based receiver antenna position estimation and reference antenna position based on PPK
4.3.2.3	TTS	G	APV,ES		Data analysis based on comparison of receiver antenna position estimation based on differenced pseudoranges and reference antenna position based on GT
4.3.2.4	ALS	G	APV,ES		Data analysis based on comparison of receiver antenna position estimation based on differenced pseudoranges and reference antenna position based on PPK
4.3.2.5	ZCU	G	APV,ES		Data analysis based on comparison of position solution from different satellite subsets
4.3.3	Data analysis and identification of factors disturbing GNSS signal and positioning solution based on raw data or specific features of receivers				
4.3.3.1	ZCU	G	APV,ES	C	Data analysis based on deviation of pseudoranges in time

4.3.3.2	ZCU	G	APV, ES	C	Analysis based on comparison of measured pseudorange and distance between SV and reference antenna position
4.3.3.3	AZD	M,V,I	APV,ES	C	C/N ₀ data based analysis
4.3.3.4	ALS	M	APV,ES	C	Code minus carrier based analysis
4.3.3.5	AZD	M	APV,ES		SSE based analysis
4.3.3.6	CAF	M	APV,ES	C	Analysis based on multipath detection and mitigation algorithm built-in receivers
4.3.3.7	RADLBS	I	ES		Analysis based on RF interference detection and mitigation algorithm built-in receiver
4.3.3.8	RADLBS	I	ES		Analysis based on AGC level evaluation
4.3.4	Identification of factors disturbing GNSS signal and position solution based on analysis of recorded RF I/Q samples				
4.3.4.1	TASF	M	APV,ES	C	Analysis based on GNSS SW receiver implementation
4.3.4.2	TUBS	I	ES		Analysis based on evaluation of RF sample histogram
4.3.4.3	RADLBS	I	(APV),ES		Analysis based on power spectral density evaluation
4.3.4.4	AZD	I	APV,ES		Analysis based on measured power spectral density
4.3.5	TUBS	V	ES		Evaluation of impact of different constellation on GNSS signal availability
4.3.A	AZD	V	APV,ES		Sky visibility assessment based on panoramic figures

Table 1: Summarization of techniques used for negative local phenomena detection and quantification

The structured description of techniques presented in Table 1 is given in Appendix 1 of this document.

2.2 ENVIRONMENT CHARACTERIZATION BASED ON TECHNIQUE OUTPUTS

Environment characterization can be performed in two successive steps.

2.2.1 Correlation in time domain

The first one is based on cross-correlation of particular APV or ES series. This step is entitled here as correlation in time domain (CTD). It is expected that APV or ES series belonging to the same group (V, M, I) should be strongly correlated, i.e. cross-correlation functions of APV or ES series should have their maxima with little offset, as techniques belonging to the same group should detect negative local phenomenon at the same time.

The situation example for CTD is presented in Figure 2.

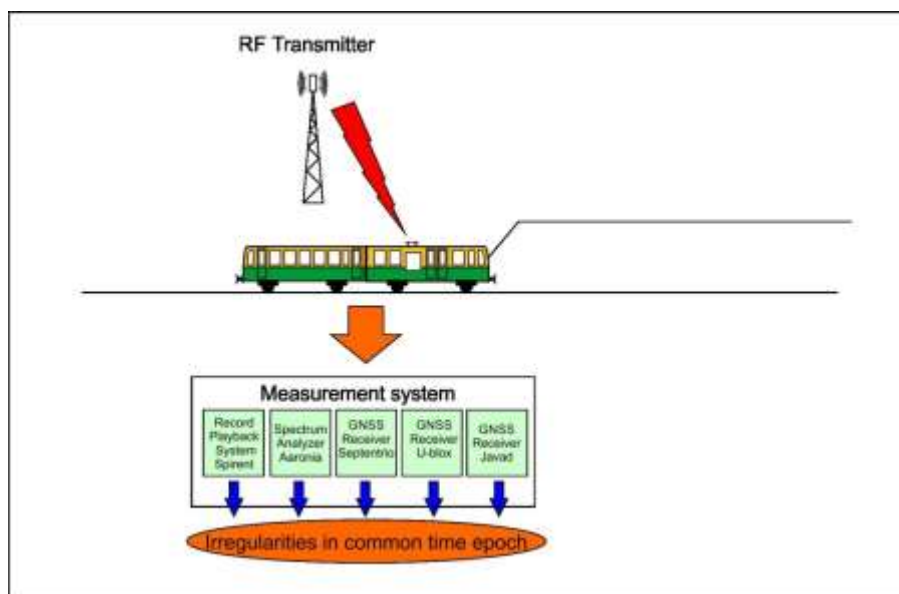


Figure 2: Principle of correlation in time domain

Technically, the correlations will be computed with the time as an independent variable. Therefore, the detected (quantified) local negative phenomena will be provided in the 1D time coordinate (for detected/quantified local negative phenomenon the time instant of occurrence will be available). This type of output is sufficient for statistical summary of a particular railway line.

2.2.2 Correlation in position domain

The second step is based on auto-correlation of APV or ES series. This step is entitled here as correlation in position domain (CPD). An arbitrary selected APV or ES series, if measurement consists of N train runs going through the identical line segment, should have N maxima of its auto-correlation function. This is a consequence of the fact that the train is passing identical locations with identical negative local phenomenon during different train runs, i.e. in different time instant.

However, to analyse what was the source (what was the obstacle, if moving interferer or stationary RF transmitter caused interference etc.) of negative phenomenon, the 1D time coordinate has to be transformed to the position coordinates. The time-position relation is available from the reference antenna position obtained from transformed ground truth position. When the 2D/3D position coordinates are available, the consideration what was the source of local negative phenomenon can be carried out with a map or with the camera figures. While the time-position transformation can be done automatically, the identification of the source on a map or using camera pictures has to be done manually.

Note that analyzing maps and pictures taken by the cameras cannot necessarily identify all sources causing local negative phenomena, and that there is also certain risk to misinterpretation.

The principle of proposed CPD is shown in Figure 3. The left train is influenced by a stationary transmitter during each passage, the right train is influenced by occasional multipath caused by non-stationary reflector. The CPD enables to distinguish between these two depicted cases.

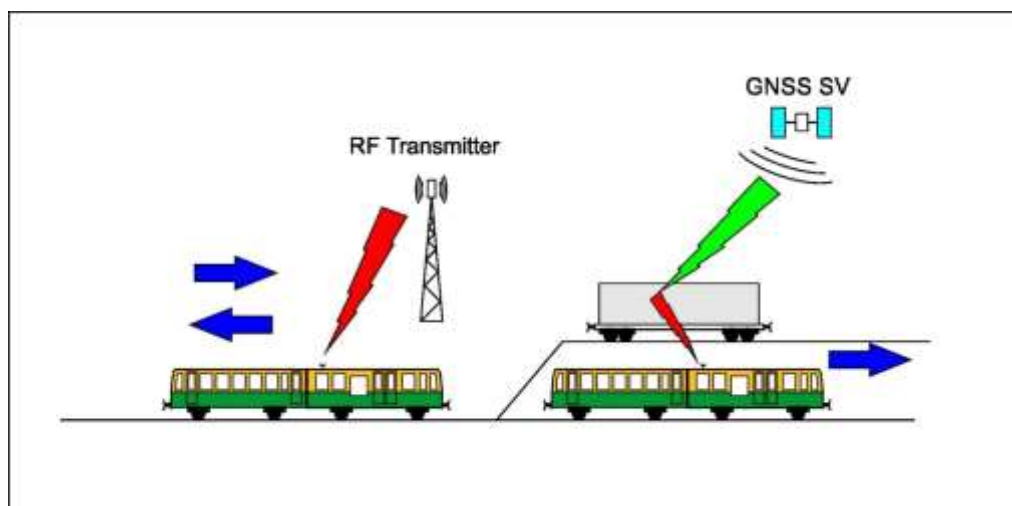


Figure 3: Principle of correlation in position domain

3 RAILWAY ENVIRONMENT CHARACTERIZATION FROM GNSS SIGNAL RECEPTION PERSPECTIVE

This section describes the principle of the proposed solution for the environment characterization of railway lines. The goal is to define a set of characteristics which provides sufficient environment characterization along the tracks from a GNSS signal reception perspective. The characteristics are simple scalar values. The criteria for an assessment of conditions of given track section for deployment of arbitrary GNSS based safety relevant application (e.g. Virtual Balise) can then have a simple form of maximal or minimal limits for these characteristics.

The list of proposed environment characteristics follows:

SVF – Sky Visibility Factor

MPL – Multipath Level

RIL – RF Interference Level

It is assumed that these characteristics are sufficient for characterizing the railway environment. With regard to the locally dependent impact on GNSS characterization, this will need to be demonstrated and proven in the STARS project solution and the analysis of the results.

Further, the characteristics are assumed to be independent of each other (degradation of one does not imply degradation of others), but this assumption will also have to be verified using the STARS data.

The description here is a top down approach based on foreseen needs (i.e. the description can help with the decision where to rely on GNSS for train positioning).

However, it should be noted that sporadic or temporary interferences also exist for the above listed characteristics, which may not be related to specific locations along the track. Such interferences can be caused by

- mobile sources that reduce satellite visibility, such as e.g. other trains, vehicles, temporary structures,
- sources that cause multipath, such as e.g. other trains, vehicles, temporary structures or weather phenomena,
- sources of RF interference, such as e.g. other trains, transmitters or jammers.

Identifying such interferences is challenging as it depends either on the analysis of large volumes of data collected over a longer time periods, which might exceed the duration of the measurement campaign within the STARS project, or even on sheer luck.

3.1 ENVIRONMENT CHARACTERISTICS

3.1.1 Sky Visibility Factor - SVF

The visibility of sky can be described as a surface of unblocked part of upper hemisphere with the center in the location of interest.

The computation of surface of unblocked area should also respect the fact that the areas on lower elevations are less significant for sky visibility evaluation. To ensure this requirement the hemisphere has to be transformed (scaled). This new shape after the transformation is denoted here as TH (Transformed Hemisphere).

As a starting point the function $\sin(\cdot)$ is used for the transformation due to simplicity. The original hemisphere with a unit radius $R = 1$ is transformed to TH according to $R = \sin(El)$. Both shapes are shown in Figure 4.



Figure 4: Hemisphere (left) and transformed hemisphere (right)

The Sky Visibility Factor (SVF) can be defined as a surface of unblocked part of TH normalized by the total area of TH, thus

$$SVF = \frac{\iint_{unblocked} TH \, d\Omega}{\iint_{total} TH \, d\Omega}$$

In the specific case when TH is created from hemisphere with $\sin(\cdot)$ function

$$SVF = \frac{\iint_{(Az, El)} \cos(El) \sin(El) \, dEl \, dAz}{\iint_{(0,0)}^{(2\pi, \frac{\pi}{2})} \cos(El) \sin(El) \, dEl \, dAz} = \frac{1}{\pi} \iint_{(Az, El)} \cos(El) \sin(El) \, dEl \, dAz$$

The SVF takes values from 0 (completely blocked sky) to 1 (completely open sky).

Note, the proposed transformation with the function $\sin(\cdot)$ is not ideal. This transformation does not consider the true tracks of GNSS satellites on the sky (orientation with respect to the local north-east coordinates, dependency on the latitude of the location of interest). This is e.g. relevant in mountain valleys, cities or between embankments, where a significant portion of the sky is visible, but where the shape of the visible part of the sky is not optimal for GNSS localization.

The effective way how to determine the unblocked area on the specific location is by processing of panoramic figure which is taken in the location of interest.

Within solution of WP4.3 a certain simplification was adopted in order to provide results in expected time. It consists of staying in 2D space, processing figures from panoramic camera and calculation of SVF without transformation into 3D space. Apart from that a lens distortion was neglected and the linear scale was used for elevation in the camera figures (circles). SVF parameter is then calculated

$$SVF(t) = \frac{\text{area of clear sky view } (t)}{\text{area of whole figure } (t)}$$

The principle of processing of figures from the panoramic camera is presented on Figure 5: .

In the first step each original figure from the panoramic camera on Figure 5: a) is properly oriented by means of information on azimuth obtained from SBF block by Septentrio receiver, see Figure 5: b). The red area in the figures represents a part of the sky covered by obstacles, the blue area represents clear sky. Subsequently, the area (the small red circle) is added through which satellite

orbits do not pass, see Figure 5: c). Finally, the SVF value is calculated for different values of elevation mask, which is represented by the yellow circle in Figure 5: d). It means according to the above written equation, but both clear sky view area and whole figure area are restricted to the area bounded by corresponding elevation mask.

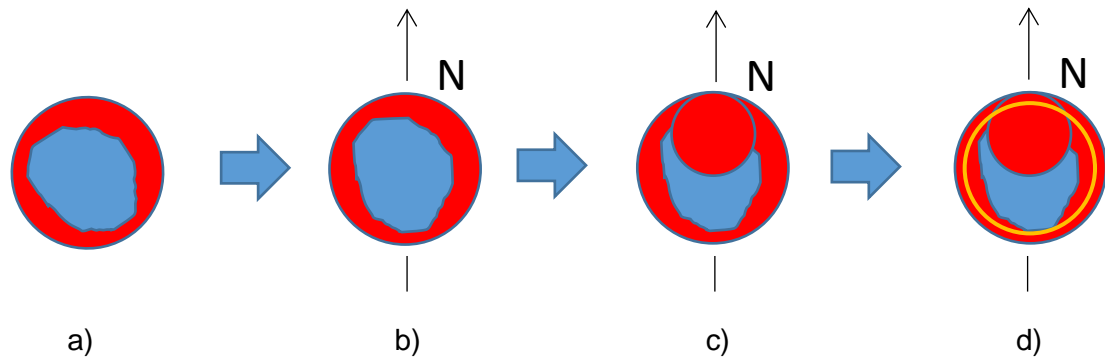
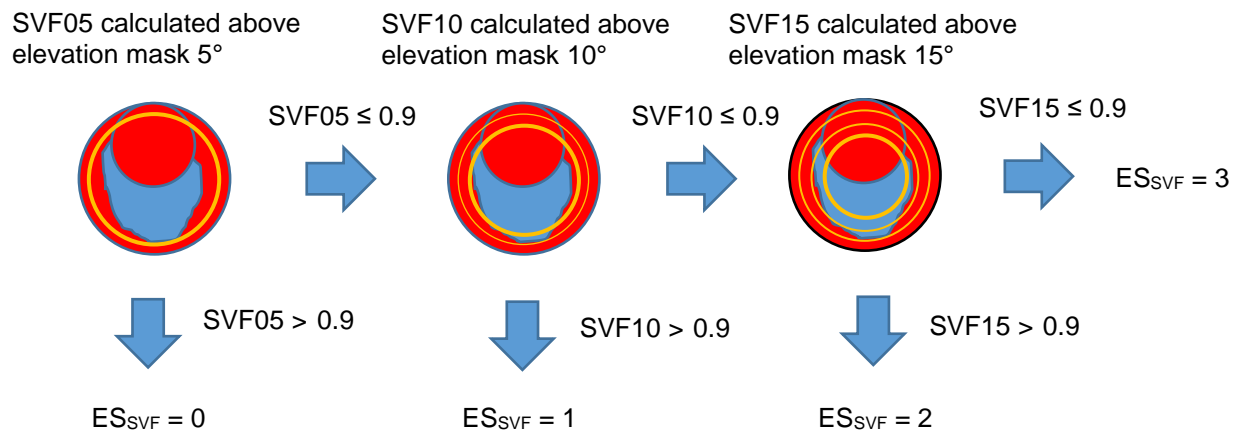


Figure 5: Principle of processing of figures from panoramic camera

To assign an appropriate ES value to SVF, three SVF values are calculated for elevation masks equal to 5, 10, 15 degrees. In the next step, each calculated value of SVF is tested at 0.9. Such value of ES is selected which corresponds to that SVF value meeting the condition to be greater than 0.9. The principle is presented by example in Figure 6.



Examples of ES_{SVF} assignment:

- a) if $SVF05 = 0.8$, subsequently $SVF10 = 0.7$ and subsequently $SVF15 = 0.7$, then **$ES_{SVF} = 3$**
- b) if $SVF05 = 0.6$, subsequently $SVF10 = 0.92$, then **$ES_{SVF} = 1$**

Figure 6: Principle of assignment of ES value

The proposed threshold value 0.9 was derived from 5 degree elevation mask considered for clear sky view. The ratio of areas (circles) of full visibility and limited visibility corresponds to ratio of their squared radii $85^2/90^2$ and is roughly equal to 0.9. It could be mentioned that a) this threshold value is tentative value, b) a simplification was implemented (evaluation in 2D) and c) a lens distortion of the camera was neglected.

3.1.2 Multipath Level - MPL

To characterize the environment from a multipath perspective, the Multipath Level (MPL) is defined as maximal multipath error estimated/measured on GNSS pseudorange and corrected to suppress values from lower elevations.

Basically, the definition MPL follows the approach of combined APV described in Section 2.1.4. Measured/estimated multipath errors on particular observables are multiplied by the correction factor $\sin(EI)$. MPL in the location of interest is then the maximum of these corrected values.

However, there are several issues with such MPL definition. First of them is a way how to measure or estimate the multipath error. In frame of STARS several techniques were proposed (code minus carrier, utilization of output of specific internal receiver algorithm, etc.). Thus multipath error is not only function of multipath but also the receiver capability of multipath detection and estimation (meaning that different receivers from different suppliers can provide different multipath error estimation in the identical location and identical time instant). Moreover multipath is also dependent of the speed of the train at time of the acquisition. Further, in case of code minus carrier, the values are proportional not only to multipath but also to noise.

Another issue is the representativeness of such MPL. MPL constructed from the measurements at one instant only might not be measured in the worst case, thus, does not represent the location. To overcome this issue, the multipath can be measured repeatedly at the same location for long time period to collect enough values. However, this approach is impractical due to high time consumption, and also because it might not be possible to park the train used for measurement at specific, critical location.

Since the multipath estimation is based on the selected GNSS signal (e.g. GPS L1 C/A), analyzed MPL value is related to this signal only and cannot be generalized for others (e.g. for Galileo E1 A+B or GPS L5).

There is no known effective way of multipath measurement which can ensure representative data for the location of interest (long time measurement is not considered as an effective way). This issue will have to be the subject of future studies based on STARS data.

3.1.3 RF Interference Level - RIL

For characterization of RF interference, the RF Interference Level (RIL) is defined. RIL is defined as a power (in [W]) of hypothetical signal which is above of defined spectral mask.

The spectral mask defines the ideal non-interfered environment. This spectral mask is not flat (constant) and thus respects different impact of spectral components on different frequencies. As a starting point, the shape of spectral mask can be inspired by the “allowed CW interference level” from Appendix C in [6] for L1 band, similarly for GPS L5 band in [7] and Galileo E5b signal in [8].

Let the power spectral density of the measured signal on the antenna port be denoted as $S_r(f)$ and the spectral mask is denoted as $S_m(f)$. The RIL is defined as

$$RIL = \int_0^{\infty} H(S_r(f) - S_m(f))(S_r(f) - S_m(f)) df$$

where $H(.)$ is a Heaviside step function, i.e. function equals to 1 for positive argument, 0 otherwise.

Meaning of previous equation is shown in Figure 7. Note, the both power spectral densities (spectral mask and measured signal) have to be in linear units, in [W/Hz] (and not in [dBW/Hz]) for the subtraction in the previous equation to be meaningful.

Note the RIL covers only stationary RF sources of interference along the track.

The effective way to determine a RIL is by means of a spectrum analyzer.

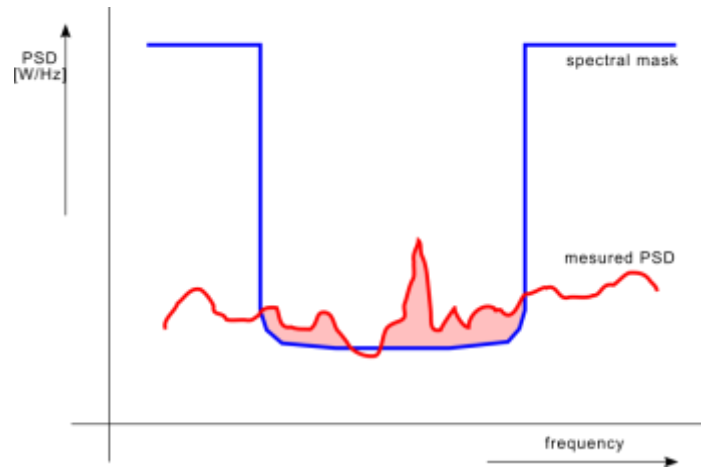


Figure 7: Explanation of RIL

To identify possible sources of RF interferers, an analysis of the signal characteristics from digitized RF data can be used.

3.1.4 Composition and determination of environment characteristics

Regarding SVF, there is only one input for calculation of APV and assignment of ES as it is explained in Section 3.1.1. Contrary, MPL and RIL parameters are results of composition of several outputs of the methods specified in Table 1. Figure 8 illustrates the principle of composition of MPL and RIL parameters from sub-task outputs.

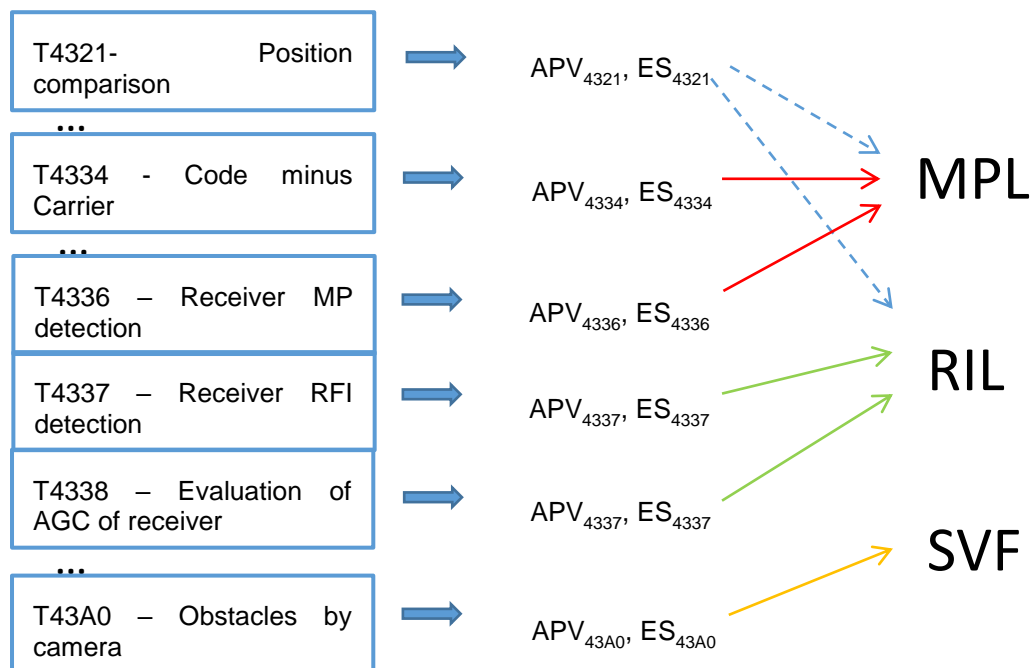


Figure 8: Principle of composition of MPL and RIL parameters

Values of both MPL and RIL parameters are calculated as double weighting sum of ES values from different tasks (methods) specified in Table 1, averaged by a number of tasks (methods) where ES output is available

$$MPL(t) = \frac{w1_{4331} \cdot w2_{4331} \cdot ES_{4331}(t) + w1_{4332} \cdot w2_{4332} \cdot ES_{4332}(t) + \dots + w1_{43xy} \cdot w2_{43xy} \cdot ES_{43xy}(t)}{n(t)}$$

$$RIL(t) = \frac{w1_{4333} \cdot w2_{4333} \cdot ES_{4333}(t) + w1_{4337} \cdot w2_{4337} \cdot ES_{4337}(t) + \dots + w1_{43wz} \cdot w2_{43wz} \cdot ES_{43wz}(t)}{n(t)}$$

where

xy is a part of the index for the methods employed for multipath detection and evaluation,

wz is a part of the index for the methods employed for RF interference detection and evaluation,

w1 is weight assigned to each method according its efficiency,

w2 is weight assigned to the ES value of individual method to strengthen its critical values of ES.

This approach allows setting any gain/attenuation of ES taking into account the different efficiency (weights $w1$) of the respective methods. ES critical values (i.e. when $ES = 2$) of individual methods can be amplified by selecting the appropriate values of $w2$ for these methods.

For this reason ES_w parameter has been introduced

$$ES_w = ES \cdot [ES \cdot (w2 - w1) - (w2 - 2 \cdot w1)] = ES \cdot [(ES - 1) \cdot w2 + (2 - ES) \cdot w1]$$

ES_w achieves following values

$$ES_w = \begin{cases} 0 & \text{if } ES = 0 \\ w1 & \text{if } ES = 1 \\ 2 \cdot w2 & \text{if } ES = 2 \end{cases}$$

E.g. normal weight ($w1 = 1$) can be considered for some method, which will lead to normal behavior of ES_w for ES smaller than its critical value ($ES_w = 0$ for $ES = 0$, $ES_w = 1$ for $ES = 1$). If critical value of ES should be amplified by this method, the weight $w2$ should be set to a value greater than one in that case. If e.g. $w2 = 2$, its $ES_w = 4$ for $ES = 2$, thus the critical value of ES was squared.

In software code of the task 4.3.7.0¹ a parametrization for $w1$ and $w2$ has been introduced

$$dw1 = w2 - w1; \quad dw2 = w2 - 2 \cdot w1$$

and weighted value ES_w of each task is calculated as

¹ Task 4.3.7.0 performs overall analysis based on the outputs of WP4.3 sub-tasks and provides the output values for the railway environment characterization (see Section 4.2).

$$ES_w = ES \cdot (ES \cdot dw1 - dw2)$$

Considering this parametrization, MPL and RIL can be simply expressed as a sum of ES_w values averaged by n , i. e. by a number of tasks (methods), where ES output is available.

$$MPL(t) = \frac{ES_{w_4331}(t) + ES_{w_4332}(t) + \dots + ES_{w_43xy}(t)}{n(t)}$$

$$RIL(t) = \frac{ES_{w_4334}(t) + ES_{w_4336}(t) + \dots + ES_{w_43wz}(t)}{n(t)}$$

4 EVALUATION OF NEGATIVE PHENOMENA AND IMPACT ON GNSS PERFORMANCE

4.1 WP4.3 OUTPUTS OF PREPARATORY SUB-TASKS

WP4.3 produces several outputs. The first of them are outputs of particular sub-tasks solved in WP4.3. These outputs, calculated by the techniques presented in Table 1, form a basis for the evaluation of negative phenomena and an assessment of their impact on GNSS performance. These outputs represent inputs for solution of task Railway environment characterization.

The technical notes (solution descriptions) of all the sub-tasks in sub-task groups 4.3.2, 4.3.3, 4.3.4 and also sub-tasks 4.3.5.0, 4.3.A.0 were prepared and preliminary analyses were carried out to check the correctness of sub-task solution and outputs. The structured descriptions of sub-tasks are compiled into Appendix 1 of this document. All these descriptions include sub-task solution principle, required input data, a format specification of output file, a justification of values of quantization thresholds and results of preliminary analysis (available only for some sub-tasks).

Full versions of descriptions including preliminary results analysis are available on Cooperation Tool.

The full set of results of all the sub-tasks was stored in STARS repository in Google Cloud.

Output data of each sub-task was uploaded in appropriate folder according to the test site, measurement date and given sub-task, in compliance with documents [3], [4].

The WP4.3 Data Inventory (in Excel file format) provides an overview of WP4.3 individual sub-task outputs stored by responsible partners in Google Cloud. This inventory is available in Google Cloud in the project *azd-stars*, the bucket *azd-normal-files* and the folder *data_inventories*.

The software code developed within solution of each sub-task was stored in the project *azd-stars*, the bucket *azd-normal-files* and the folder *sw_tools* in Google Cloud.

Output data rate in these files is mostly 10Hz, 1Hz output data rate has been used in case of panoramic camera, RF measurements and Septentrio receiver in Siemens measurement set.

4.2 RAILWAY ENVIRONMENT CHARACTERIZATION – DATA PROCESSING, OUTPUT SPECIFICATION

Main goals of WP4.3 Task 4.3.7.0 Railway environment characterization are: 1) processing of output data of all the sub-tasks described in Section 4.1 and calculation of the three parameters for railway characterization, 2) analysis and evaluation of these three output parameters.

The outputs of the sub-tasks described in Section 4.1 are processed by a script developed in Matlab. The actual version of the script is *t4370_19.m*. In this version most of WP4.3 sub-tasks is included in processing, but due to insufficient time some sub-tasks, mainly RF interference focused sub-tasks, have not been included. In **Table 2** is presented the list of WP4.3 sub-tasks comprised in calculation and analysis carried out by the current version of the script in frame of Task 4.3.7.0.

Specification of sub-task group	Group (see Section 2.1.2)	Sub-tasks included in the matlab script, version 19 (<i>t4370_19.m</i>)
4.3.2. - Identification of factors disturbing GNSS signal and positioning solution based on comparison in position domain	G	4.3.2.1 - 4.3.2.5 (all sub-tasks included)

4.3.3 - Data analysis and identification of factors disturbing GNSS signal and positioning solution based on raw data or specific features of receivers	G, M, V, I	4.3.3.1 - 4.3.3.8 (all sub-tasks included)
4.3.4 - Identification of factors disturbing GNSS signal and position solution based on analysis of recorded RF I/Q samples	M, I	4.3.4 includes 4 sub-tasks, no subtask included yet
4.3.5 - Evaluation of impact of different constellation on GNSS signal availability	V	4.3.5 includes only 1 sub-task, the subtask is not included yet
4.3.A - Sky visibility assessment based on panoramic figures	V	4.3.A.0 (4.3.A includes only 1 sub-task)

Table 2: List of sub-tasks included in processing and analysis in matlab script version t4370_19.m

The sorting and composition of input data of sub-task 4.3.7.0 are carried out according to GPS time. Four output files are provided by this script as depicted in Table 3.

File suffix	Description of file contents
.CHA	GPS time, XYZ coordinates, APV values of all the sub-tasks quoted in Section 4.1
.CHR	GPS time, XYZ coordinates, ES values of all the sub-tasks quoted in Section 4.1
.CHT	GPS time, XYZ coordinates, MPL, RIL and SVF parameters
.CHE	GPS time, XYZ coordinates, Epsilon_H for tasks in position domain Z4321-Z4324. Epsilon_H is horizontal error from comparison of GNSS estimated position and reference position from ground truth or PPK.

Table 3 Description of output files of Task 4.3.7.0 - Railway environment characterization

Full description of output file formats can be found in [9].

Matlab script is available in STARS repository in Google Cloud, in the project *azd-stars*, the bucket *azd-normal-files*, and the folder *sw_tools*.

The values of MPL, RIL and SVF parameters were calculated for selected cases (specified in next Section 4.3) according equations given in Section 3.1.4 and stored together with figures in STARS repository in Google Cloud, in appropriate project, in the directory representing a day of a measurement and the sub-directory Z4370.

4.3 RAILWAY ENVIRONMENT CHARACTERIZATION – ANALYSIS OF SPECIFIC SCENARIOS

In the origin of the analysis the individual outputs of sub-tasks quoted in Section 4.1 (inputs for sub-task 4.3.7.0) and calculated MPL, RIL and SVF parameters were visually inspected. The poor correlation of these individual outputs contributing MPL or RIL was observed for several reasons. One of them was different approach in threshold setting in each sub-task providing input data for sub-task 4.3.7.0. Second one was initial bugs in some scripts developed in frame of individual sub-tasks.

In the next step the horizontal position error HNSE was employed in the analysis and correlation between HNSE and sub-task outputs was looked for. This approach helped to quickly find bugs in

scripts of the subtasks and also showed the possible way how to analyze output data characterizing railway environment.

The values of horizontal position error HNSE have been calculated from comparison of estimated position calculated by different software tools (Septentrio PP-SDK, RTKLIB, TAS-F SPRING) and reference position obtained from ground truth or PPK. All estimated position data were obtained by only post-processing, EGNOS data from EDAS server was used in EGNOS-based solution.

It should be mentioned that some differences can be seen between the values of HNSE in dependence on different estimated position provided by different software positioning tools. This problem of different horizontal error HNSE has been deeply investigated by AZD and TAS-F and the causes gradually are identified. To obtain similar results from all the software tools, some input parameters had to be unified (e.g. EDAS data, common SBAS satellite etc.) and other input parameters in PP-SDK and RTKLIB had to be modified (DOP maximum value).

Currently some difference can be still observed for different reasons. One of them is limited setting of maximum value of DOP, next one could be internal hidden RAIM in PP-SDK and RTKLIB. Generally, it seems that PP-SDK and RTKLIB are trying to provide to the user a position solution with small position error every time. On the other hand, SPRING takes in position solution even the pseudorange measurements, which are affected by negative local phenomena and thus it is more sensitive for detection of occurrence of these phenomena. For these reason SPRING has been evaluated as most effective tool for analysis and evaluation of MPL, RIL and SVF parameters. But it should be mentioned that SPRING occasionally indicated high values of HNSE without apparent reason in several cases. Complementary information provided by RTKLIB and PPSDK toolsets, also useful for analysis, has enabled the SPRING outputs to be verified

The part of analysis regarding the comparison in position domain, calculation of HNSE by use of different software tools and ground truth error influence is documented in a separate document [10].

Considering the huge amount of measured data, it has been decided to focus on analysis of only several cases representing specific railway environment.

The selected scenarios included in the analysis are listed below:

- Clear sky view (ASTS, Sardinia test track)
- Clear sky view in the station (ASTS, Sardinia test track)
- Odd case in vicinity of a military airport (ASTS, Sardinia test track)
- Forest, normal case (AZD, South Bohemia test track)
- Forest, extreme case (AZD, South Bohemia test track)
- Mountain (SIE, Switzerland test track)
- Acceleration from the station (SIE, Switzerland test track)
- Camera measurement² (AZD, South Bohemia test track)

Some conditions or limitations were introduced and they are valid for the analysis of all the cases:

- Only L1/E1, L5/E5a signals were included in the analysis as they are primarily intended for railway safety applications.

² Note: Camera measurement is not really a scenario. It is a supplement of measurement scenarios, which do not include a camera tool.

- HNSE of multifrequency and multiconstellation solutions was calculated and results uploaded on the cloud. But this solution has not been further analysed. Main focus was paid only to EGNOS solution because EGNOS performance is one of main WP5 objectives.
- The weights w_1 and w_2 for all members (methods) defined in Section 3.1.4 were set as $w_1 = 1$, $w_2 = 2$ for calculation of MPL, RIL in all the cases by the matlab script of version t4370_19.m. Therefore the range of values of MPL and RIL is interval (0; 4) as individual methods provide quantized ES in range 0, 1, 2. Based on these values then influence of local negative phenomena can be considered negligible for MPL, RIL values around 0, middle for MPL, RIL values around 1, strong for MPL, RIL values above 1 and very strong for MPL, RIL values around 4.
- Only outputs of some sub-tasks have been involved in carried out analysis in dependence on their availability in the cloud in time of data processing in frame of task 4.3.7.0 Railway environment characterization. Therefore their number can differ for each test site.
- Raw data only from Septentrio AsteRx4 receiver was included in the analysis since only this receiver was selected into the measurement set common to all three companies responsible for measurement campaign.
- Output rate of HNSE provided by SPRING is 1Hz, output rates of HNSE provided by PP-SDK and RTKLIB is 10Hz (data rate for AZD and ASTS campaigns) or 1 Hz (data rate for SIE campaign).
- MPL was calculated at output rates 1Hz and 10Hz, where 1Hz output is an extraction of 10Hz output. RIL and SVF were calculated 1Hz due to the output rate 1Hz of the source data. The purpose of 1Hz MPL output is better visual comparability with RIL and SVF parameters. The purpose of 10Hz MPL output is that some cases of high value MPL are not shown in 1Hz output.
- SVF was calculated only for AZD data since DMU operating test track in the South Bohemia was equipped by panoramic camera³. Data from the camera are available only for the second half of AZD measurement campaign due to camera malfunction. In presented “camera cases” the set of GNSS signals was reduced to only GPS L1 signal. The reasons are that 1) main intention is to show correlation of the SVF and HNSE data in these cases (sections) and not correlation of the SVF and MPL data, 2) only GPL L1 signal is used in HNSE calculation. On the other hand, figures with DOP parameter are included in these “camera cases” to highlight DOP and SVF_{APV} relationship.
- PVT solution in “camera cases” is provided by composition of PP-SDK and RTKLIB position solutions. Primarily, PP-SDK solution was used if available, otherwise the RTKLIB solution was used⁴.
- Output of C/N_0 analysis (Task 4333) is not available for SIE and ASTS due to the method used in the analysis. This method requires data from measurements in both RHCP and LHCP polarizations. Nevertheless, values of C/N_0 parameter are available from all measurements from all the test sites in the Google Cloud.

Analyses of all the cases are provided in following sections.

³ Since the panoramic camera was not approved for installation on the trains used by ASTS and SIE in the measurement campaign, approved non-panoramic cameras were installed instead. Although the output of non-panoramic cameras does not allow SVF calculation, it has provided valuable information on the characteristics of obstacles along a track and helped to explain causes of higher HNSE values.

⁴ Configuration of PP-SDK and RTKLIB sw tools is available in the Google Cloud (azd-stars project -> azd-normal-files -> config -> 4230)

4.3.1 Case of clear sky view

This case represents optimal conditions for the highest GNSS performance. The analysis is carried out from data obtained from measurement performed on November 7 (2017), at Sardinia test track.

Source file of raw data: SAR_1975_1711071350_49M_10Z.SBF

Source file of reference position data: SAR_4250_1711071359_37M_10Z.RPO

Analysis carried out in GPS Time interval: 1194100344 s – 1194100499 s.

The real situation is depicted in Figure 9. In this figure the spatial points represent ground truth based reference position of a train. To show these points on a track in Google map the reference position data stored in .RPO files has been converted into the gpx file format and the .gpx file has been imported in Google map.



Figure 9: Case of clear sky view (ASTS test track at Sardinia)

In Figure 10, the HNSE of EGNOS-based solution provided by SPRING, PP-SDK and RTKLIB is presented. The reference position is provided by ground truth.

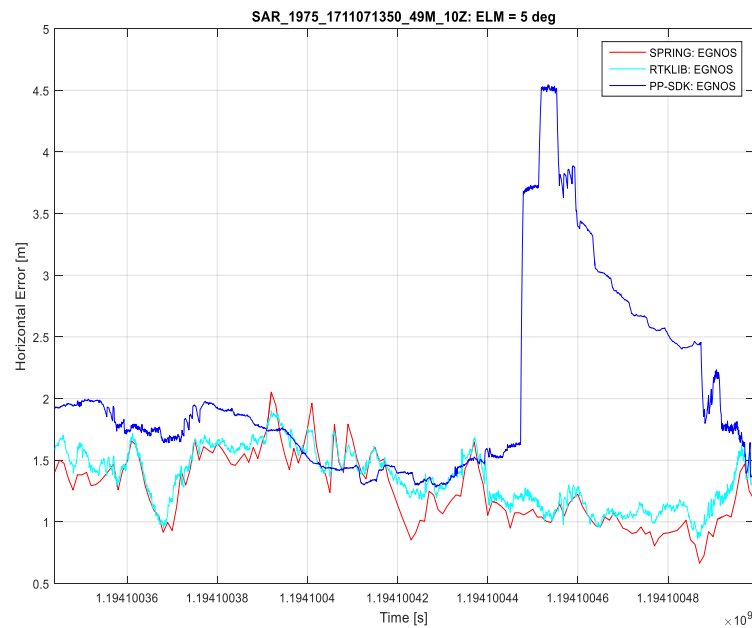


Figure 10: Case of clear sky view - HNSE values

It's evident that HNSE is low as expected under favorable conditions of sky visibility. Significant correlation is obvious between HNSE outputs provided by SPRING and RTKLIB. The difference in HNSE from PP-SDK is due to the use of fewer satellites in the EGNOS-based solution (less by 2 to 3 satellites than for the other SW tools) and the difference is not too large.

The number of satellites is shown in Figure 11.

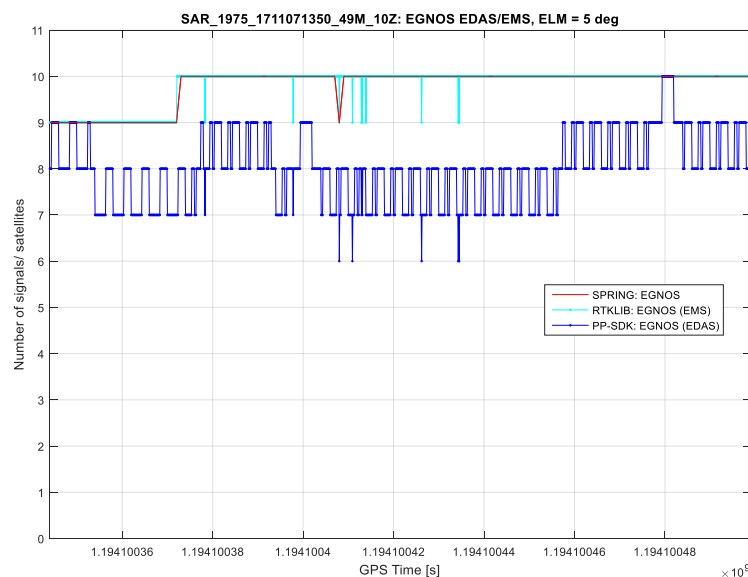


Figure 11: Case of clear sky view - Number of satellites

The train speed profile is presented in Figure 12.

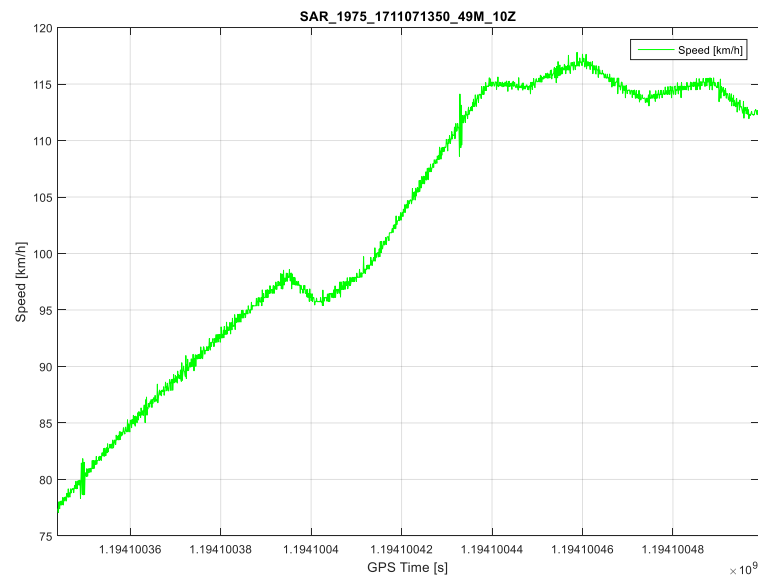


Figure 12: Case of clear sky view – Train speed profile

Set of figures from Figure 13 to Figure 18 shows MPL parameter values in selected time range of this case for signals GPS L1, Galileo E1 and GPS L1+ Galileo E1 and output rates 1Hz and 10Hz.

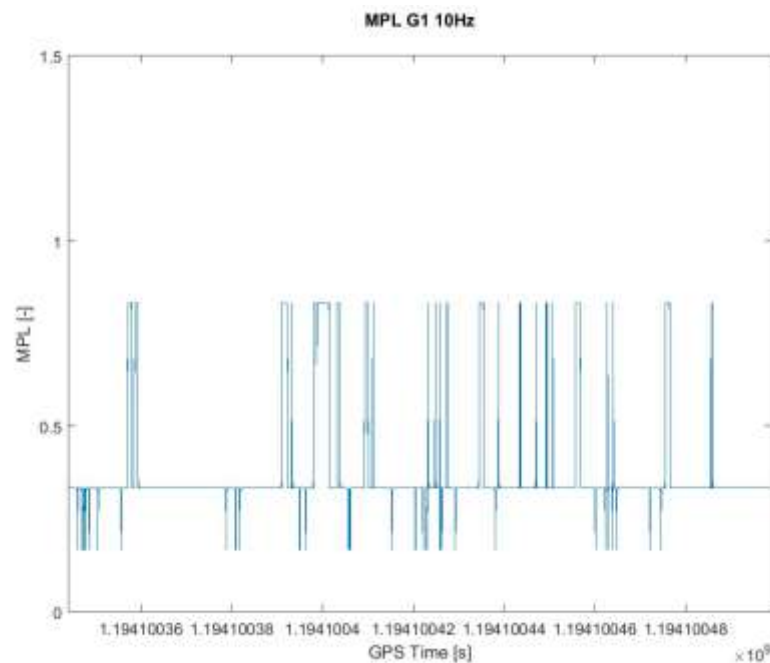


Figure 13: Case of clear sky view – MPL_GPS_L1 (10Hz output rate)

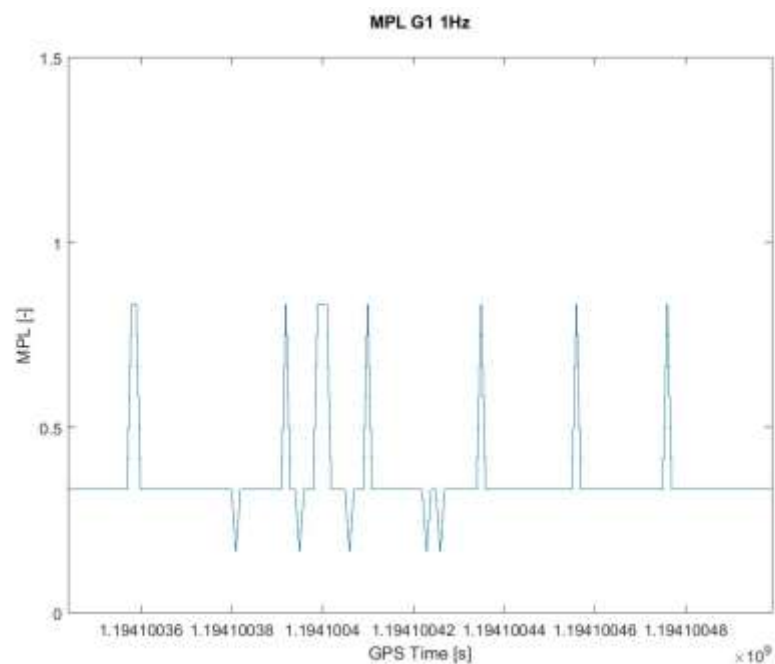


Figure 14: Case of clear sky view – MPL_GPS_L1 (1Hz output rate)

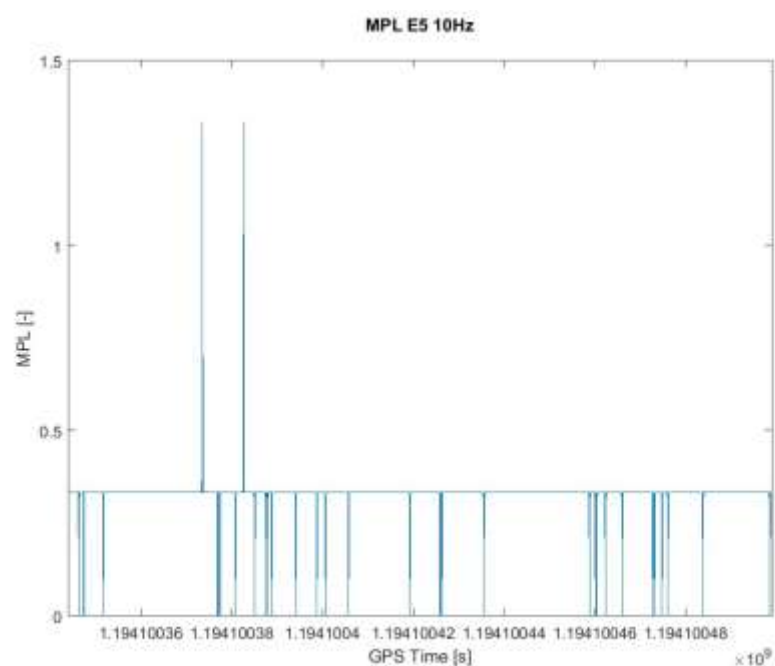


Figure 15: Case of clear sky view – MPL_GAL_E1 (10Hz output rate)

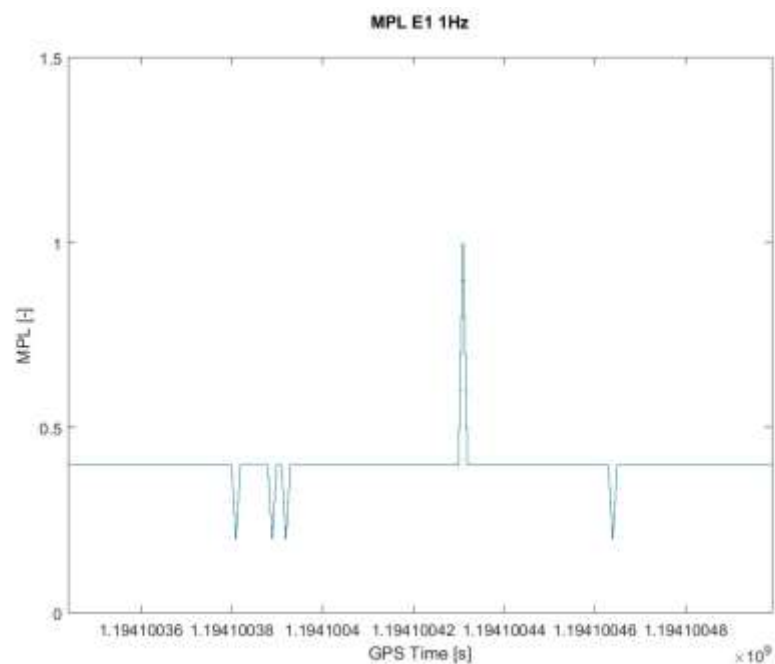


Figure 16: Case of clear sky view – MPL_GAL_E1 (1Hz output rate)

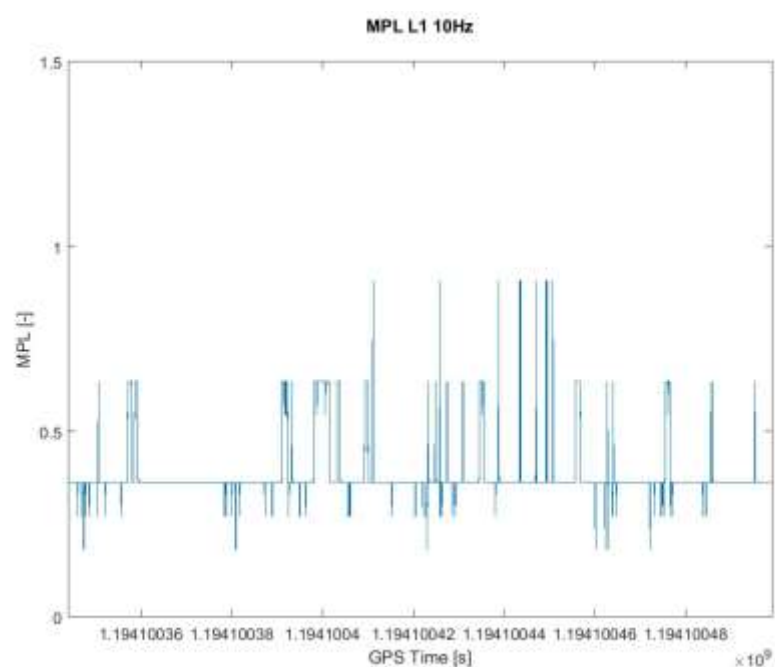


Figure 17: Case of clear sky view – MPL_GPS_L1+GAL_E1 (10Hz output rate)

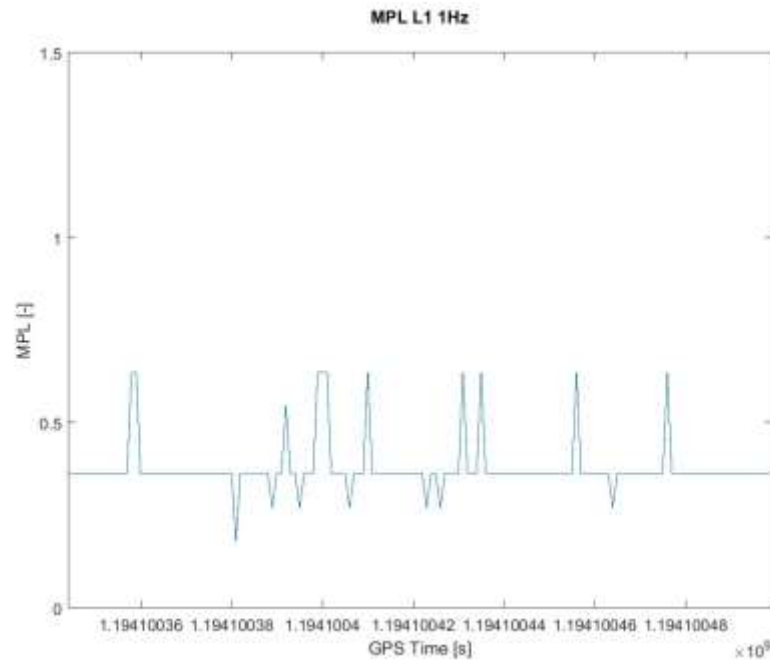


Figure 18: Case of clear sky view – MPL_GPS_L1+GAL_E1 (1Hz output rate)

The curves presented in figures from Figure 13 to Figure 18 show that MPL parameter values are mostly low, implying low multipath for both GPS L1 and Galileo E1 signals, occasionally MPL reaches up to value “1” indicating middle multipath.

The curves presented in Figure 19 and Figure 20 show MPL parameter values calculated for both GPS L5 and Galileo E5 signals (only 10Hz output rates). It seems that these signals are more resistant to multipath effect.

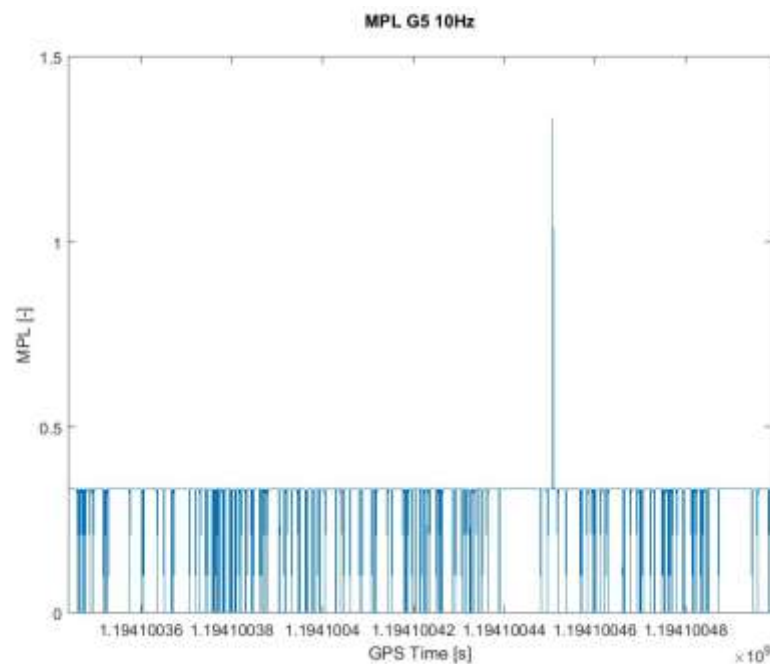


Figure 19: Case of clear sky view – MPL_GPS_L5 (10Hz output rate)

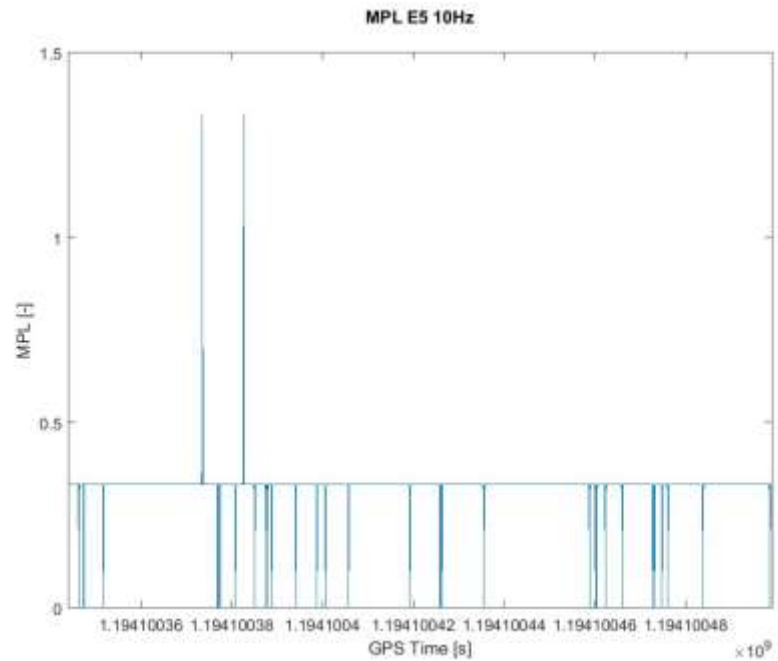


Figure 20: Case of clear sky view – MPL_GAL_E5 (10Hz output rate)

RIL parameter values for L1/E1 and L5/E5 bands are presented in Figure 21 and Figure 22. No interference was detected in selected time interval.

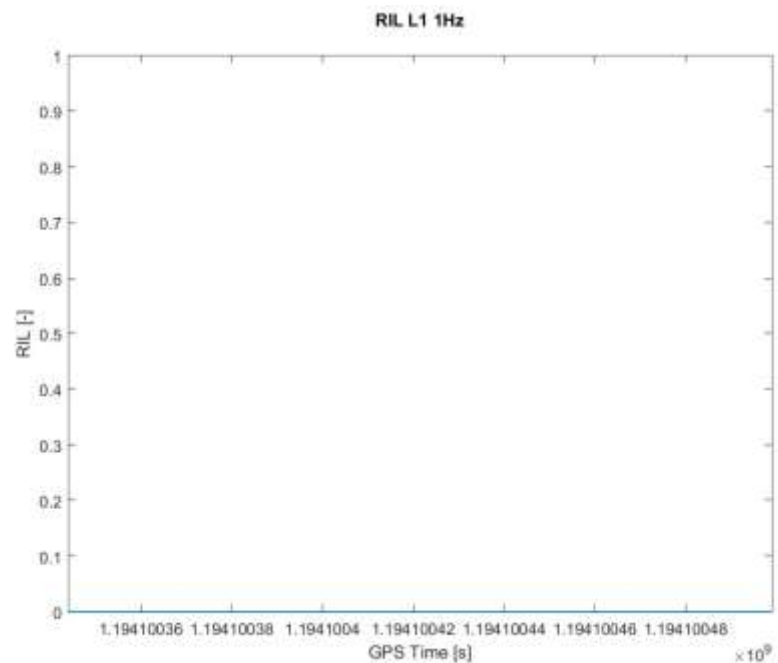


Figure 21: Case of clear sky view – RIL_ L1/E1 (1Hz output rate)

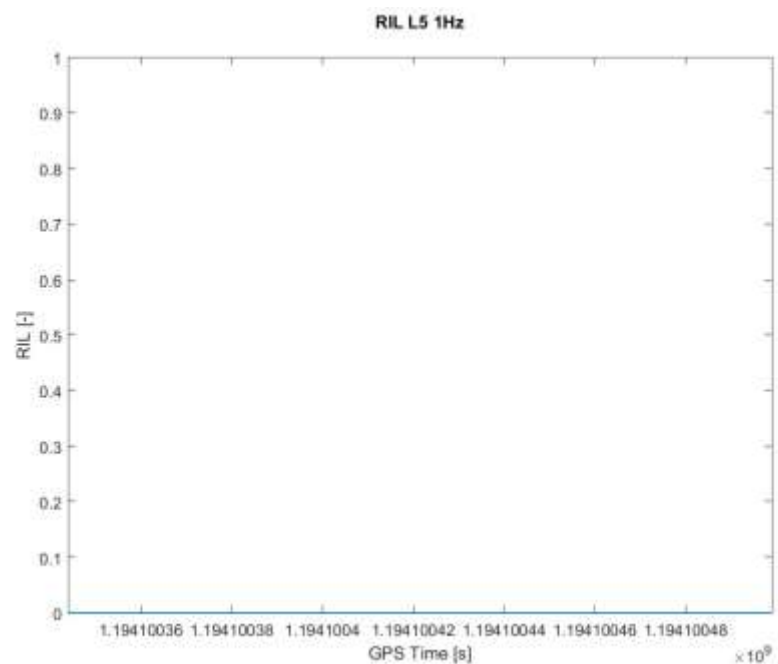


Figure 22: Case of clear sky view – RIL_ L5/E5 (1Hz output rate)

4.3.2 Case of clear sky view in a station

The analysis is carried out from data obtained from measurement performed on November 7 (2017), at Sardinia test track.

Source file of raw data: SAR_1975_1711071350_49M_10Z.SBF

Source file of reference position data: SAR_4250_1711071359_37M_10Z.RPO

Analysis carried out in GPS Time interval: 1194098436 s – 1194098525 s.

The real situation is depicted in Figure 23.



Figure 23: Case of clear sky view in a station (ASTS test track at Sardinia)

In Figure 24, the HNSE of EGNOS-based solution provided by SPRING, PP-SDK and RTKLIB is presented. In comparison to other figures drawing HNSE in this document the Figure 24 uses two references (RPO and PPK). The reason is to emphasize that the RPO errors achieve several metres for this case, which can significantly influence the evaluation of results.

The partial correlation can be seen between all HNSE outputs. In time when SPRING detects higher values of HNSE, the PP-SDK gives HNSE values only under some threshold and RTKLIB doesn't provide any values at all.

PDOP is very good for this case (from 1.6 to 1.8) and PVT was calculated from 8 to 10 satellites in the PP-SDK.

The HNSE from GPS L1 solution was also calculated by RTKLIB for this case [10]. RTKLIB provides GPS L1 solution in the first half of the figure and matches well with the EGNOS-based solution by SPRING. It is also interesting that growth of the HNSE from SPRING appears just before stopping of the train in the station, which shows the impact of the surrounding obstacles of the station. Therefore, RTKLIB may not be able to provide a solution for EGNOS mode due to unfavourable conditions, whereas the PP-SDK was evidently able to suppress them effectively. It seems that higher availability of HNSE derived from PP-SDK is probably achieved by PP-SDK internal hidden filtering based on movement dynamics. The flat course of HNSE presented in Figure 24 very well

corresponds with the standstill of a train. The course of HNSE curves obtained from PP-SDK in all selected cases strengthens this hypothesis. Unfortunately, due to this filtering in PP-SDK, effects of local phenomena can be suppressed.

But in general, it has been often observed that PP-SDK or RTKLIB don't provide position solution under unfavorable conditions while SPRING indicates higher values of HNSE.

Some additional notes on sw tools are given in Section 4.4.8.

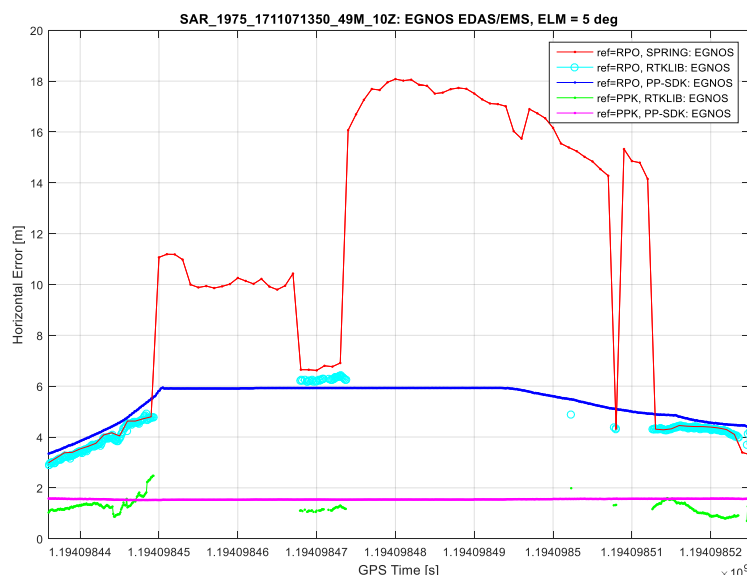


Figure 24: Case of clear sky view in a station - HNSE values

The number of satellites is shown in Figure 25.

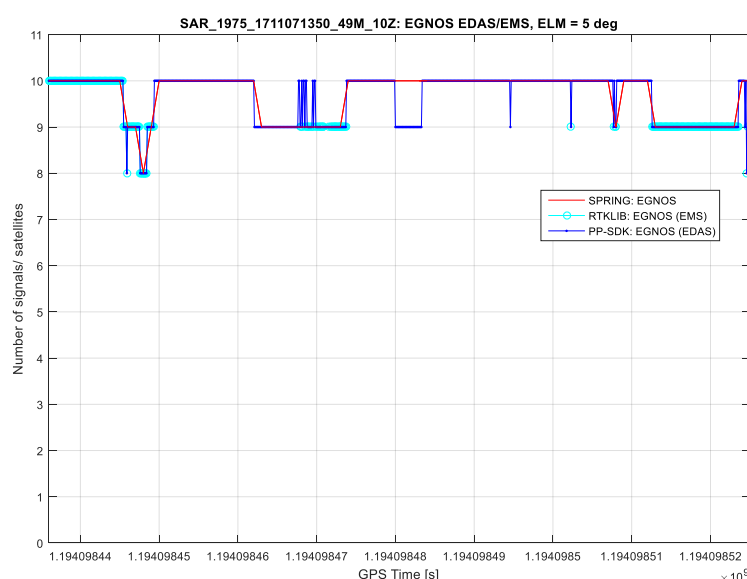


Figure 25: Case of clear sky view in a station - Number of satellites

The train speed profile is presented in Figure 26.

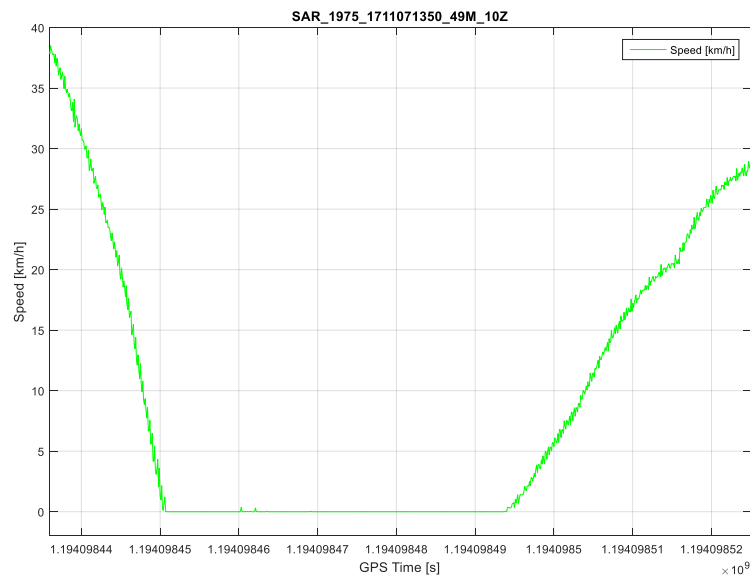


Figure 26: Case of clear sky view in a station – Train speed profile

Set of figures from Figure 27 to Figure 32 shows MPL parameter values in selected time range of this case for signals GPS L1, Galileo E1 and GPS L1+ Galileo E1 and output rates 1Hz and 10Hz.

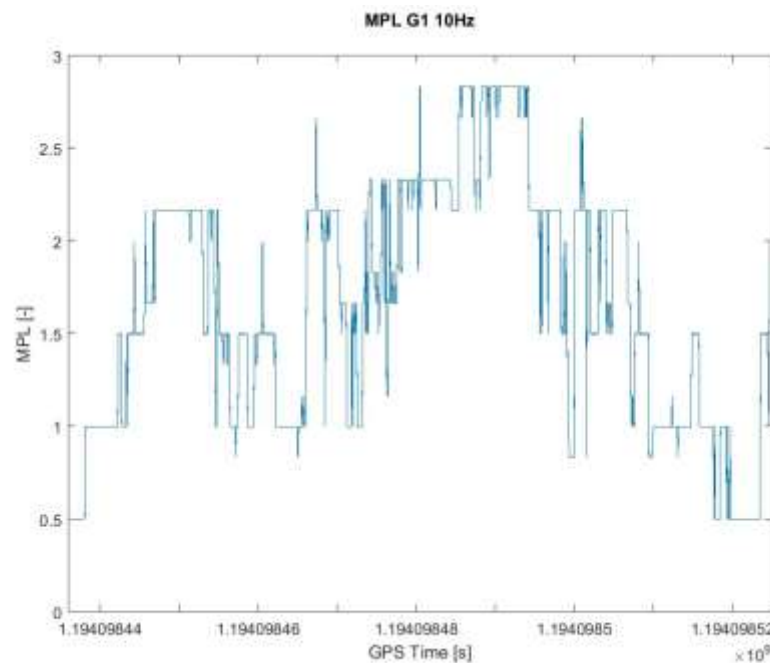


Figure 27: Case of clear sky view in a station – MPL_GPS_L1 (10Hz output rate)

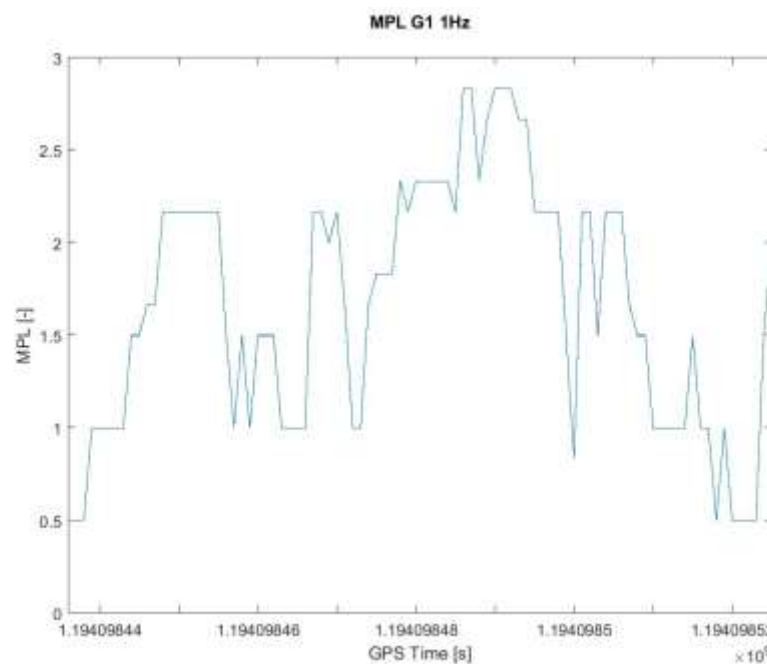


Figure 28: Case of clear sky view in a station – MPL_GPS_L1 (1Hz output rate)

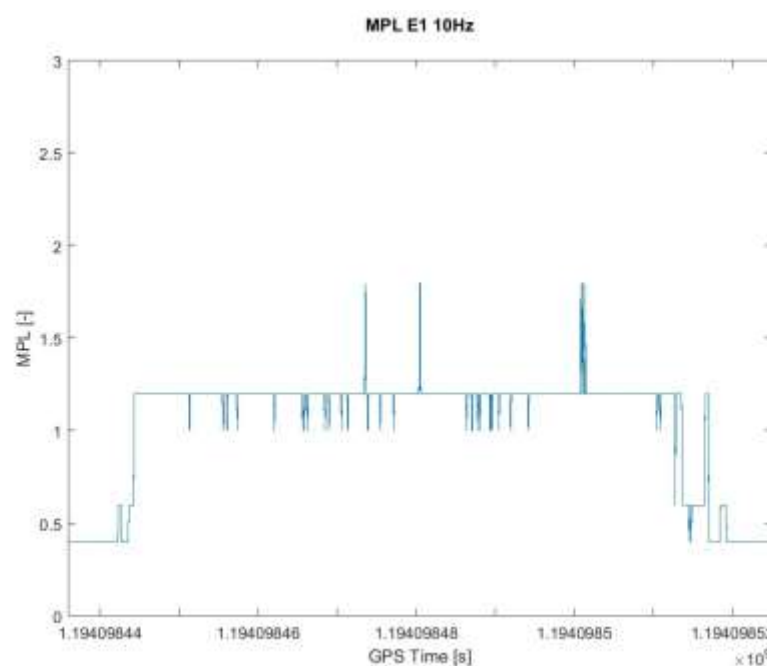


Figure 29: Case of clear sky view in a station – MPL_GAL_E1 (10Hz output rate)

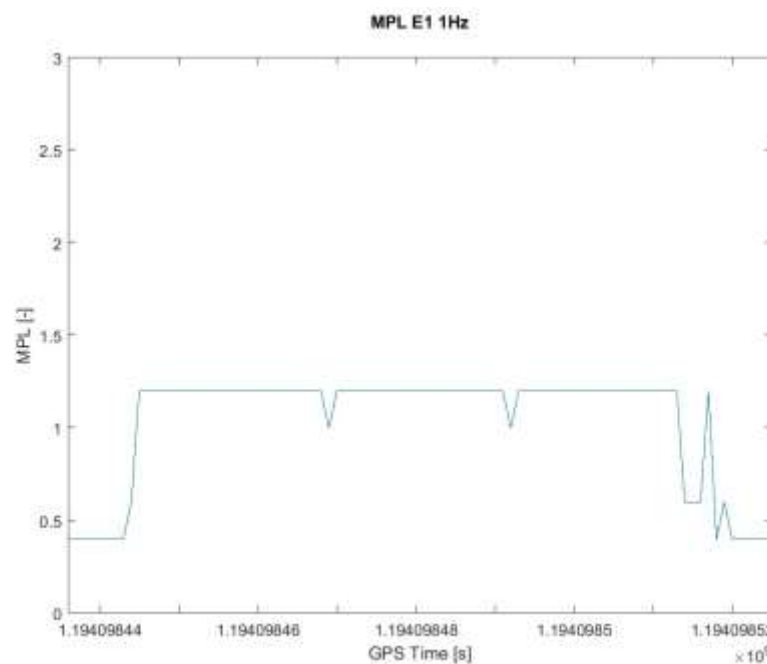


Figure 30: Case of clear sky view in a station – MPL_GAL_E1 (1Hz output rate)

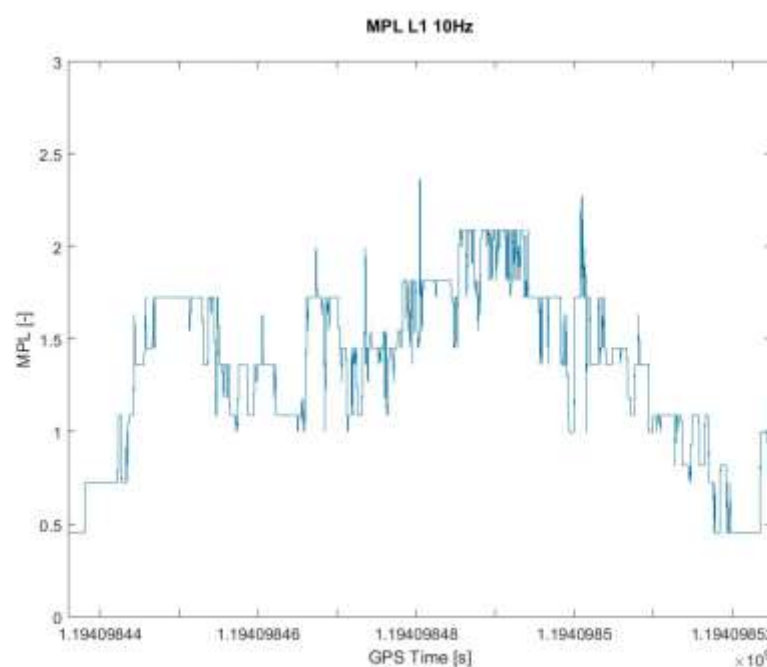


Figure 31: Case of clear sky view in a station – MPL_GPS_L1+GAL_E1 (10Hz output rate)

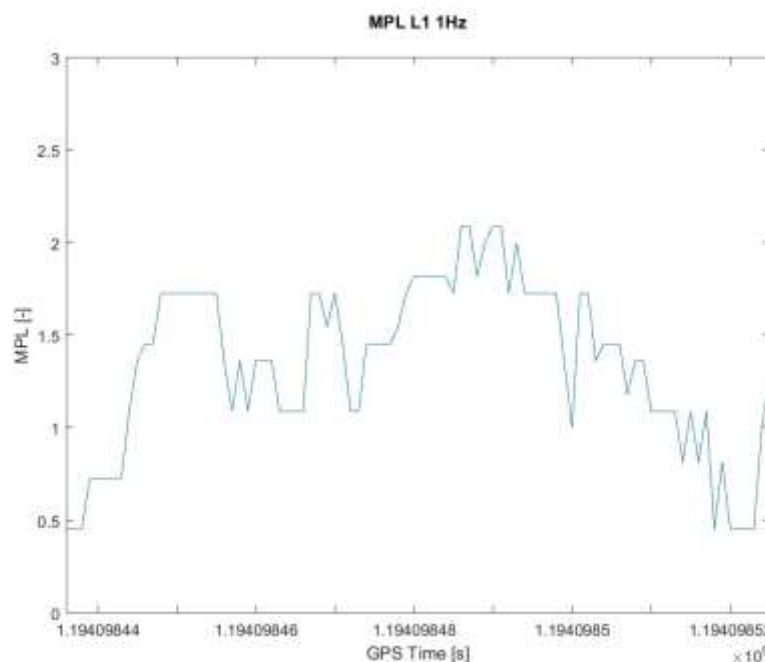


Figure 32: Case of clear sky view in a station – MPL_GPS_L1+GAL_E1 (1Hz output rate)

The curves presented in figures from Figure 27 to Figure 32 show that MPL parameter values increase when the train passes a railway station and indicate the presence of stronger multipath. There is well evident strong correlation between HNSE for EGNOS-based solution calculated by SPRING and MPL calculated for GPS L1 signals. Higher multipath level is also indicated for Galileo E1 signals during train passage through the station. This reinforces that the methods used to detect multipath are a good estimate of the PVT solution confidence since the calculated values of MPL and the results obtained from the SPRING are correlated. Furthermore, even if SPRING is able to provide values where RTKLIB isn't, it seems that this is only the case when GNSS performance could be expected poor due to unfavourable conditions.

The curves presented in Figure 33 and Figure 34 show MPL parameter values calculated for both GPS L5 and Galileo E5 signals (only 10Hz output rates). The MPL for GPS L5 signals presented in Figure 33 indicates higher resistance of these signals to multipath in comparison with Galileo E5 signals and calculated MPL for Galileo E5 signals, depicted in Figure 34.

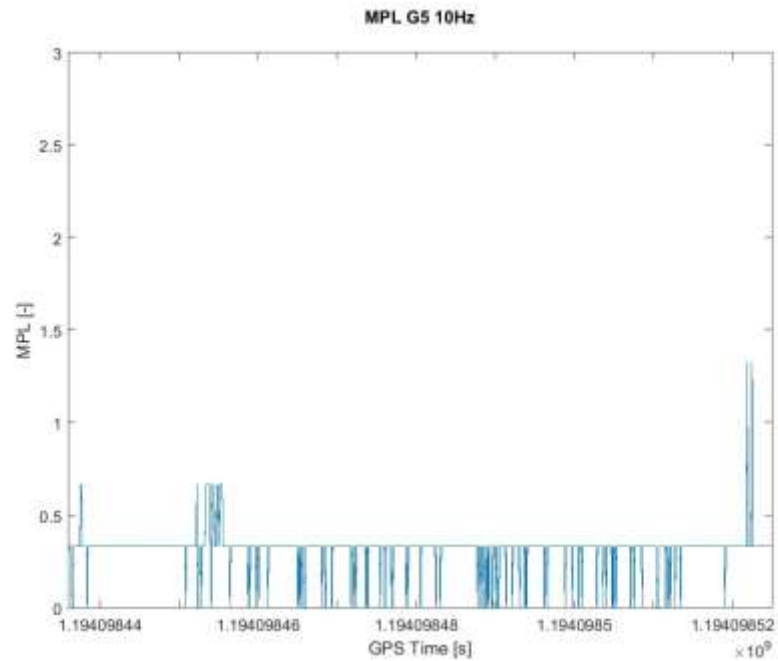


Figure 33: Case of clear sky view in a station – MPL_GPS_L5 (10Hz output rate)

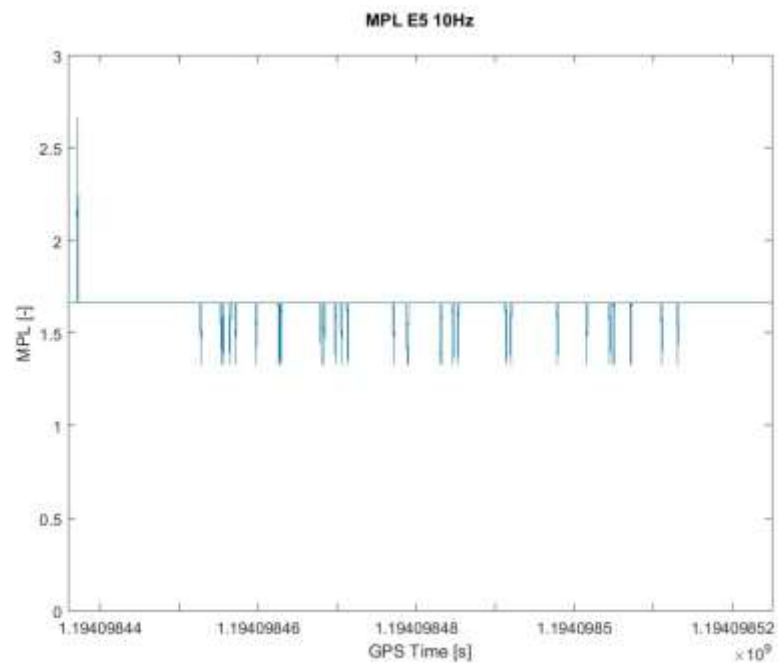


Figure 34: Case of clear sky view in a station – MPL_GAL_E5 (10Hz output rate)

RIL parameter values for L1/E1 and L5/E5 bands are presented in Figure 35 and Figure 36. No interference was detected in the selected time interval.

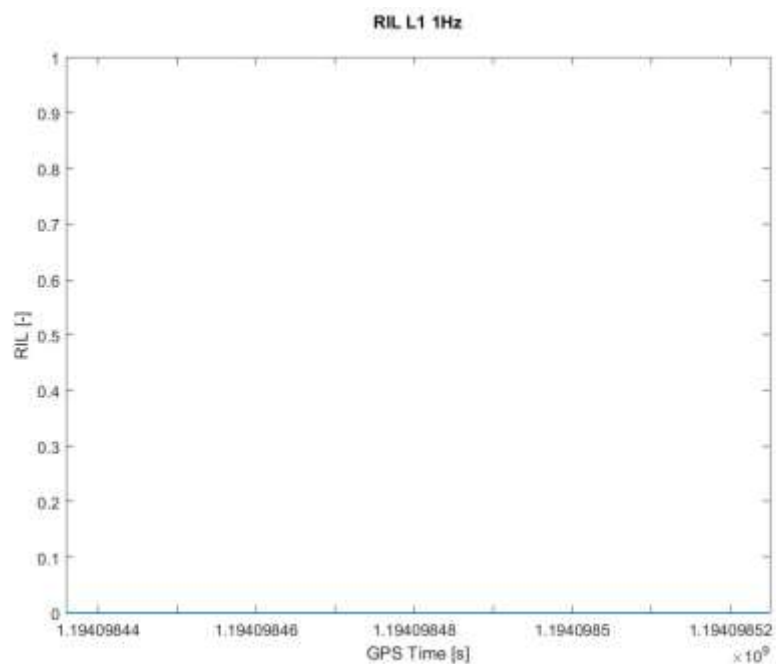


Figure 35: Case of clear sky view in a station – RIL_ L1/E1 (1Hz output rate)

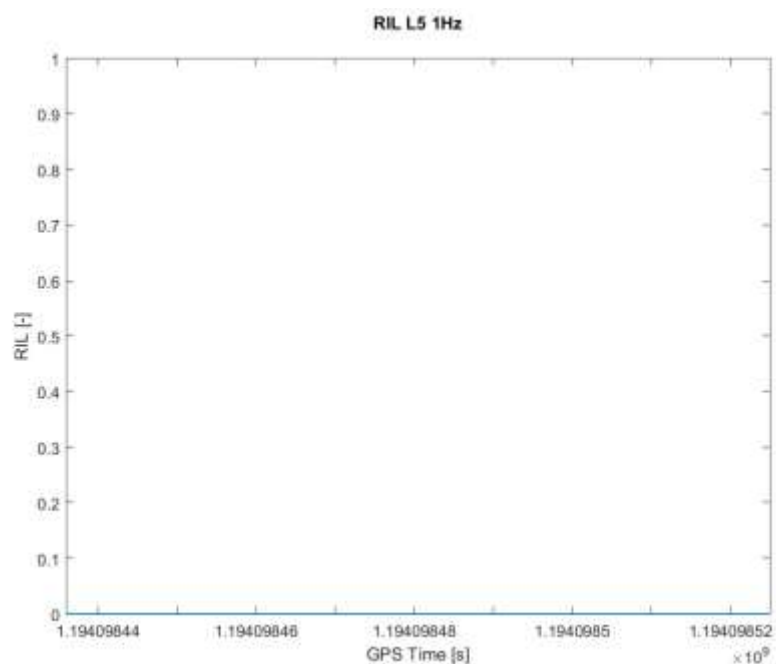


Figure 36: Case of clear sky view in a station – RIL_ L5/E5 (1Hz output rate)

4.3.3 Case of test track in vicinity of a military airport

The analysis is carried out from data obtained from measurement performed on June 13 (2017), at Sardinia test track.

Source file of raw data: SAR_1975_1706131118_01H_10H.SBF

Source file of reference position data: SAR_4250_1706131118_01H_10H.RPO

Analysis carried out in GPS Time interval: 1181382072 s – 1181382145 s.

The real situation is depicted in Figure 37.



Figure 37: Case of test track in vicinity of a military airport (ASTS test track at Sardinia)

In Figure 38, the HNSE of EGNOS-based solution provided by SPRING, PPSDK and RTKLIB is presented. The reference position is provided by ground truth. HNSE by PPSDK and RTKLIB seem to be correlated, any correlation is not apparent between HNSE from SPRING and HNSE from PPSDK and RTKLIB. Some outages of HNSE provided by PP-SDK around the center of observation

interval indicate a problem in position solution caused by limited sky visibility during passage under the bridge.

On the other hand SPRING provided high values of HNSE longer time without an obvious reason (no change in raw data of Septentrio receiver, open sky terrain). The HNSE from other SW tools were determined very small (below 2 m) for the same time period, that is totally different result from SPRING. The same number of satellites was used for PVT calculation as in SPRING tool. Due to these facts this may be a case of incorrect behaviour of SPRING tool.

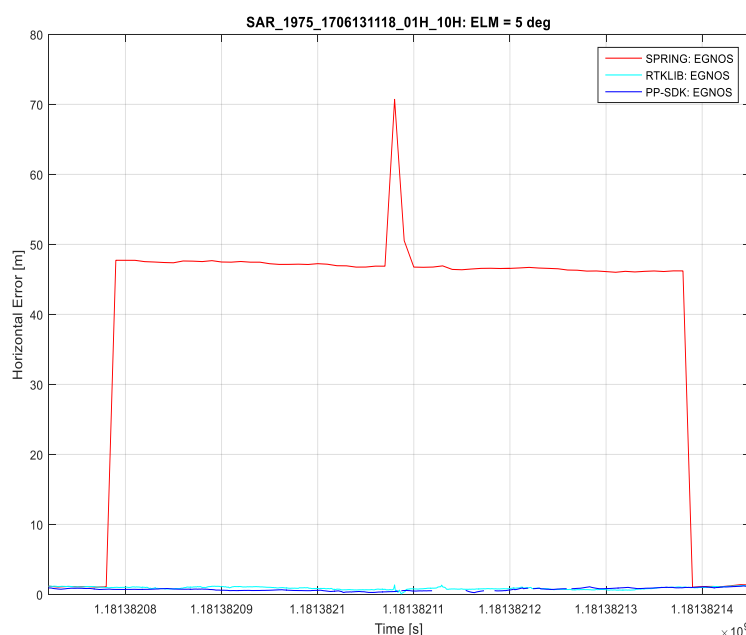


Figure 38: Case of test track in vicinity of military airport – HNSE values

The number of satellites is shown in Figure 39.

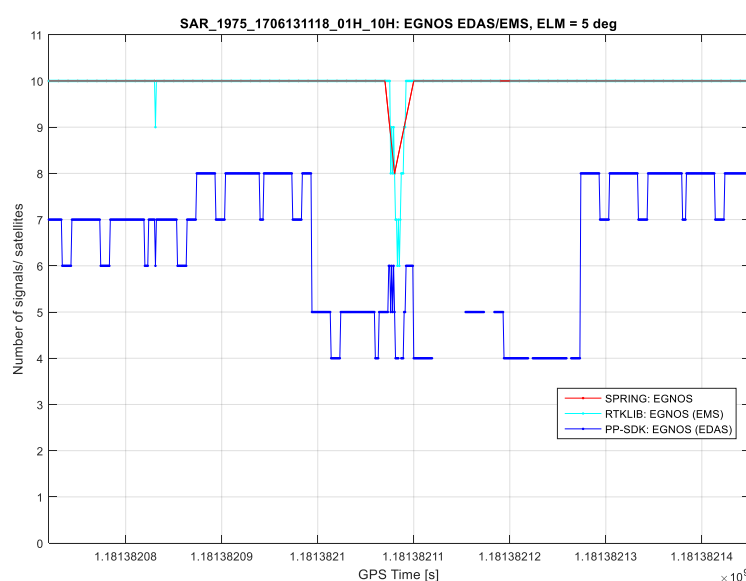


Figure 39: Case of test track in vicinity of military airport – Number of satellites

The train speed profile is presented in Figure 40.

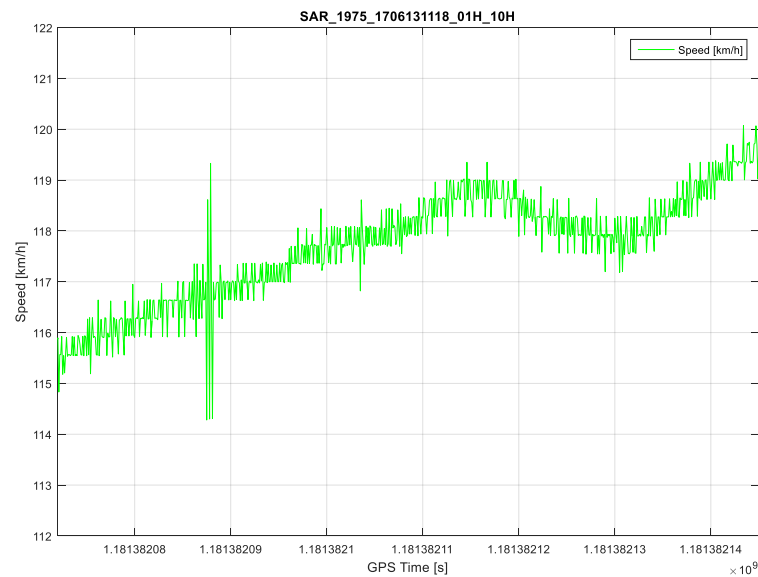


Figure 40: Case of test track in vicinity of military airport – Train speed profile

The set of figures from Figure 41 to Figure 46 shows MPL parameter values in the selected time range of this case for signals GPS L1, Galileo E1 and GPS L1+ Galileo E1 and output rates 1Hz and 10Hz.

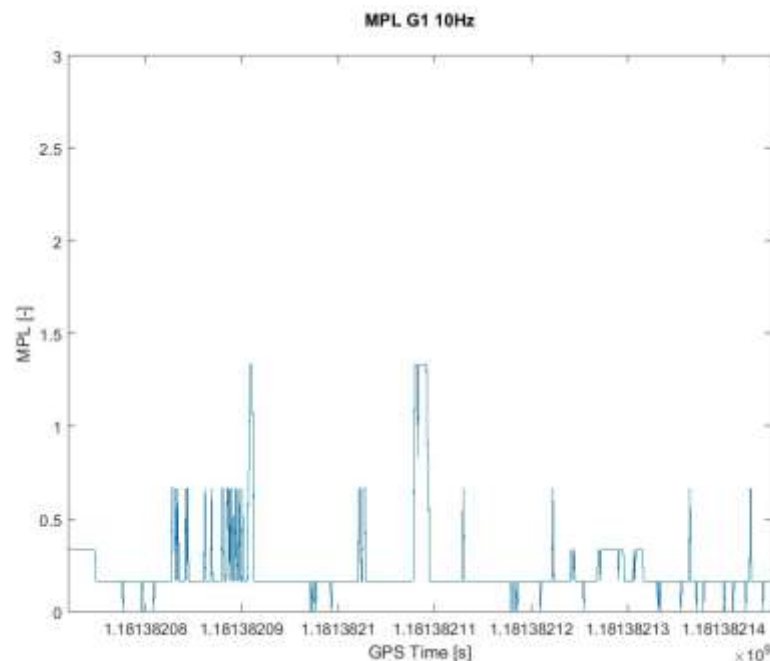


Figure 41: Case of test track in vicinity of military airport – MPL_GPS_L1 (10Hz output rate)

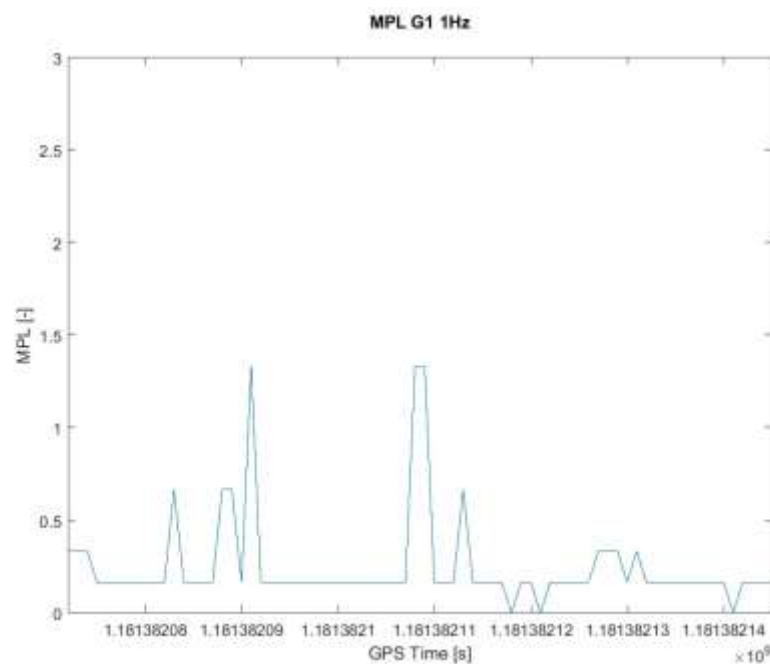


Figure 42: Case of test track in vicinity of military airport – MPL_GPS_L1 (1Hz output rate)

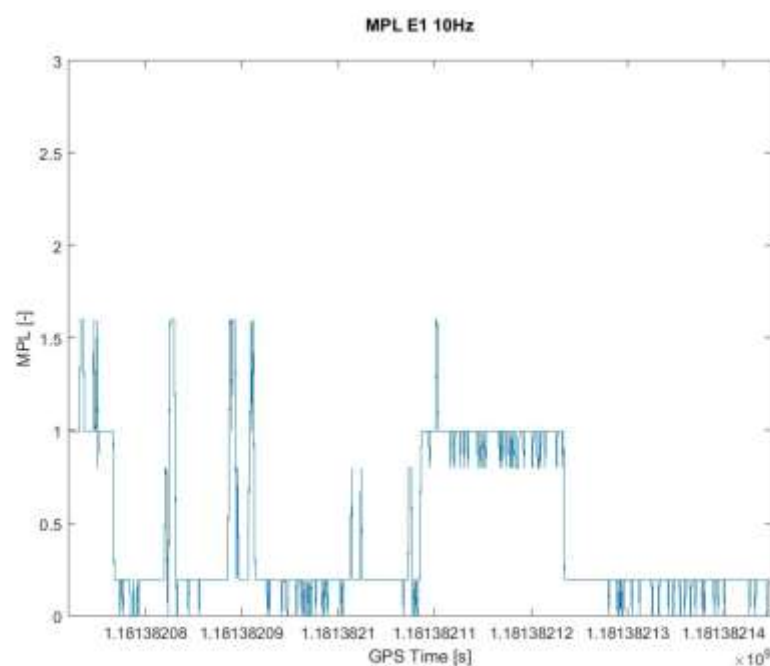


Figure 43: Case of test track in vicinity of military airport – MPL_GAL_E1 (10Hz output rate)

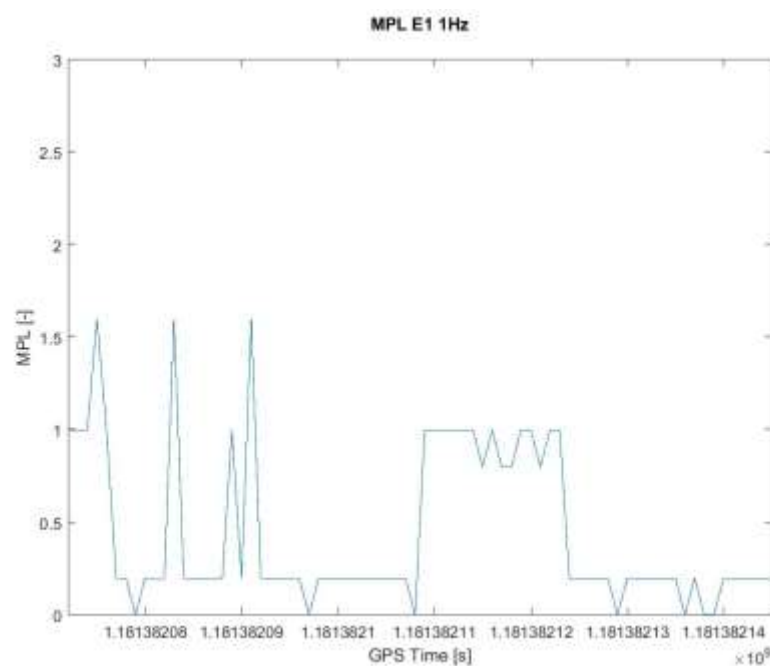


Figure 44: Case of test track in vicinity of military airport – MPL_GAL_E1 (1Hz output rate)

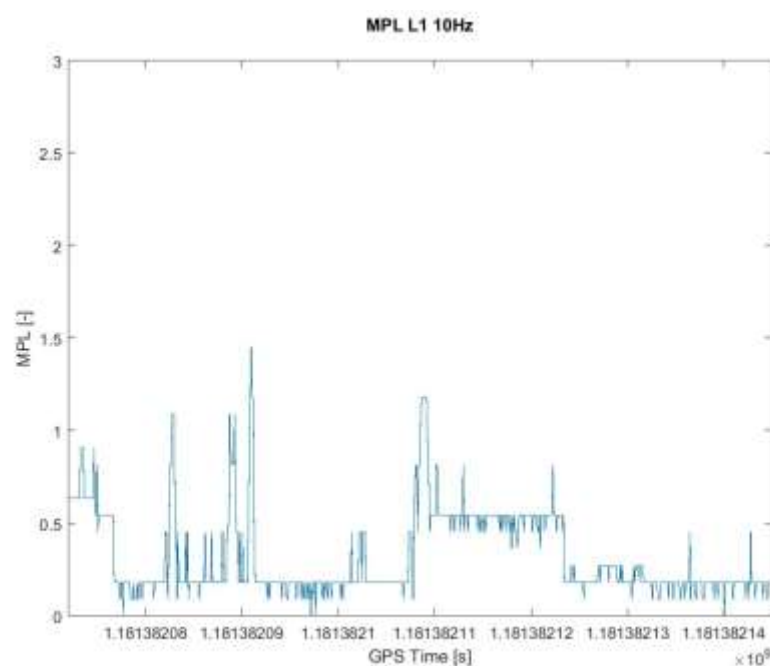


Figure 45: Case of test track in vicinity of military airport – MPL_GPS_L1+GAL_E1 (10Hz output rate)

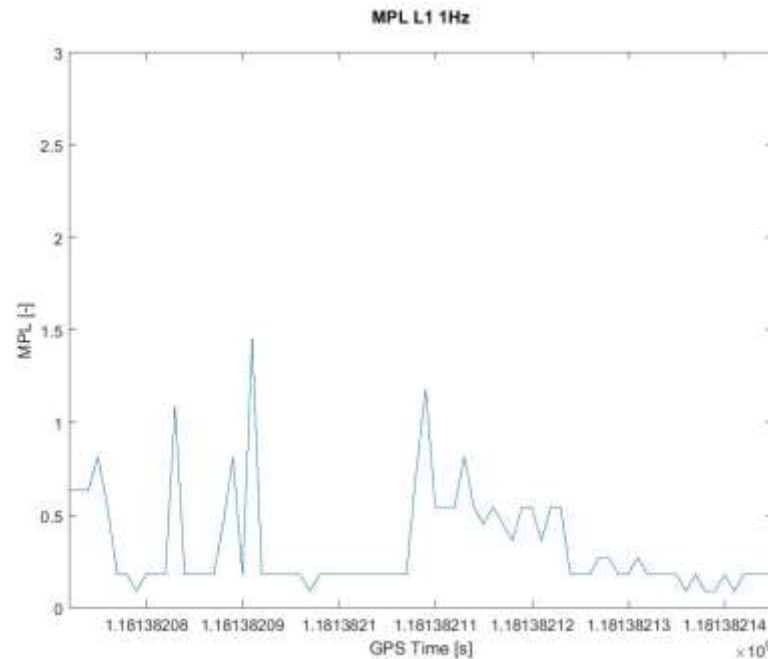


Figure 46: Case of test track in vicinity of military airport – MPL_GPS_L1+GAL_E1 (1Hz output rate)

In Figure 41 to Figure 46 the values of MPL parameter indicate mostly presence of low multipath and middle multipath only in several epochs. MPL peak value in the middle of time interval is correlated for both GNSS signals. Another significant correlation between MPLs in L1 band appears around the time epochs 1181382083 s, 1181382088 s and 1181382092 s.

The curves presented in figures from Figure 47 and Figure 48 show MPL parameter values calculated for both GPS L5 and Galileo E5 signals (only 10Hz output rates). The MPL for GPS L5 signals presented in Figure 47 indicates higher resistance of these signals to multipath in comparison with Galileo E5 signals and calculated MPL for Galileo E5 signals depicted in Figure 48. The highest values of MPL GPS L5 significantly correlate with the highest values of both MPLs of L1 band. Some correlation can also be seen for highest values of MPL GAL E5 and MPL GAL E1 up to time epoch 1181382110 s.

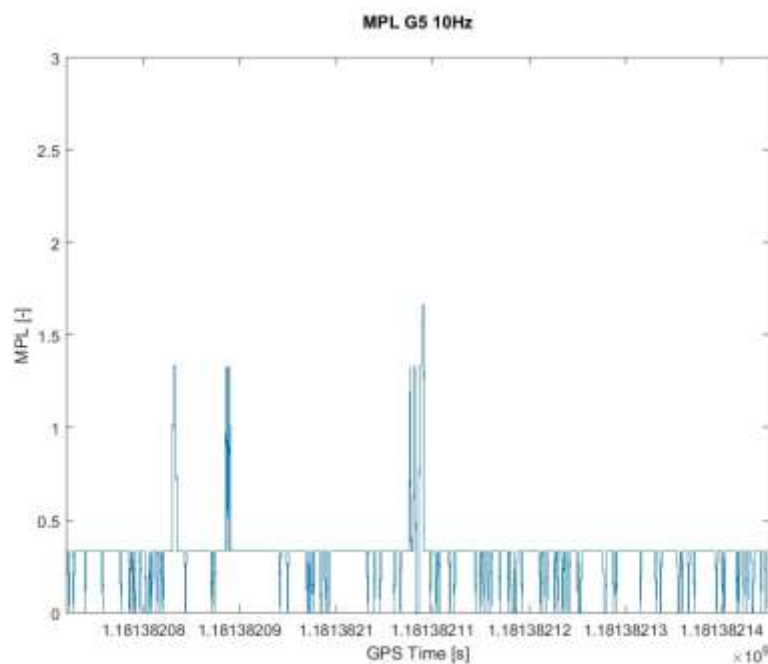


Figure 47: Case of test track in vicinity of military airport – MPL_GPS_L5 (10Hz output rate)

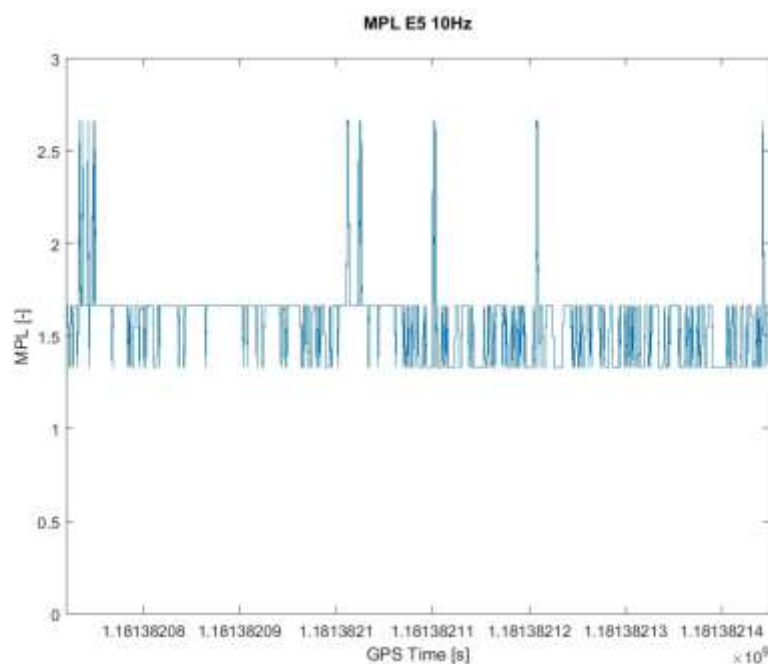


Figure 48: Case of test track in vicinity of military airport – MPL_GAL_E5 (10Hz output rate)

RIL parameter values for L1/E1 and L5/E5 bands are presented in Figure 49 and Figure 50. No interference was detected in selected time interval.

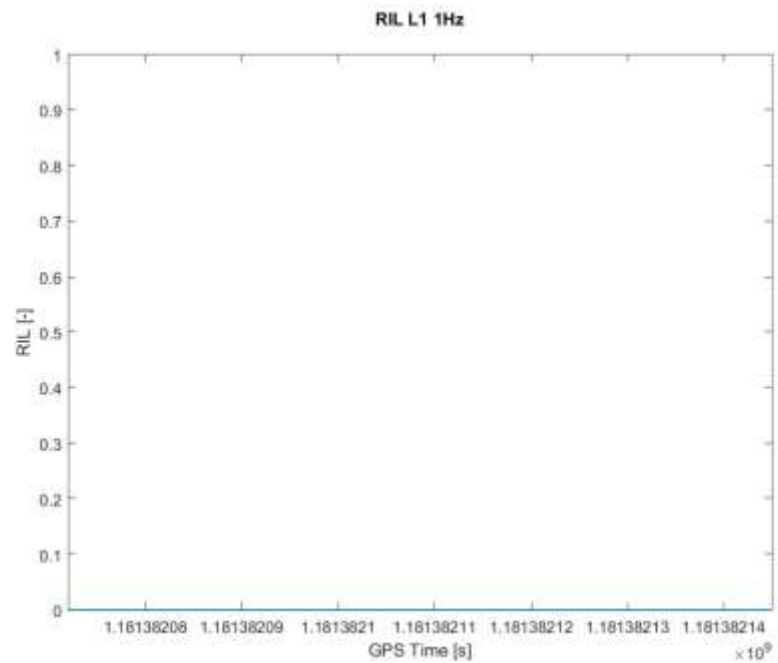


Figure 49: Case of test track in vicinity of military airport – RIL_L1/E1 (1Hz output rate)

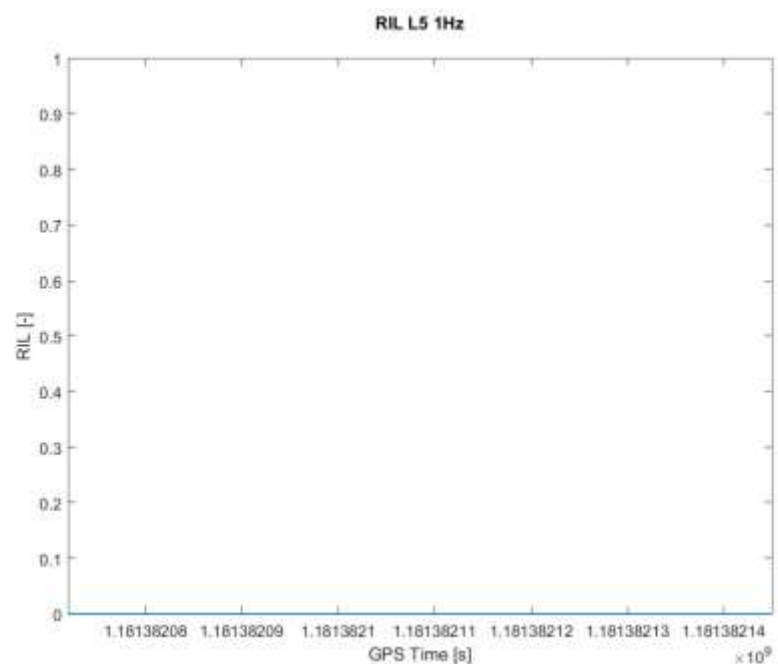


Figure 50: Case of test track in vicinity of military airport – RIL_L5/E5 (1Hz output rate)

The cause of higher values of HNSE is lower sky visibility during short time passage of a train under a road bridge.

4.3.4 Case of test track in mountain range

The analysis is carried out from data obtained from measurement performed on March 25 (2017), at Switzerland test track. This example does not represent only mountain issue but also a tunnel exit and tunnel entering in the middle of the mountains.

Source file of raw data: BAG_0005_1703250653_01H_01S.SBF

Source file of reference position data: BAG_4250_1703250653_01H_10Z.CSV

Analysis carried out in GPS Time interval: 1174460950 s – 1174461046 s.

The real situation is depicted in Figure 51.



Figure 51: Case of test track in mountain range (SIE test track at Switzerland)

In Figure 52, the HNSE of EGNOS position solution provided by SPRING, PP-SDK and RTKLIB is presented. The reference position is provided by ground truth. Strong correlation occurs for outputs provided by SPRING and RTKLIB, PP-SDK doesn't provide solution output when problem is indicated by outputs from SPRING and RTKLIB. Outages in calculation of HNSE are caused by insufficient number of satellites as presented in Figure 52.

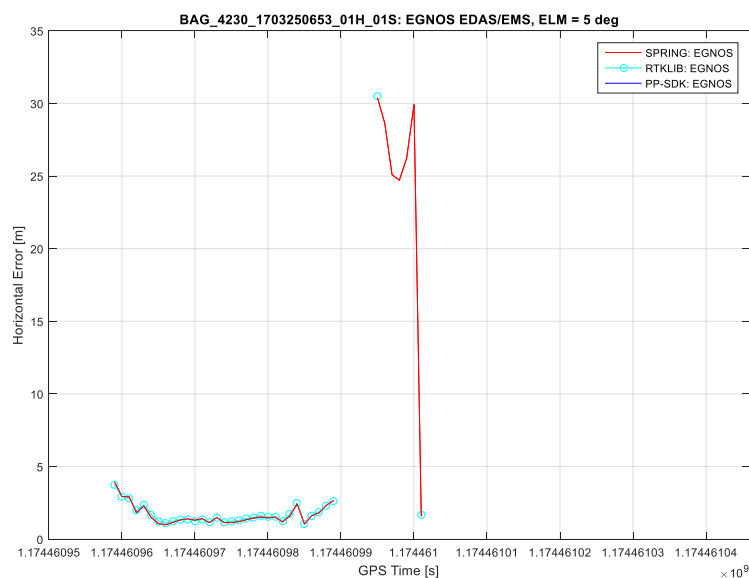


Figure 52: Case of test track in mountain range - HNSE values

The number of satellites is shown in Figure 53.

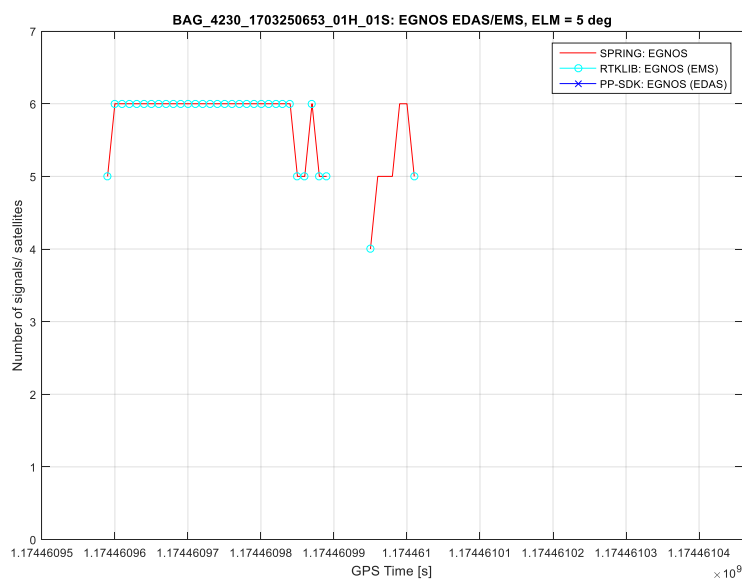


Figure 53: Case of test track in mountain range - number of satellites

The train speed profile is presented in Figure 54.

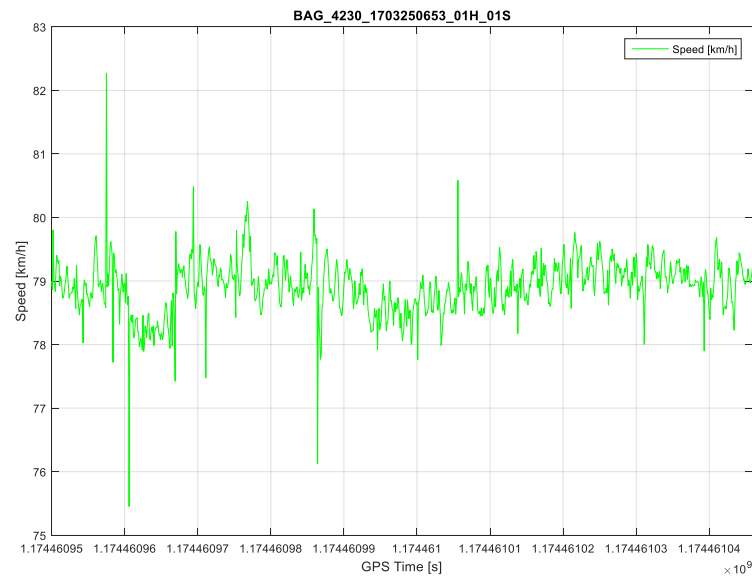


Figure 54: Case of test track in mountain range – Train speed profile

The set of figures from Figure 55 to Figure 57 shows MPL parameter values for signals GPS L1, Galileo E1 and GPS L1+ Galileo E1 and output rate 1Hz in selected time range of this case.

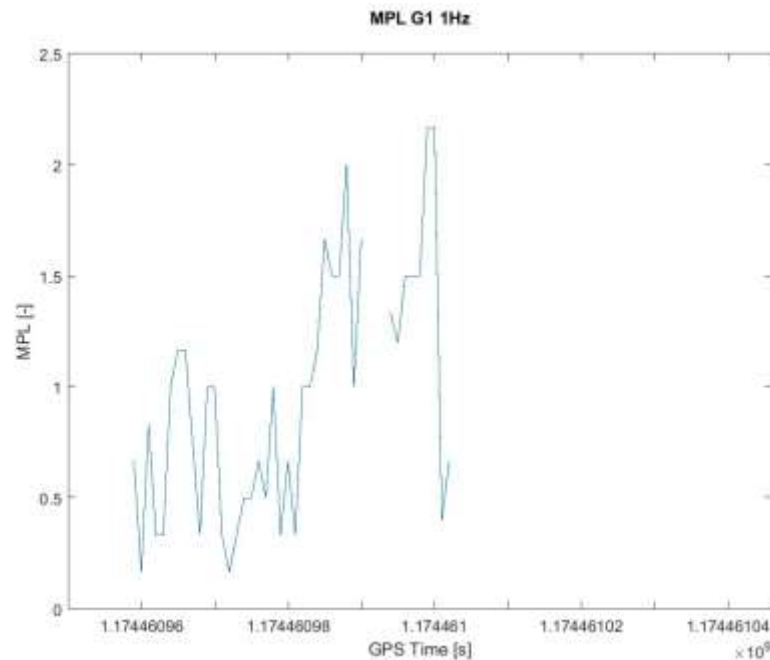


Figure 55: Case of test track in mountain range – MPL_GPS_L1 (1Hz output rate)

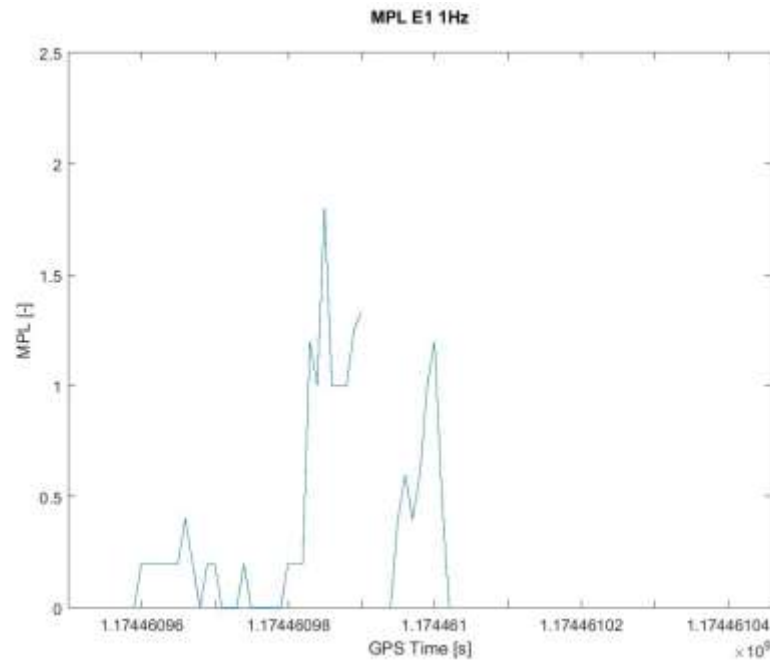


Figure 56: Case of test track in mountain range – MPL_GAL_E1 (1Hz output rate)

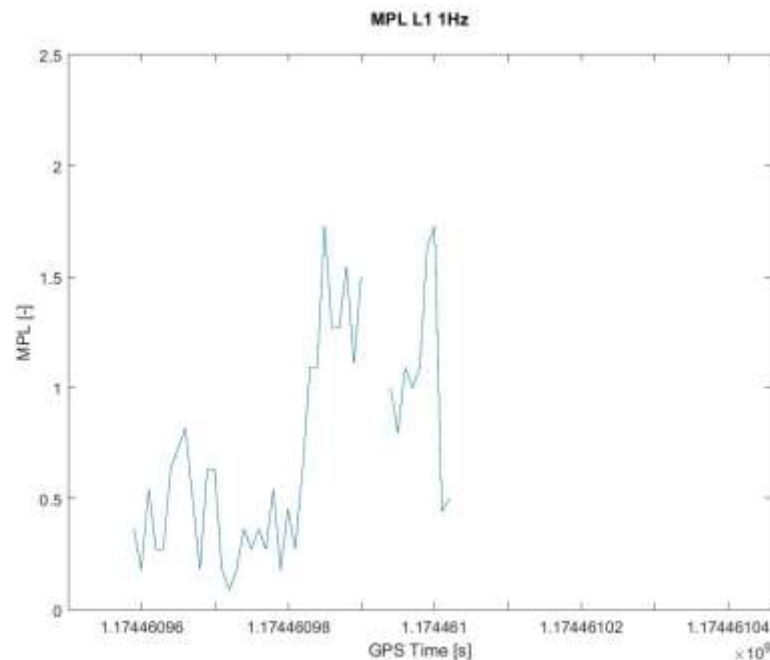


Figure 57: Case of test track in mountain range – MPL_GPS_L1+GAL_E1 (1Hz output rate)

Low, middle and stronger multipath is indicated in whole time interval of this case. Strong correlation is observed for MPL and HNSE values.

The curves presented in Figure 58 and Figure 59 show MPL parameter values calculated for both GPS L5 and Galileo E5 signals (only 1Hz output rates). The calculated values of MPL for GPS L5

signals in Figure 58 and MPL for Galileo E5 signals in Figure 59 exhibit significant correlation of MPL values for GPS L1 and Galileo E1 signals.

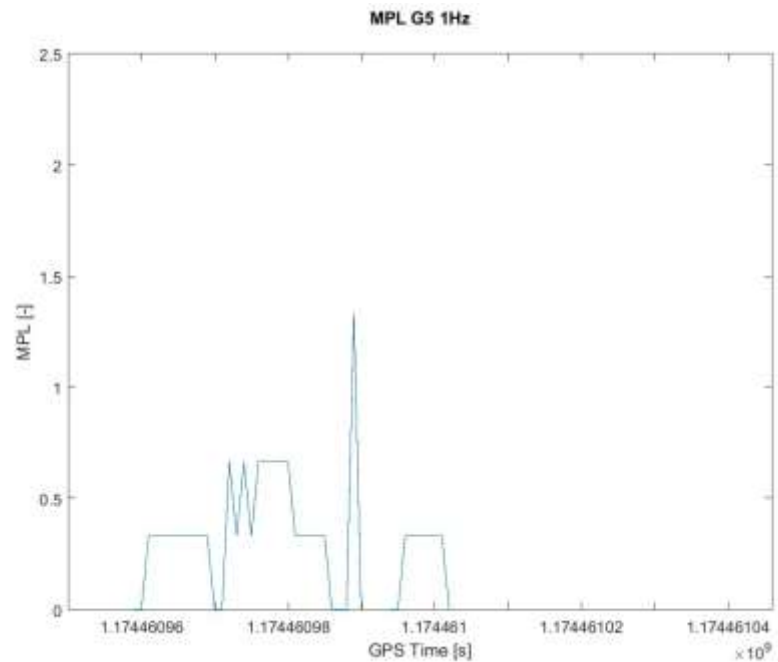


Figure 58: Case of test track in mountain range – MPL_GPS_L5 (1Hz output rate)

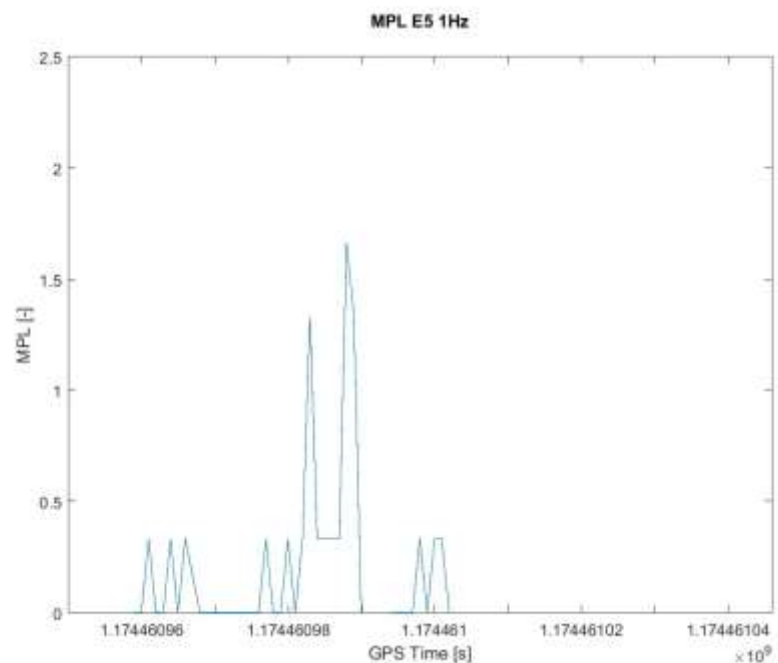


Figure 59: Case of test track in mountain range – MPL_GAL_E5 (1Hz output rate)

RIL parameter values for L1/E1 and L5/E5 bands are presented in Figure 60 and Figure 61. No interference was detected in selected time interval.

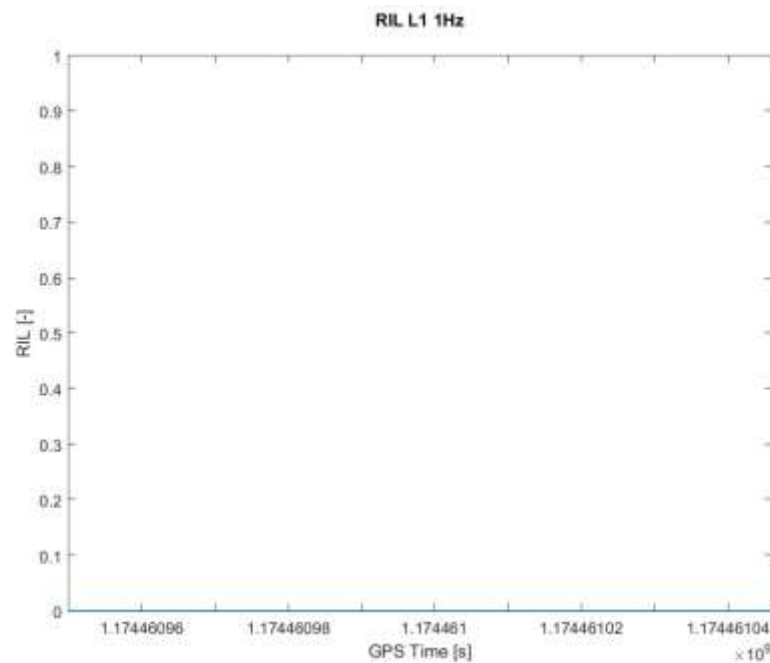


Figure 60: Case of test track in mountain range – RIL_L1/E1 (1Hz output rate)

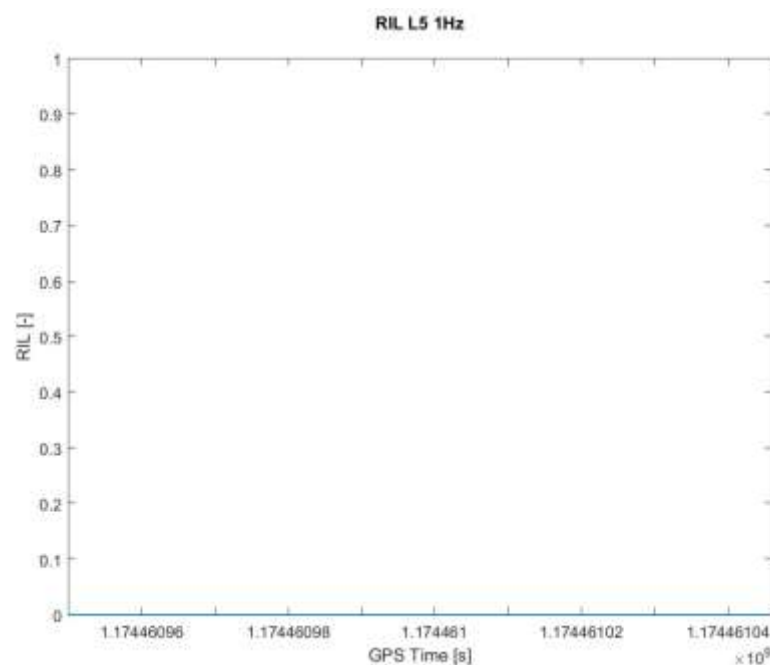


Figure 61: Case of test track in mountain range – RIL_L5/E5 (1Hz output rate)

4.3.5 Case of train acceleration from a station

The analysis is carried out from data obtained from measurement performed on November 2 (2017), at Switzerland test track.

Source file of raw data: GGC_0005_1711021000_11H_01S.SBF

Source file of reference position data: GGC_4250_1711021000_11H_01S.CSV

Analysis carried out in GPS Time interval: 1193655142 s – 1193655342 s.

The real situation is depicted in Figure 62.

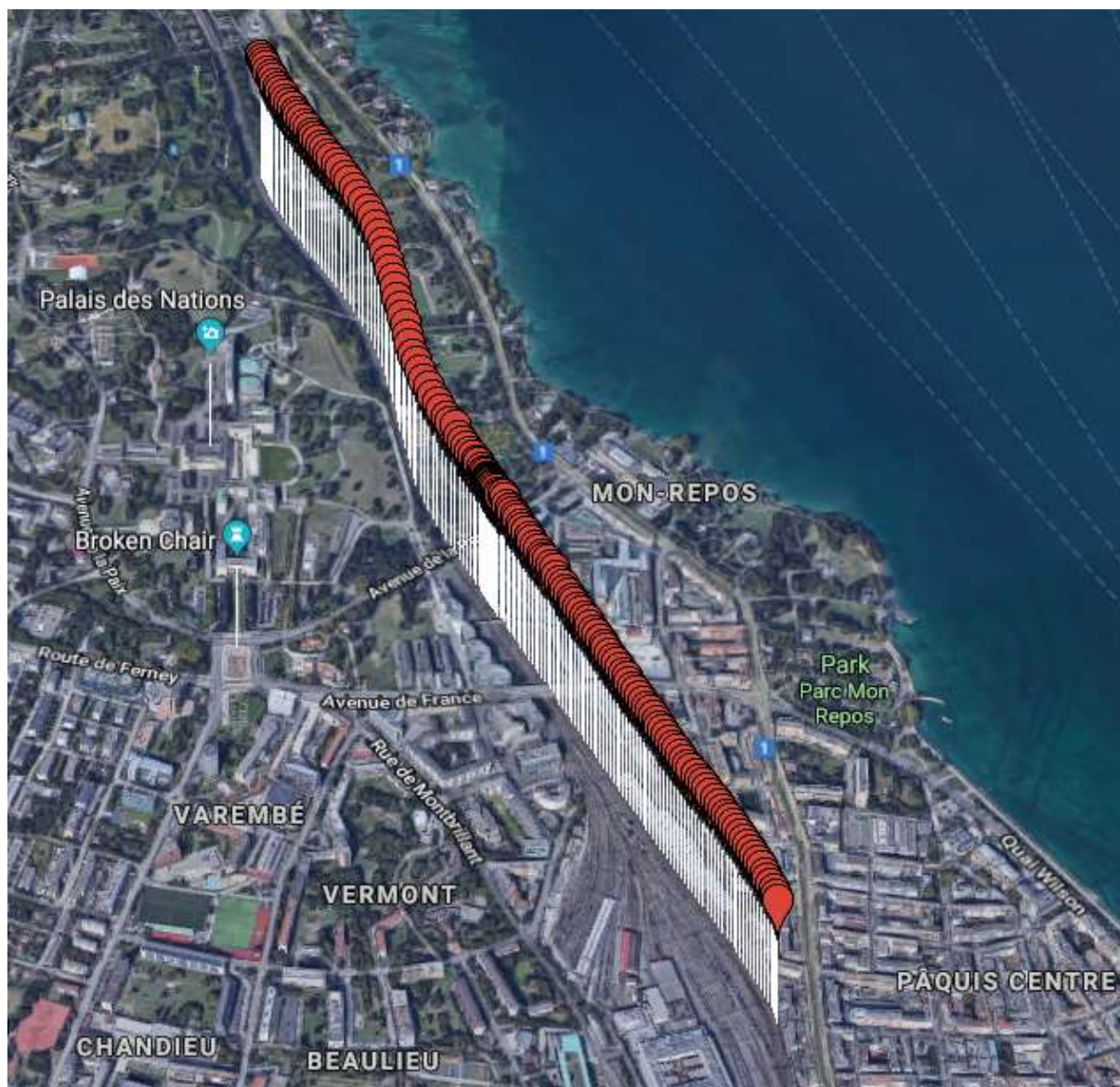


Figure 62: Case of train acceleration from a station (SIE test track at Switzerland)

In Figure 63, the HNSE of EGNOS position solution provided by SPRING, PP-SDK and RTKLIB is presented. The reference position is provided by ground truth. Strong correlation occurs for outputs provided by SPRING and RTKLIB, PP-SDK doesn't provide solution output when problem is indicated by outputs from SPRING and RTKLIB.

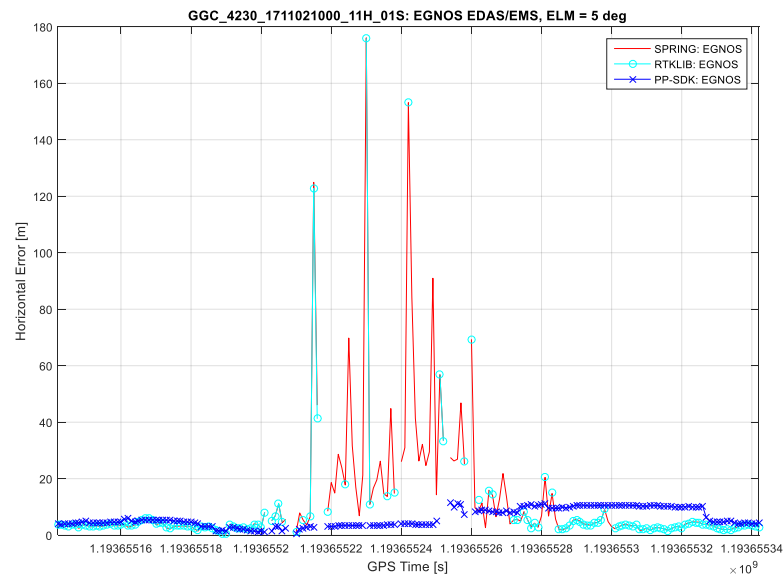


Figure 63: Case of train acceleration from a station – HNSE values

The number of satellites is shown in Figure 64.

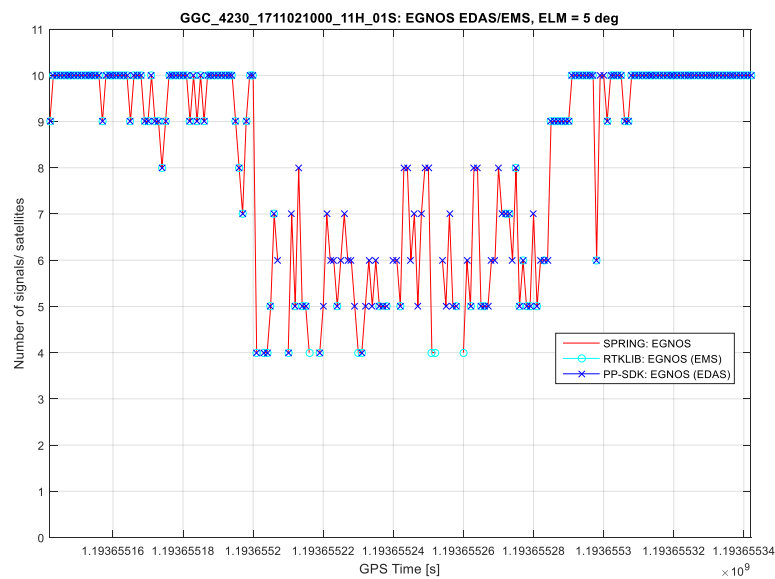


Figure 64: Case of train acceleration from a station – Number of satellites

The train speed profile is presented in Figure 65.

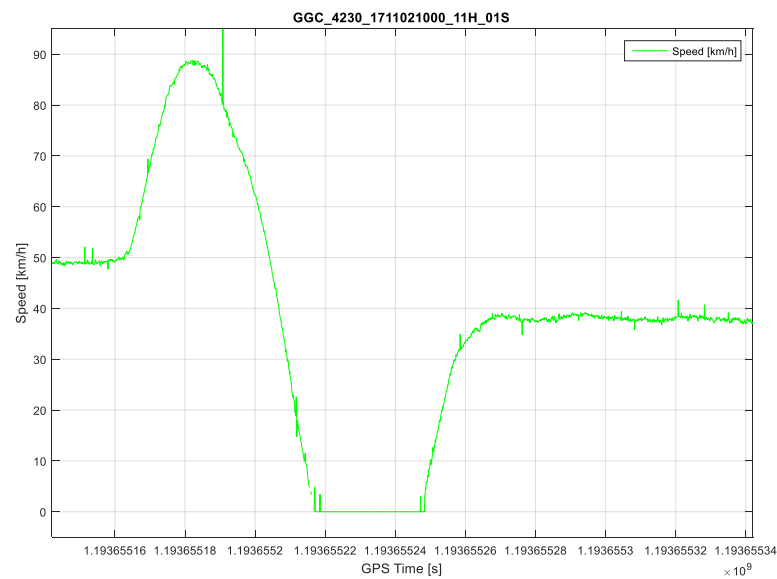


Figure 65: Case of train acceleration from a station – Train speed profile

The set of figures from Figure 66 to Figure 68 shows MPL parameter values for signals GPS L1, Galileo E1 and GPS L1+ Galileo E1 and output rate 1Hz in selected time range of this case.

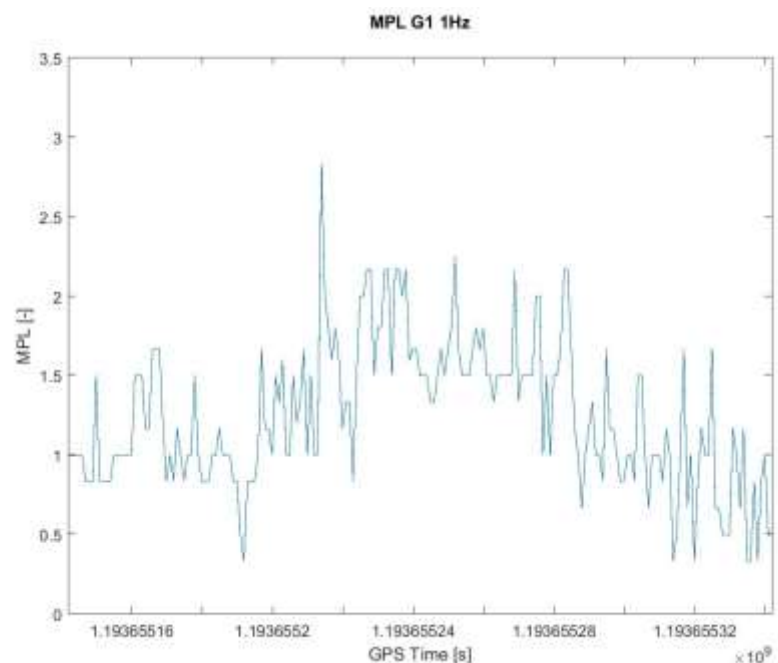


Figure 66: Case of train acceleration from a station – MPL_GPS_L1 (1Hz output rate)

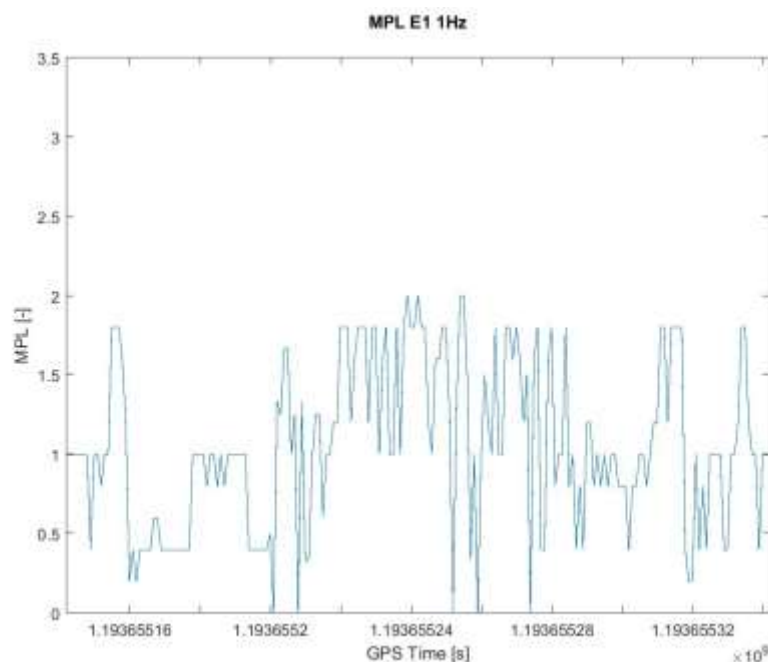


Figure 67: Case of train acceleration from a station – MPL_GAL_E1 (1Hz output rate)

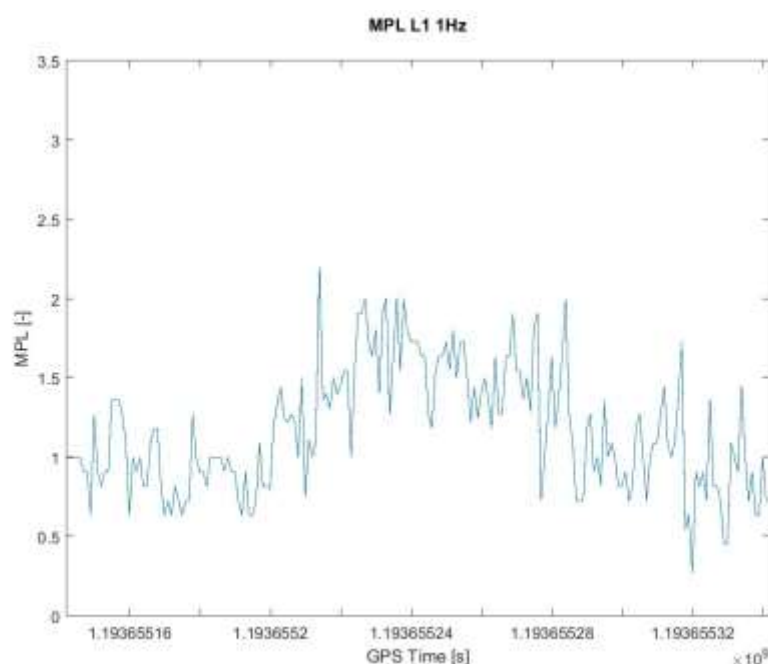


Figure 68: Case of train acceleration from a station – MPL_GPS_L1+GAL_E1 (1Hz output rate)

Middle and stronger multipath is indicated in this case. Stronger correlation is observed for MPL and HNSE values.

The curves presented in Figure 69 and Figure 70 show MPL parameter values calculated for both GPS L5 and Galileo E5 signals (only 1Hz output rates). Calculated values of MPL for GPS L5 signals in Figure 69 exhibit certain correlation with MPL values for GPS L1 signal and also with HNSE values.

MPL values for Galileo E5 signals in Figure 70 exhibit poor correlation with HNSE and indicate lower resistance of this signal to multipath in comparison with GPS L5.

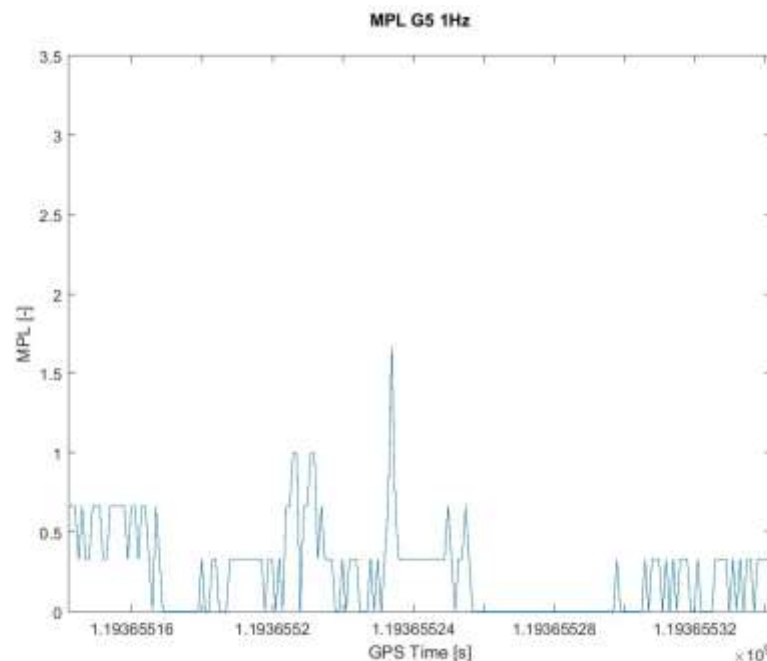


Figure 69: Case of train acceleration from a station – MPL_GPS_L5 (1Hz output rate)

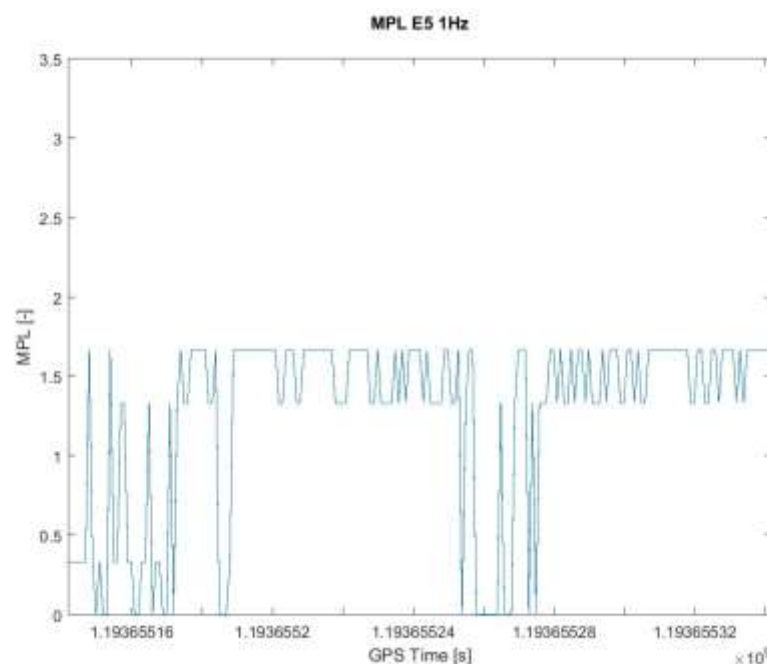


Figure 70: Case of train acceleration from a station – MPL_GAL_E5 (1Hz output rate)

RIL parameter values for L1/E1 and L5/E5 bands are presented in Figure 71 and Figure 72. Stronger RF interference appears when train accelerates from a station. The observed RF interference can significantly contribute to higher values of HNSE as it can cause a loss of lock of some satellites or

an additional noise in pseudorange measurements. The similar cases were already observed in analysis prepared by Siemens [11]. There are presented repeated train runs where HNSE increases during train acceleration from a station and GNSS receiver switches from the SBAS aided mode to the Stand-Alone mode.

But in this selected case high HNSE errors are mainly the result from multipath. There are higher buildings on both sides of the track. Much higher buildings on the opposite side are not visible in Figure 62. Moreover, the train passes under the road bridge before stopping.

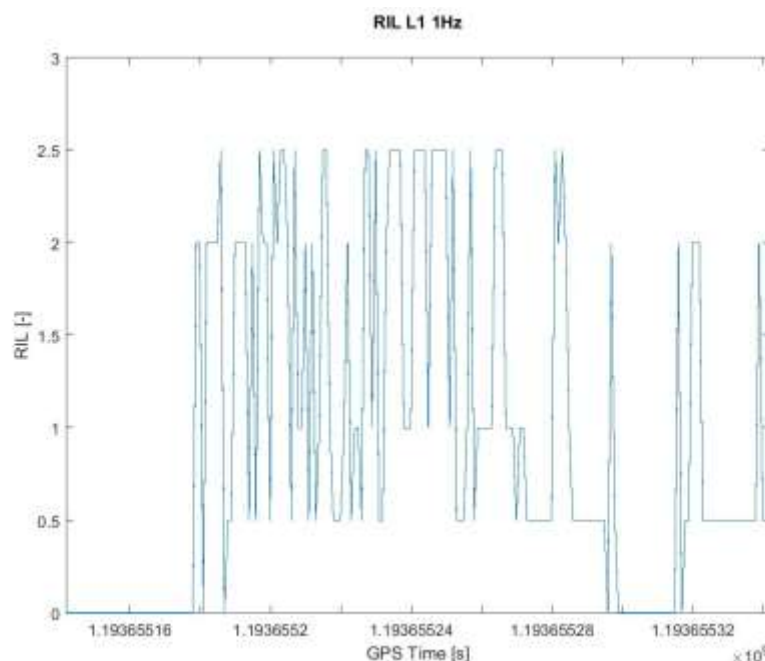


Figure 71: Case of train acceleration from a station – RIL_L1/E1 (1Hz output rate)

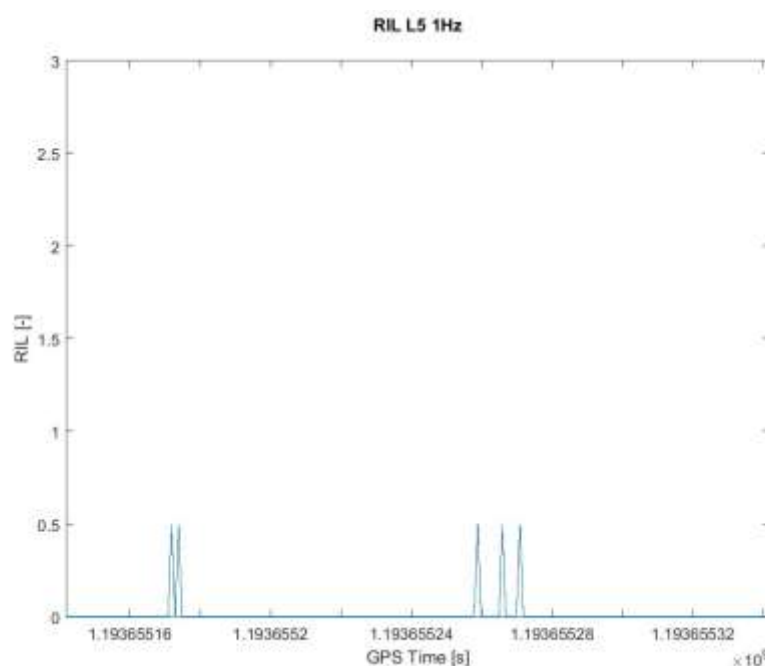


Figure 72: Case of train acceleration from a station – RIL_L5/E5 (1Hz output rate)

4.3.6 Case of forest (normal case)

The analysis is carried out from data obtained from measurement performed on August 4 (2017), at South Bohemia test track.

Source file of raw data: CVO_0925_1708040136H_02H.SBF

Source file of reference position data: CVO_4250_1708040217_01H_10Z.RPO

Analysis carried out in GPS Time interval: 1185851711 s – 1185851736 s.

The real situation is depicted in Figure 73.

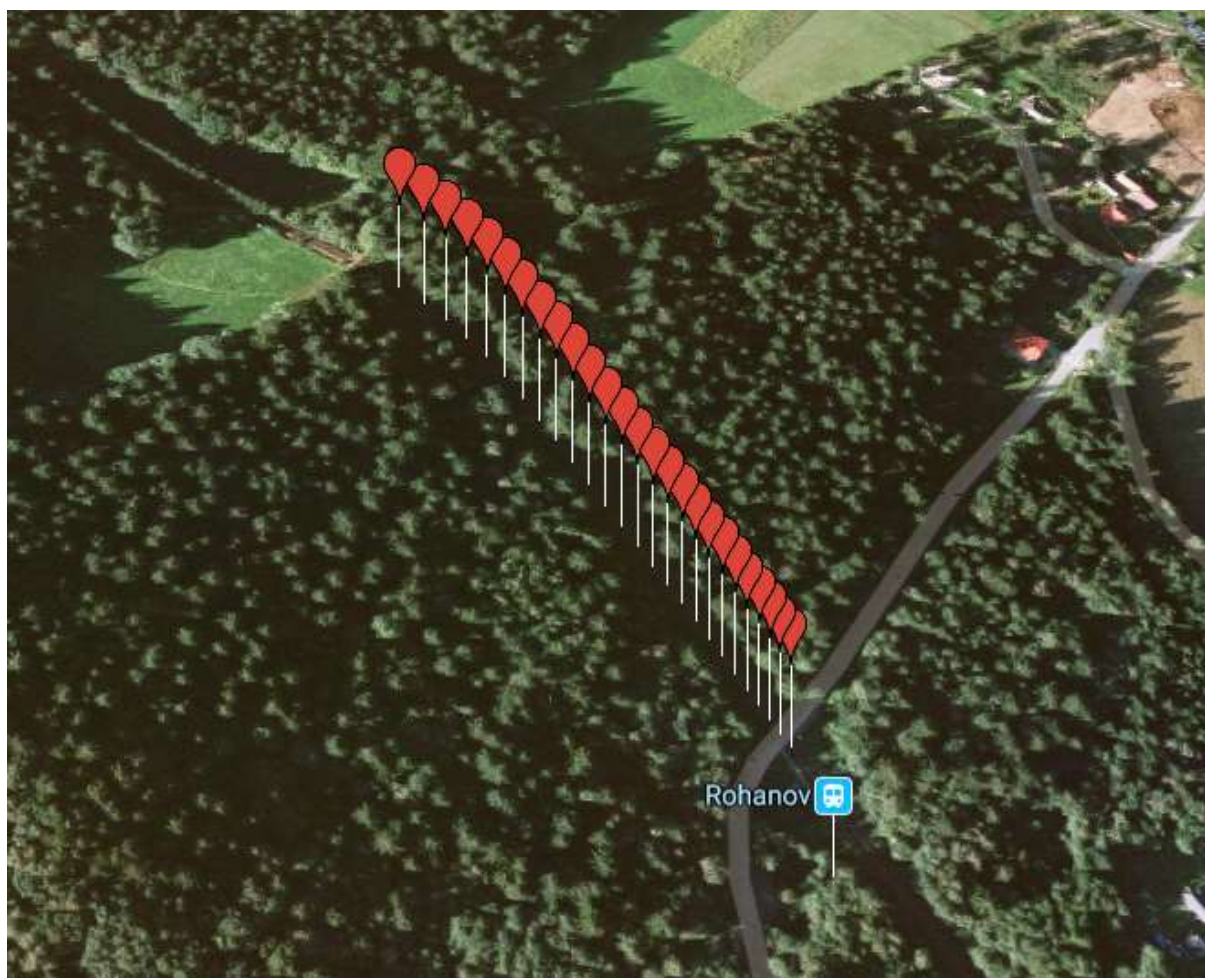


Figure 73: Case of nominal forest (AZD test track at the South Bohemia)

In Figure 74, the HNSE of EGNOS-based solution provided by SPRING, PP-SDK and RTKLIB is presented. The reference position is provided by ground truth. Some outages of HNSE provided by PP-SDK and RTKLIB were caused insufficient (unavailable) differential corrections. MPL and RIL parameters indicate presence of both stronger multipath and RF interference.

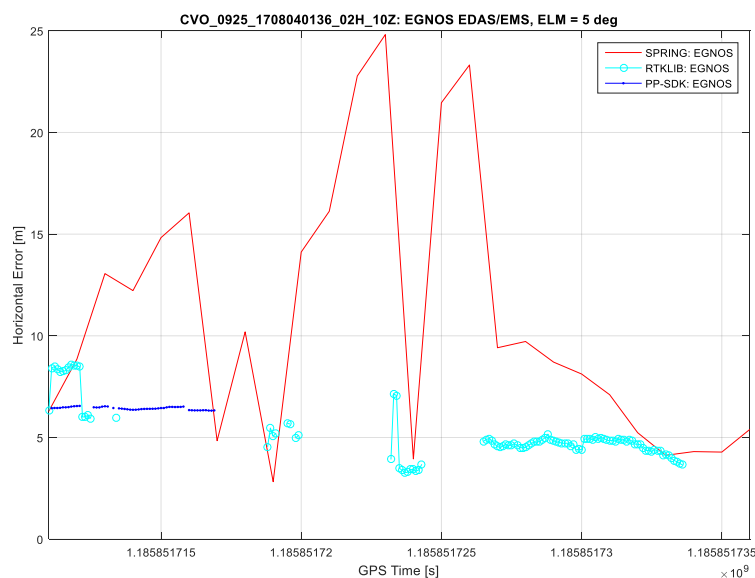


Figure 74: Case of nominal forest – HNSE values (10Hz output rate)

The number of satellites is shown in Figure 75.

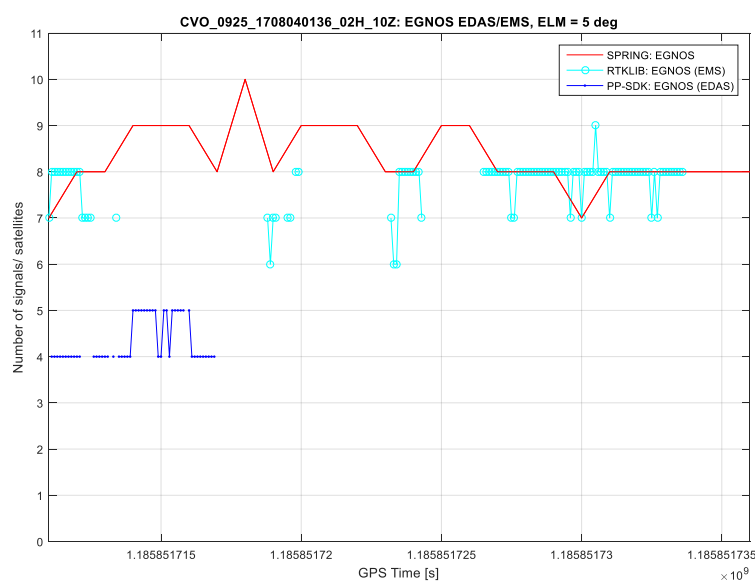


Figure 75: Case of nominal forest – Number of satellites

The train speed profile is presented in Figure 76.

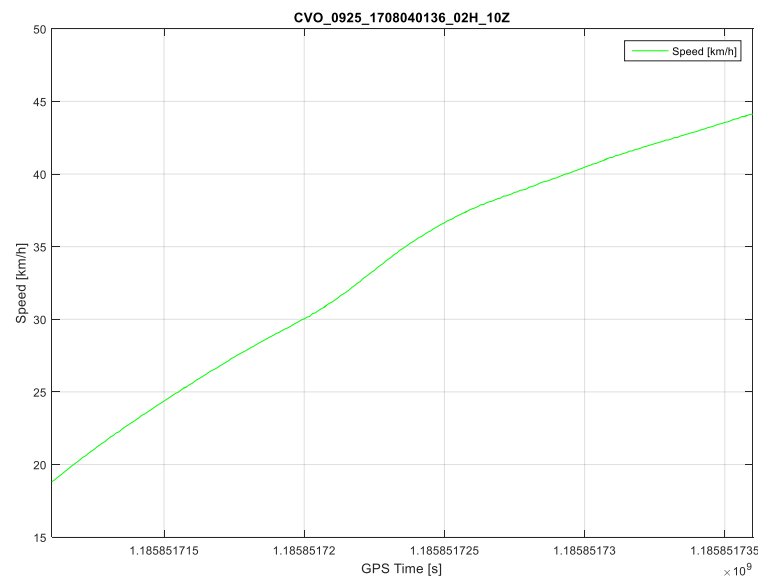


Figure 76: Case of nominal forest – Train speed profile

The set of figures from Figure 77 to Figure 82 shows MPL parameter values in selected time range of this case for signals GPS L1, Galileo E1 and GPS L1+ Galileo E1 and output rates 1Hz and 10Hz.

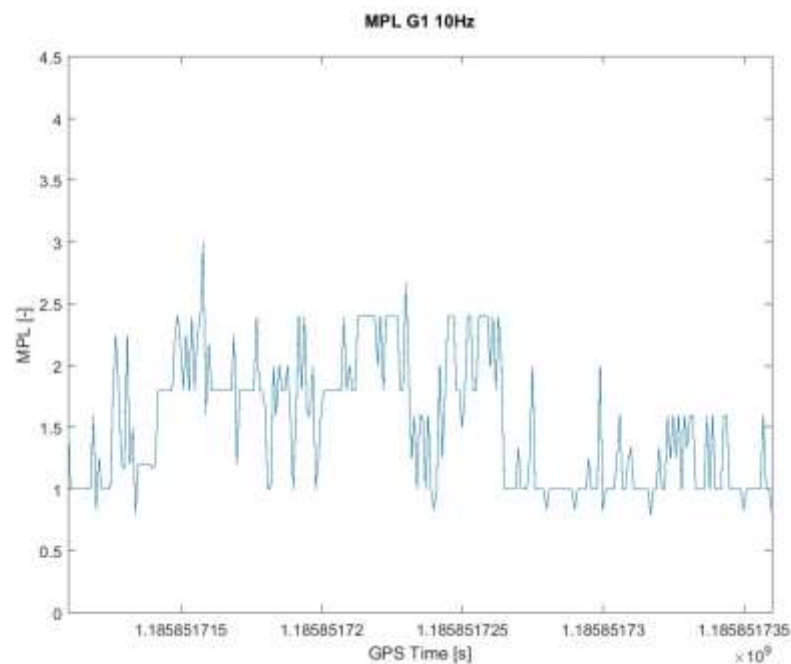


Figure 77: Case of nominal forest – MPL_GPS_L1 (10Hz output rate)

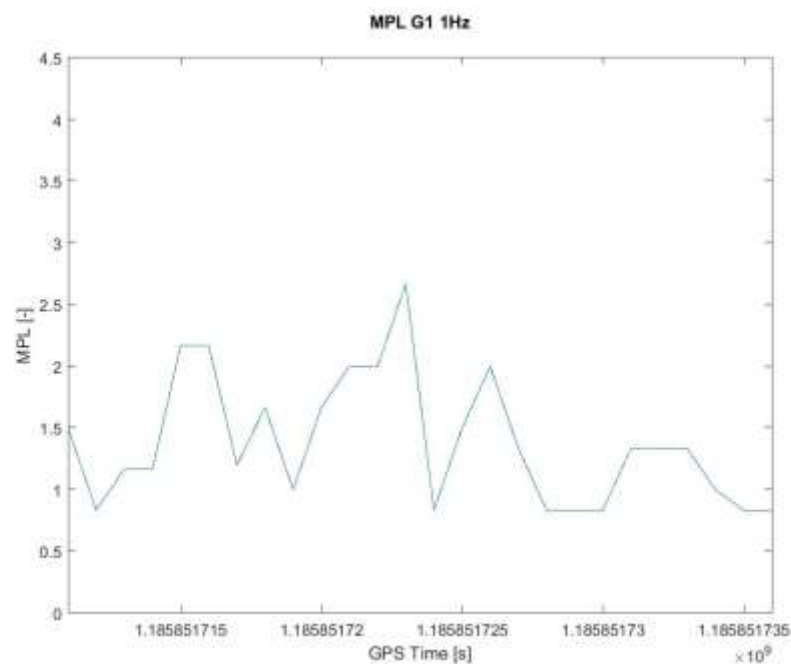


Figure 78: Case of nominal forest – MPL_GPS_L1 (1Hz output rate)

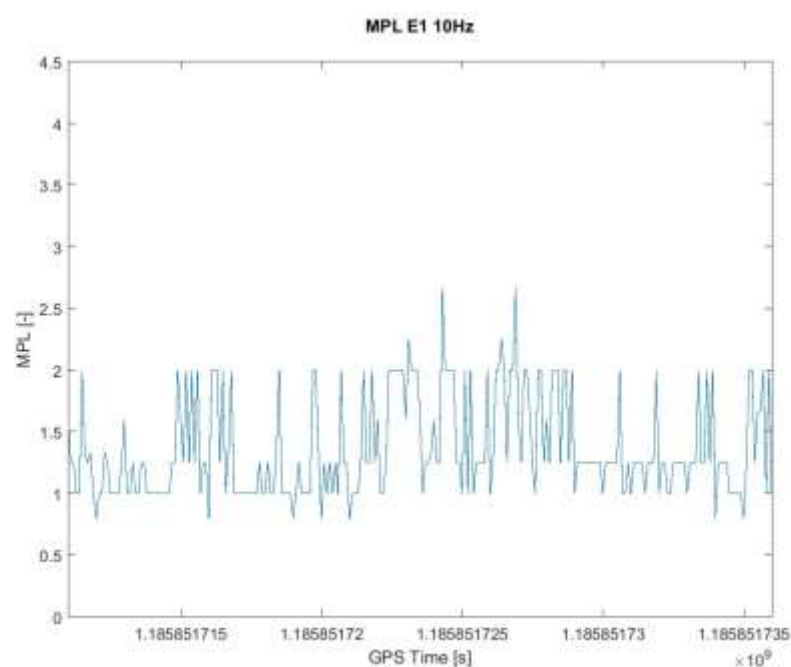


Figure 79: Case of nominal forest – MPL_GAL_E1 (10Hz output rate)

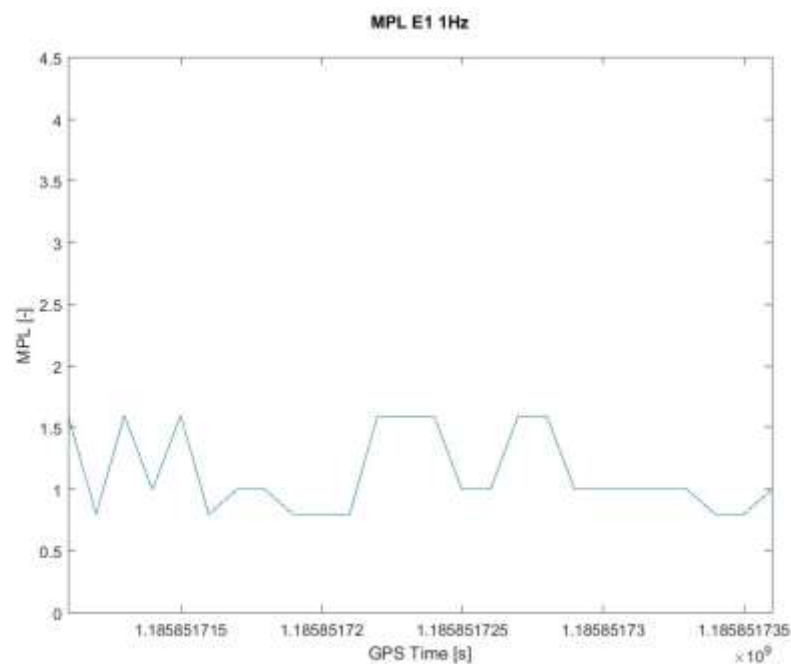


Figure 80: Case of nominal forest – MPL_GAL_E1 (1Hz output rate)

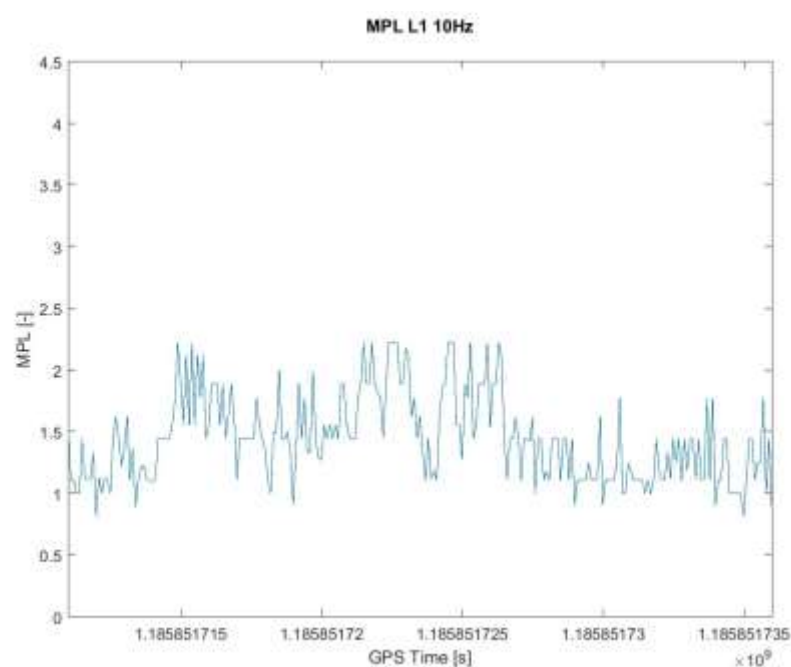


Figure 81: Case of nominal forest – MPL_GPS_L1+GAL_E1 (10Hz output rate)

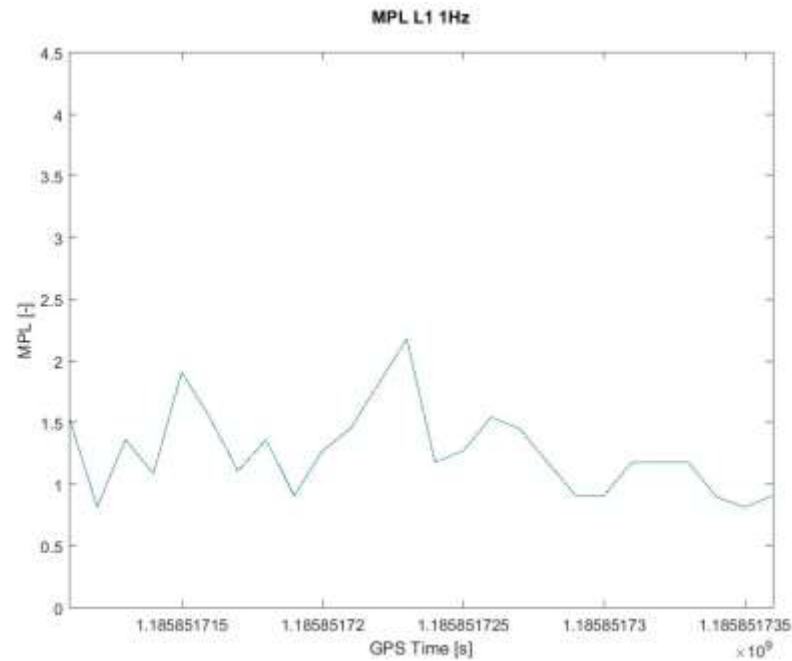


Figure 82: Case of nominal forest – MPL_GPS_L1+GAL_E1 (1Hz output rate)

In figures from Figure 77 to Figure 82 the values of MPL parameter indicate presence of middle and stronger multipath in strong correlation with HNSE provided by SPRING.

The curves presented in Figure 83 and Figure 84 show MPL parameter values calculated for both GPS L5 and Galileo E5 signals (only 10Hz output rates). The MPL for GPS L5 signals presented in Figure 83 indicates better resistance of these signals to multipath in comparison to Galileo E5 signals and calculated MPL for Galileo E5 signals depicted in Figure 84.

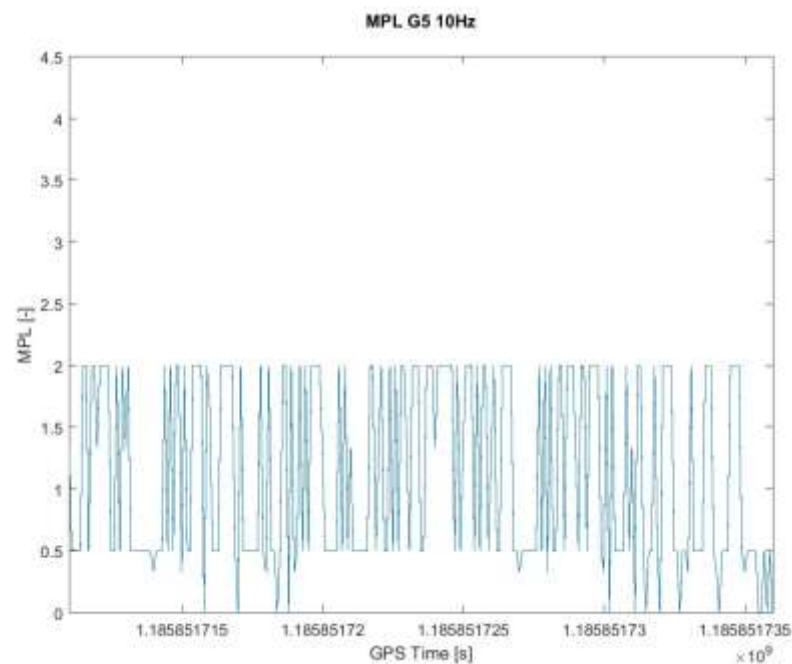


Figure 83: Case of nominal forest – MPL_GPS_L5 (10Hz output rate)

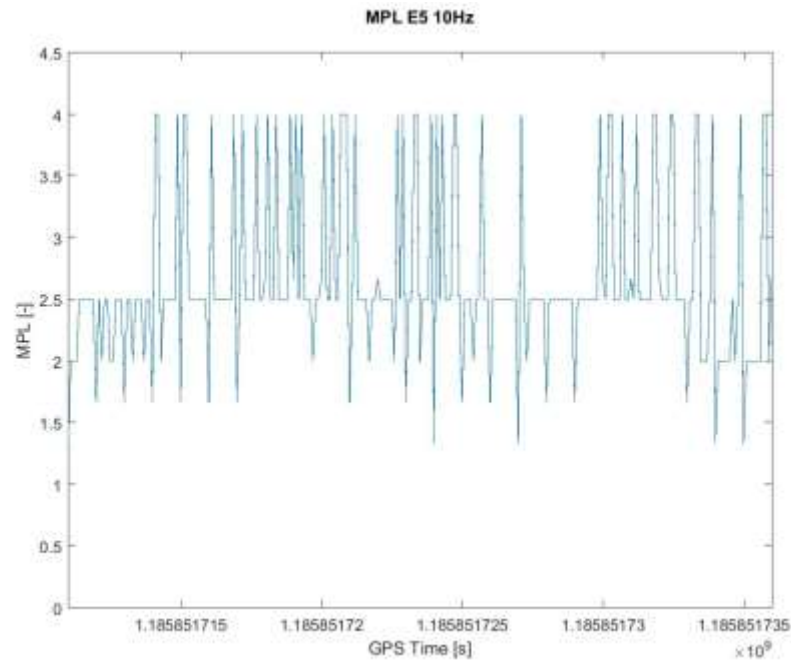


Figure 84: Case of nominal forest – MPL_GAL_E5 (10Hz output rate)

RIL parameter values for L1/E1 and L5/E5 bands are presented in Figure 85 and Figure 86. No interference was detected in selected time interval.

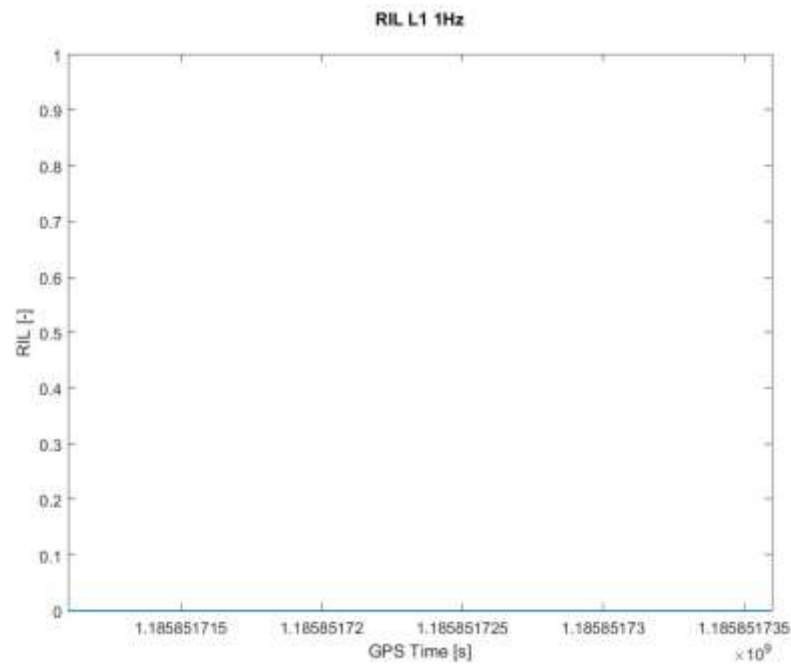


Figure 85: Case of nominal forest – RIL_L1/E1 (1Hz output rate)

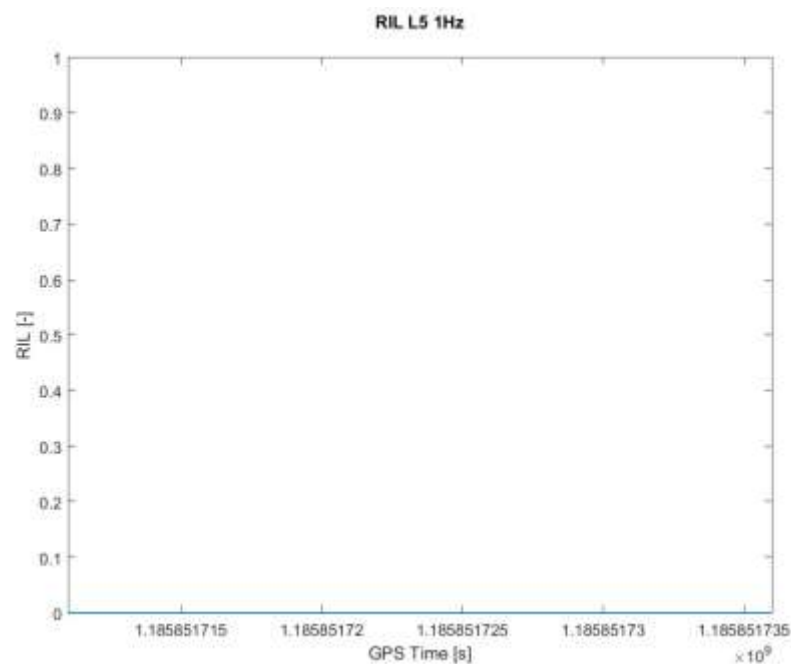


Figure 86: Case of nominal forest – RIL_L5/E5 (1Hz output rate)

4.3.7 Case of forest (extreme case)

The analysis is carried out from data obtained from measurement performed on August 4 (2017), at South Bohemia test track.

Source file of raw data: CVO_0925_1708091720H_02H.SBF

Source file of reference position data: CVO_4250_1708091756_01H_10Z.RPO

Analysis carried out in GPS Time interval: 1186340200 s – 1186340210 s.

The real situation is depicted in Figure 87.

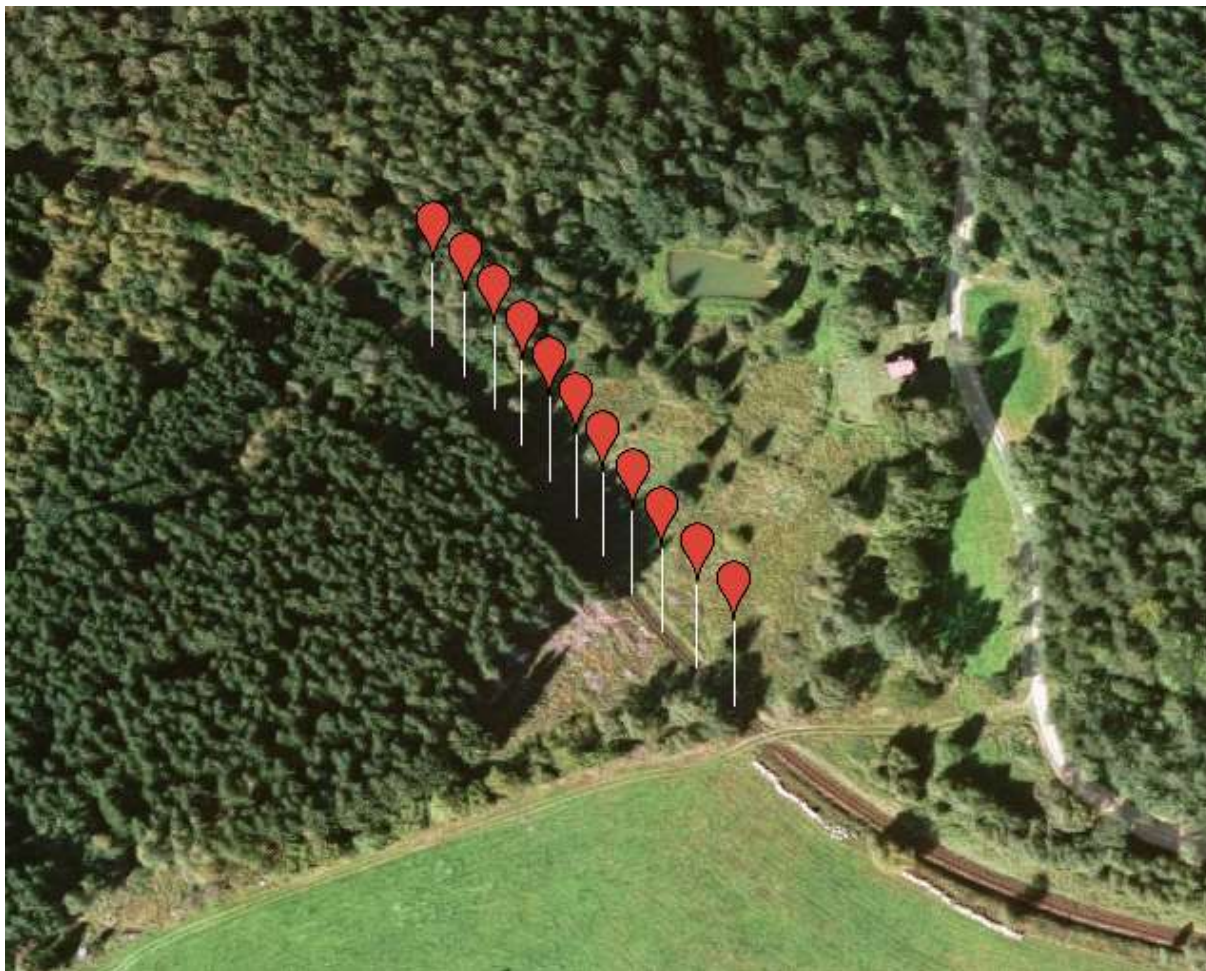


Figure 87: Case of extreme forest (AZD test track at the South Bohemia)

In Figure 88, the HNSE of EGNOS-based solution provided by SPRING, PP-SDK and RTKLIB is presented. The reference position is provided by ground truth. HNSE calculated by SPRING gives high values for several epochs, on the other hand PP-SDK and RTKLIB don't detect any significant deviation for the same time epochs.

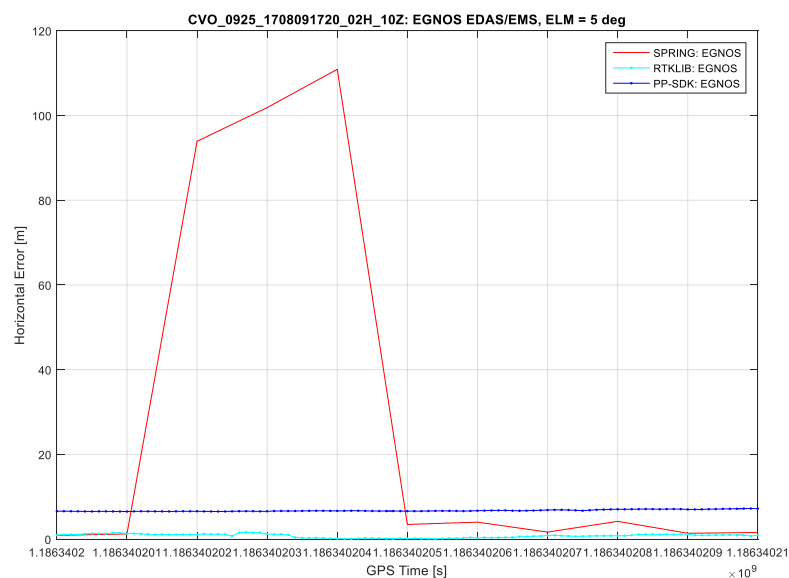


Figure 88: Case of extreme forest HNSE values

The number of satellites is shown in Figure 89.

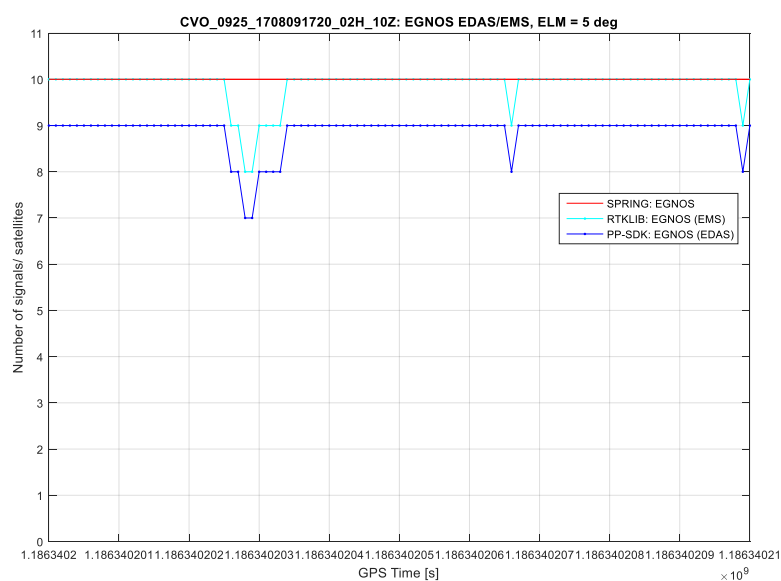


Figure 89: Case of extreme forest – Number of satellites

The train speed profile is presented in Figure 90.

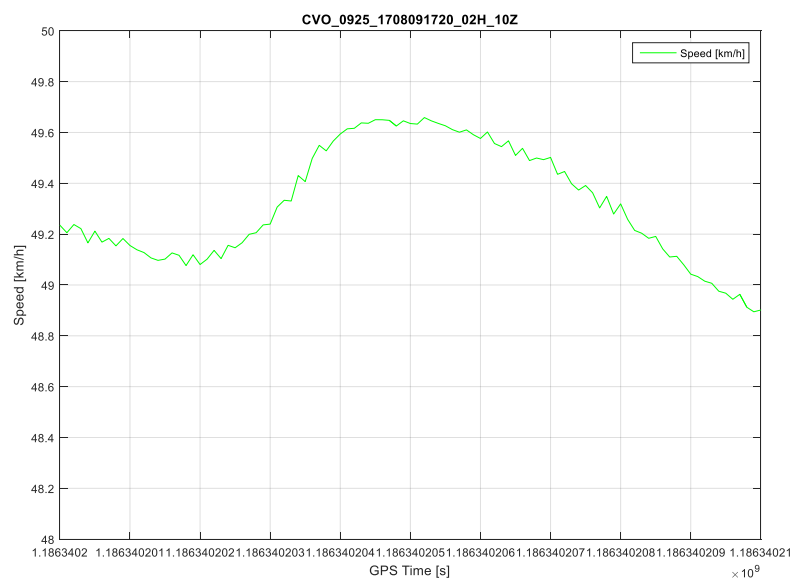


Figure 90: Case of extreme forest – Train speed profile

The set of figures from Figure 91 to Figure 95 shows MPL parameter values in selected time range of this case for signals GPS L1, Galileo E1 and GPS L1+ Galileo E1 and output rates 1Hz and 10Hz.

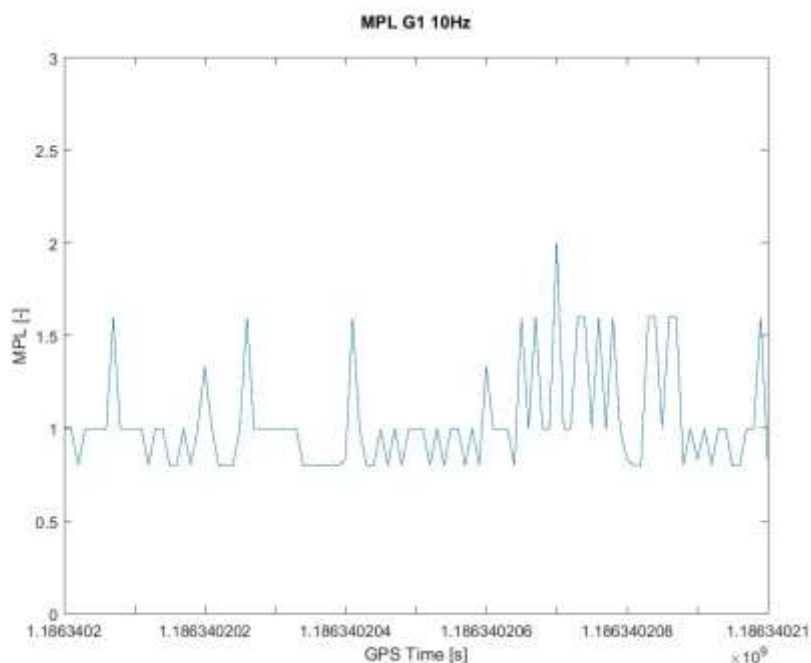


Figure 91: Case of extreme forest – MPL_GPS_L1 (10Hz output rate)

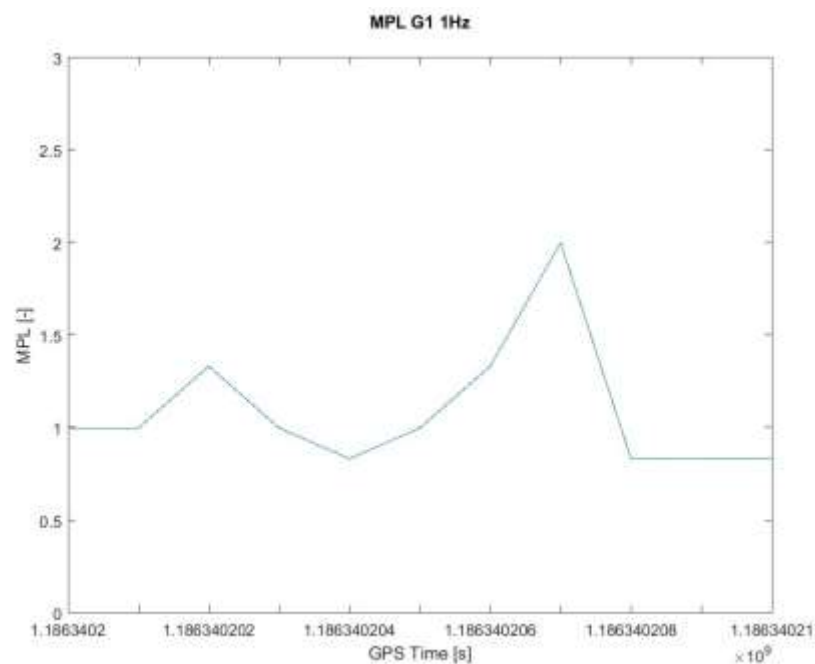


Figure 92: Case of extreme forest – MPL_GPS_L1 (1Hz output rate)

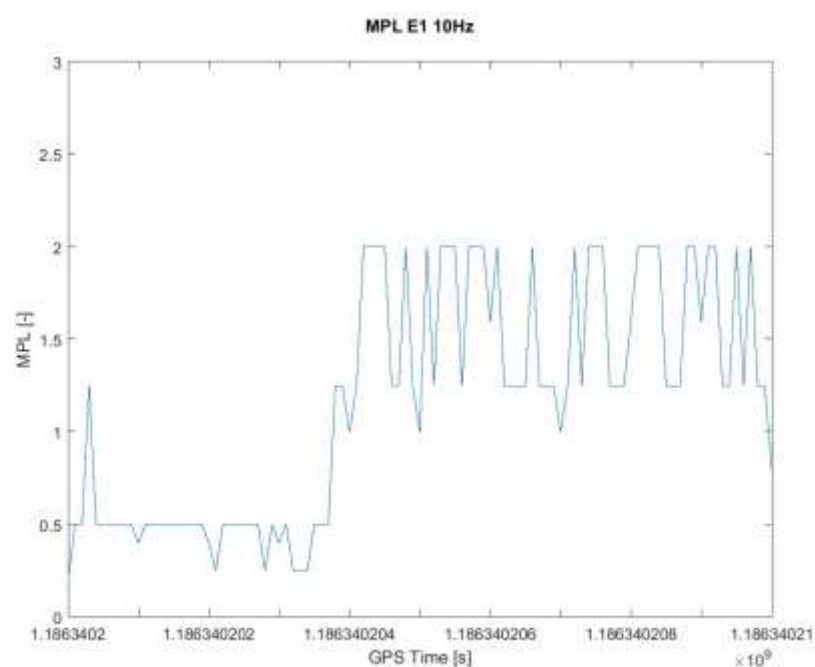


Figure 93: Case of extreme forest – MPL_GAL_E1 (10Hz output rate)

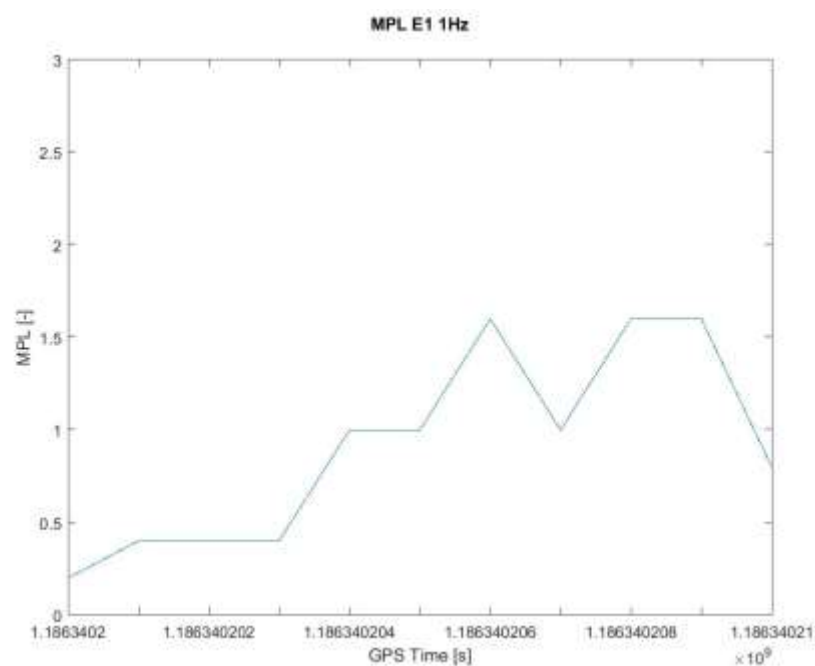


Figure 94: Case of extreme forest – MPL_GAL_E1 (1Hz output rate)

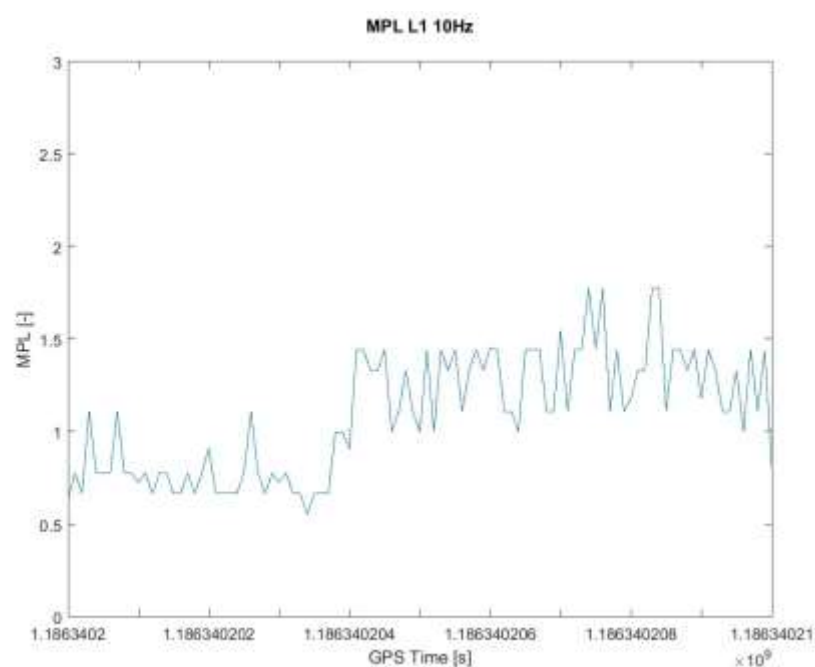


Figure 95: Case of extreme forest – MPL_GPS_L1+GAL_E1 (10Hz output rate)

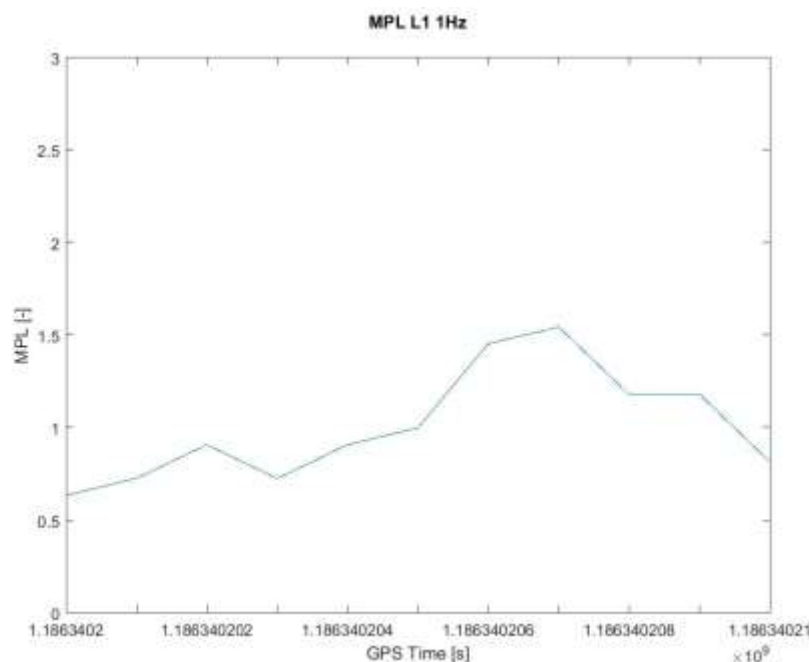


Figure 96: Case of extreme forest – MPL_GPS_L1+GAL_E1 (1Hz output rate)

In Figure 91, Figure 95 and Figure 96 MPL parameter values indicate presence of middle and stronger multipath but not correlated with HNSE provided by SPRING⁵.

The curves presented in Figure 97 and Figure 98 show MPL parameter values calculated for both GPS L5 and Galileo E5 signals (only 10Hz output rates). The MPL for both these signals indicates middle and stronger multipath but not correlated with the HNSE provided by SPRING⁵.

⁵ Subsequent deep analysis revealed that software tools SPRING and TEQC do not correctly decode SBF binary files of Septentrio receiver including concurrently recorded data from both antenna inputs of the receiver. Therefore, the values of HNSE provided by PPSDK or RTKLIB may be considered correct. Despite above mentioned fact it was decided to leave this case without changes as an model example of high multipath.

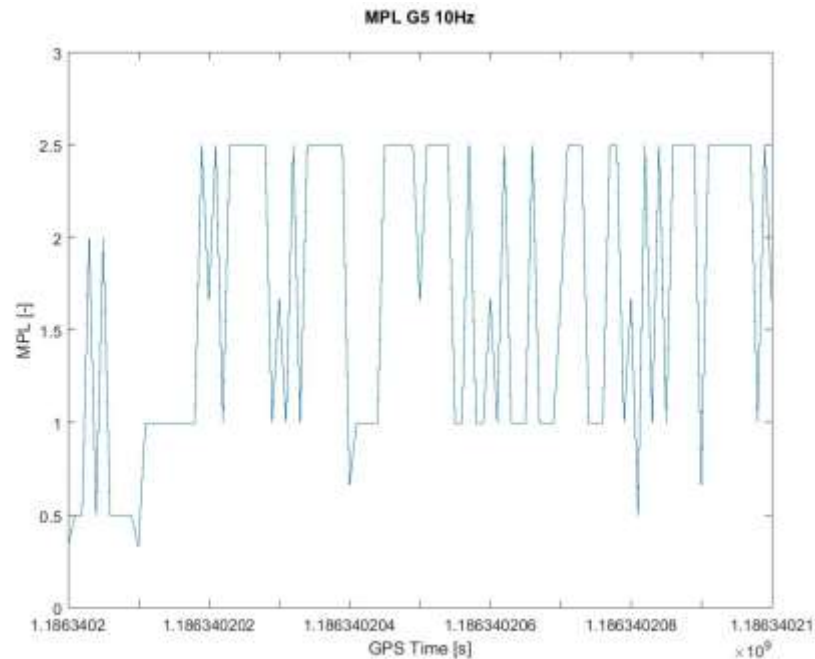


Figure 97: Case of extreme forest – MPL_GPS_L5 (10Hz output rate)

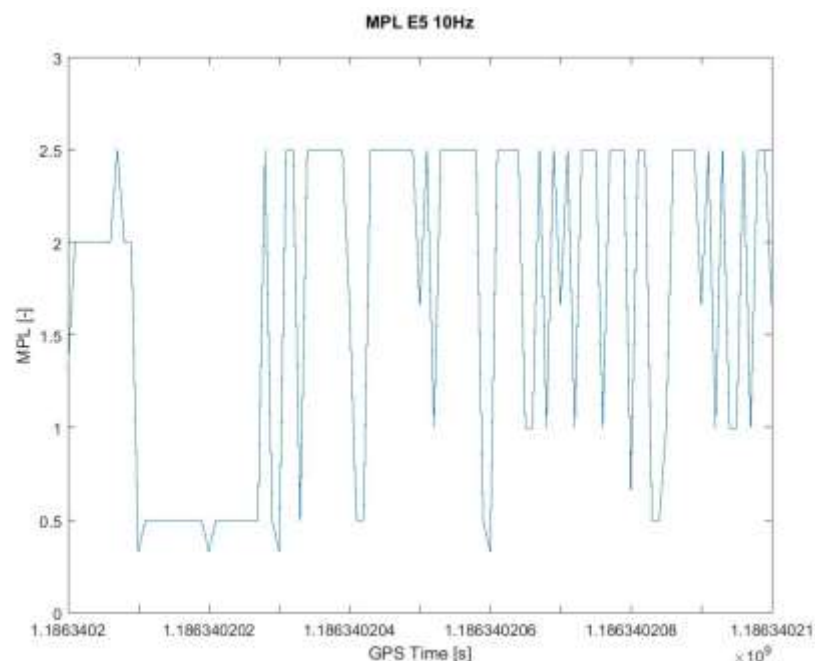


Figure 98: Case of extreme forest – MPL_GAL_E5 (10Hz output rate)

There is not visible any significant influence of detected multipath on the HNSE. The analysis⁵ showed that the reason is sufficient number of satellites unaffected by multipath entering in position solution. On the other hand output of multipath detection function is based on a comparison of a threshold and output of maximum function on a set of satellites, where only 1 or 2 the most affected satellites are selected by maximum function for the comparison.

RIL parameter values for L1/E1 and L5/E5 bands are presented in Figure 99 and Figure 100. No interference was detected in selected time interval.

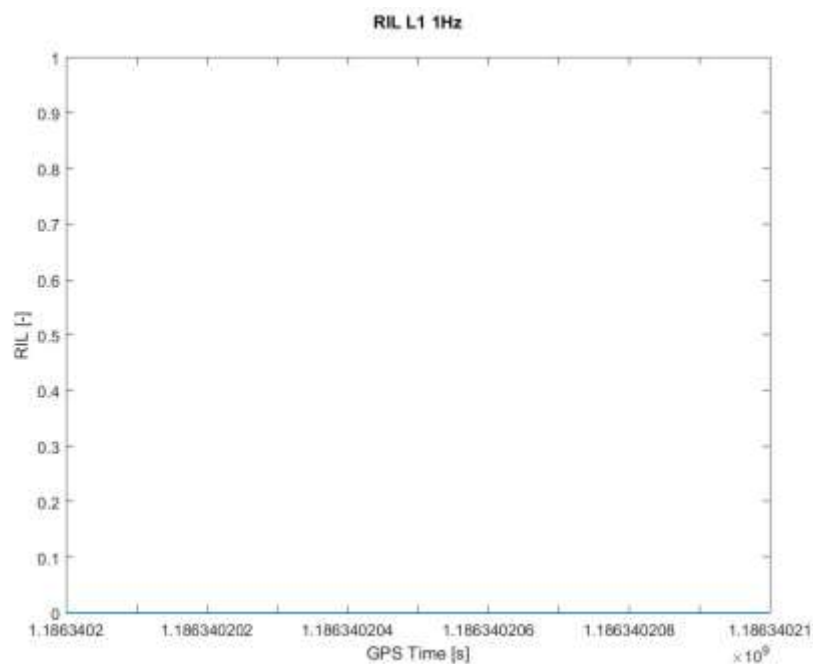


Figure 99: Case of extreme forest – RIL_L1/E1 (1Hz output rate)

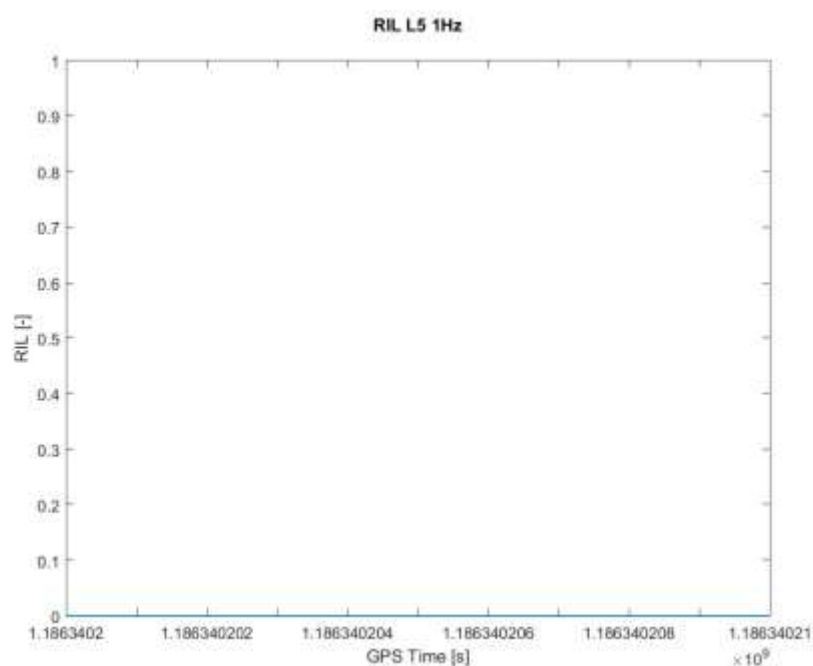


Figure 100: Case of extreme forest – RIL_L5/E5 (1Hz output rate)

4.3.8 Case of panoramic camera measurement 1

The analysis is carried out from data obtained from measurement performed on November 24 (2017), at South Bohemia test track.

Source file of raw data: CVO_4250_1711241102_10H_10Z.SBF

Source file of reference position data: CVO_4250_1711241145_08H_10Z.RPO

Analysis carried out in GPS Time interval: 1195561937 s – 1195562552 s.

The real situation is depicted in Figure 101.

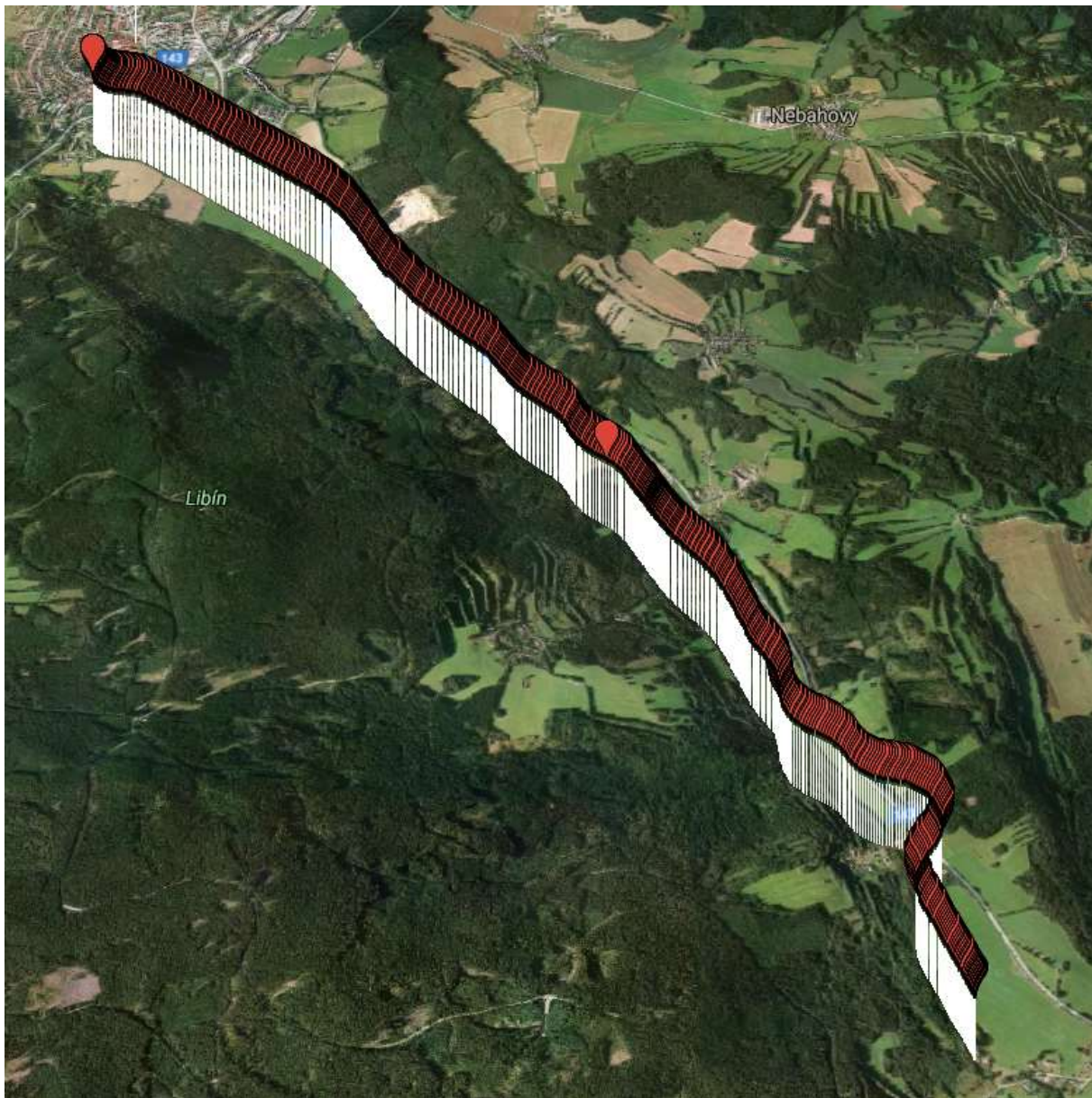


Figure 101: Case of panoramic camera measurement 1 (AZD test track at the South Bohemia)

The HNSE of EGNOS-based solution is presented in Figure 102, the HNSE of GPS L1 solution is outlined in Figure 103. Both outputs are provided by the composition of PP-SDK and RTKLIB solution outputs. The reference position is provided by ground truth. The HNSE from both position solutions

is relatively low. Some increase appears around time epoch 1195562240 s. Outputs of both solutions seem to be correlated.

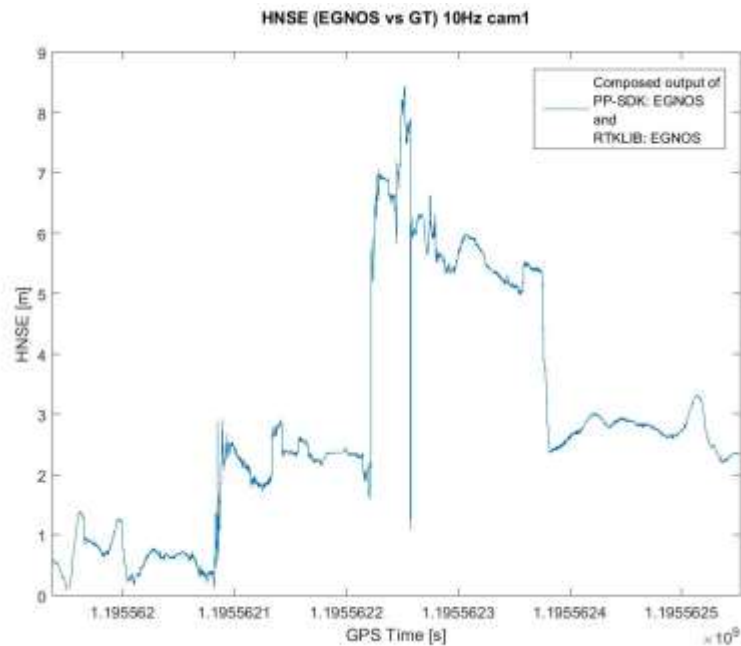


Figure 102: Case of camera measurement 1 – HNSE EGNOS values (10Hz output rate)

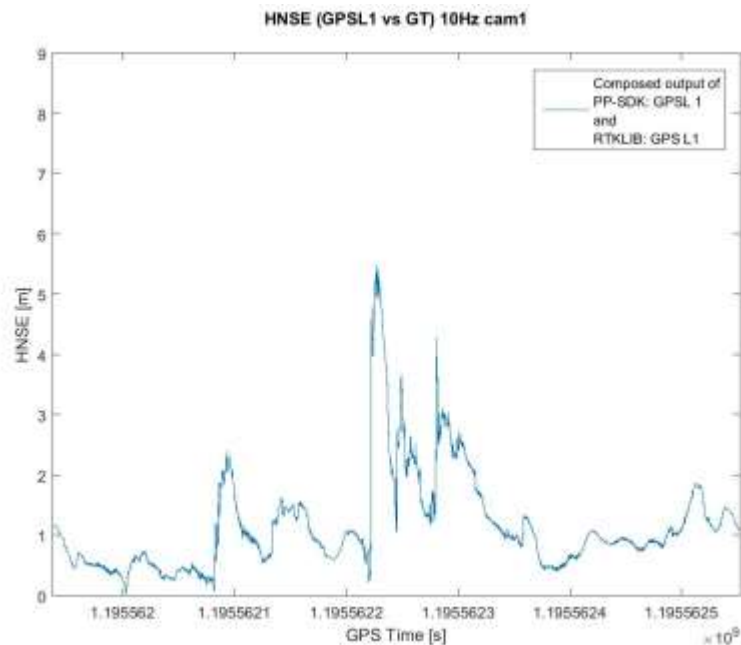


Figure 103: Case of camera measurement 1 – HNSE GPSL1 values (10Hz output rate)

The number of satellites is shown in Figure 104 and Figure 105.

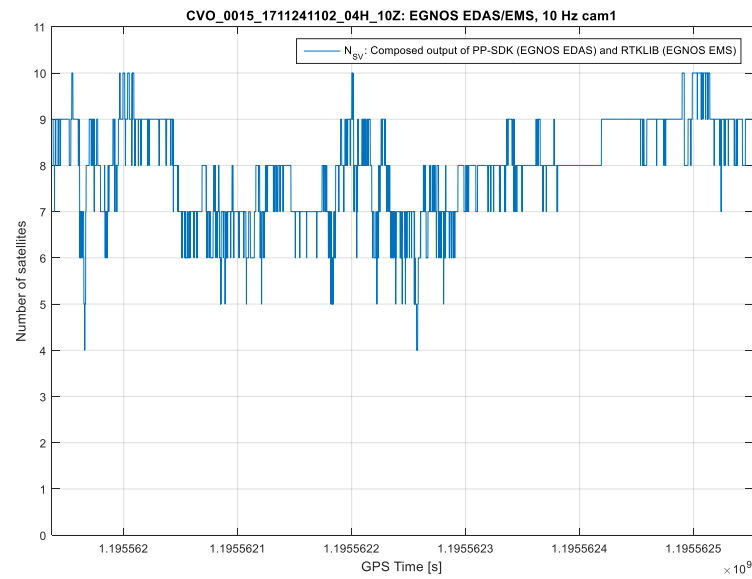


Figure 104: Case of camera measurement 1 – Number of satellites (EGNOS solution)

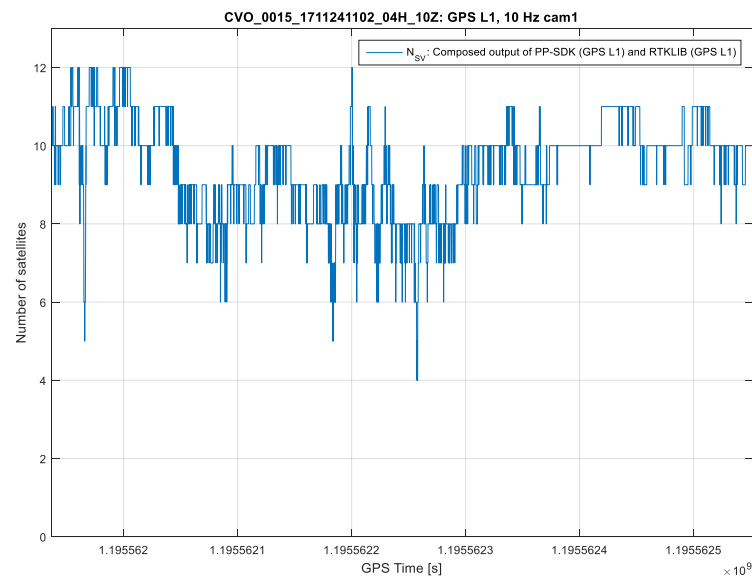


Figure 105: Case of camera measurement 1 – Number of satellites (GPS L1 solution)

The train speed profile is presented in Figure 106. PDOP parameter is depicted in Figure 107.

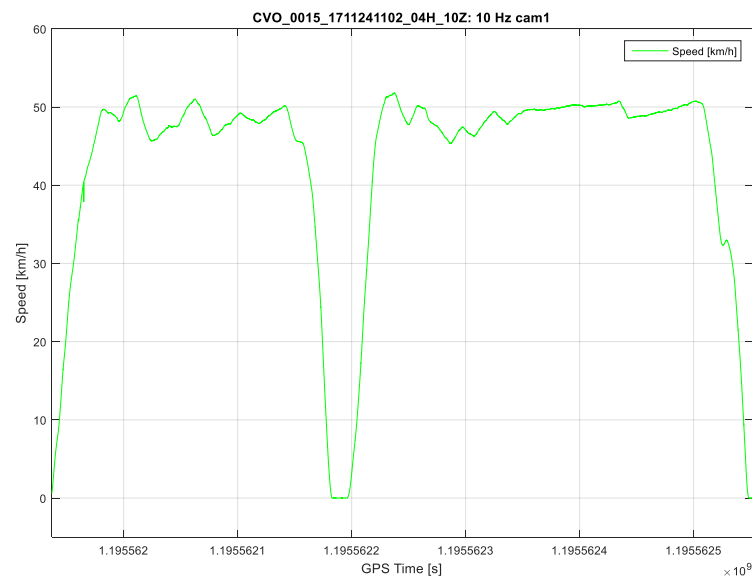


Figure 106: Case of camera measurement 1 – Train speed profile

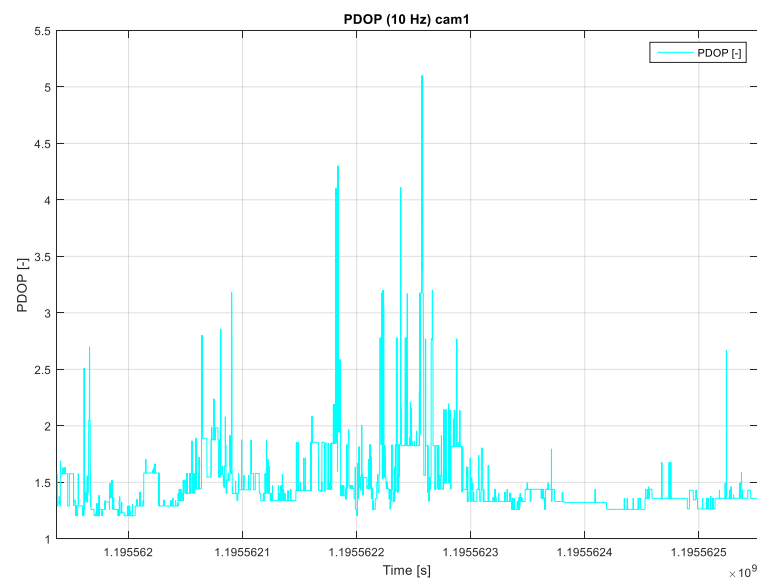


Figure 107: Case of camera measurement 1 – PDOP (10 Hz output rate)

Figure 108 shows MPL parameter values in selected time range of this case for signal GPS L1 and output rate 10Hz. Low multipath is indicated around time epoch 1195562240 s which is correlated with HNSE.

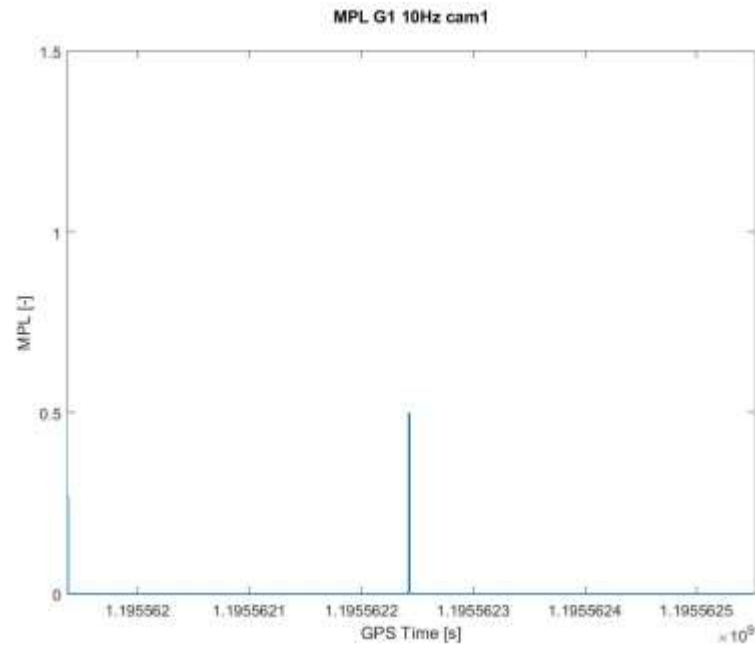


Figure 108: Case of camera measurement 1 – MPL_GPS_L1 (10Hz output rate)

SVF_{APV} parameter values are presented in Figure 109. There is well evident correlation of SVF_{APV} with HNSE in selected time interval of this case for signals GPS L1 and output rate 10Hz. A decrease of SVF_{APV} corresponds to an increase of HNSE. Regarding different magnitude of HNSE compared to the same (low) magnitude of SVF in some epochs, the HNSE magnitude cannot be considered to be directly corresponding to the magnitude of SVF from camera. HNSE depends on many factors: not only the number of satellites, but also on actual DOP (satellite deployment), quality of measurement, measurement errors etc. These above figures in this section well illustrate the correlation between HNSE and SVF factor especially for locations with reduced visibility.

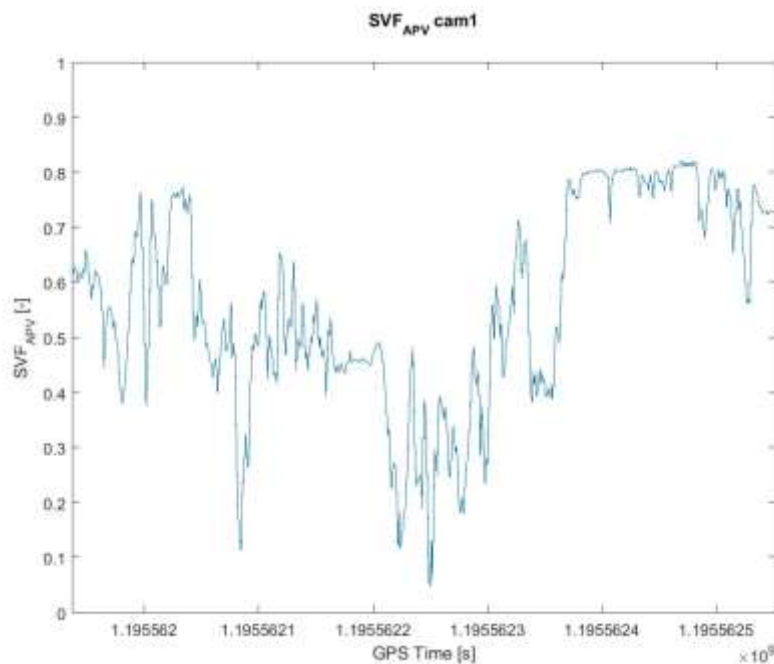


Figure 109: Case of camera measurement 1 – SVF_{APV} (1Hz output rate)

SVF_{ES} parameter values are presented in Figure 110. It can be seen that significant loss of information occurs due to a quantization. There is also evidence that output values are enough restrictive. It indicates that stringent thresholds were set in the sub-task focused on processing data from the panoramic camera. For these reasons only SVF_{APV} is included in presented results of analyses of next measurements with the camera. Further investigation is needed in this field. The current SVF thresholds were intuitively set for the analysis and the comparisons given within STARS project. The future investigation could comprise e.g. modelling of visibility conditions (number of available LOS satellites) for given thresholds. Appropriate SVF thresholds could be set according to the requirement of given application on number of available LOS satellites.

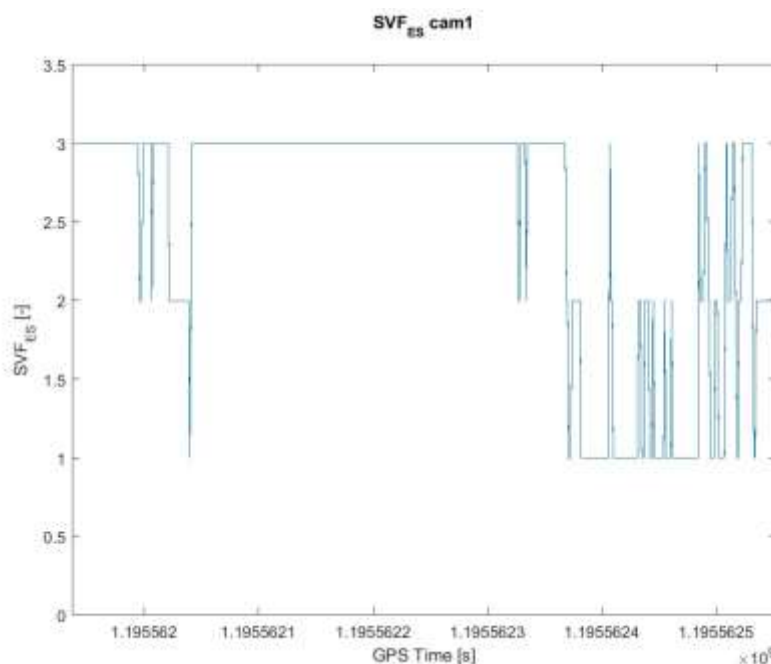


Figure 110: Case of camera measurement 1 – SVF_{ES} (1Hz output rate)

RIL parameter values for L1/E1 and L5/E5 bands are presented in Figure 111 and Figure 112. Occasionally stronger RF interference is indicated in L1/E1 bands in selected time interval⁶, but no influence on HNSE is observed. Low level RF interference is also indicated in L5/E5 bands in selected time interval. The observed RF interference was detected and probably partially suppressed by the receiver as the output ES = 1 indicates “*RF interference detected and suppressed*” and the output ES = 4 indicates “*RF interference detected*”. Moreover, the nature of RF interference determines a degree of impact on GNSS measurement.

⁶ It should be noted that the previously performed measurements at the AZD test site did not exhibit RF interference. Something has probably been modified on the vehicle or a new device has been installed on board.

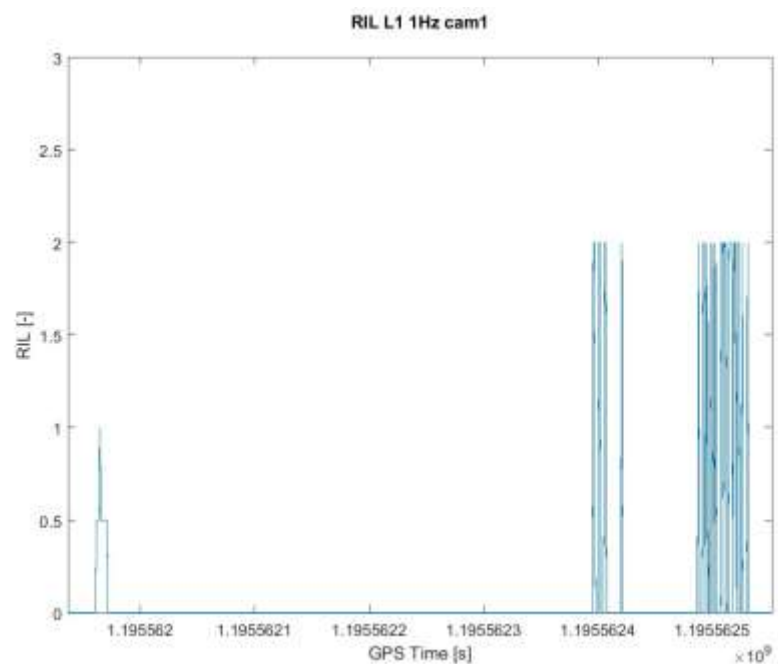


Figure 111: Case of camera measurement 1 – RIL_L1/E1 (1Hz output rate)

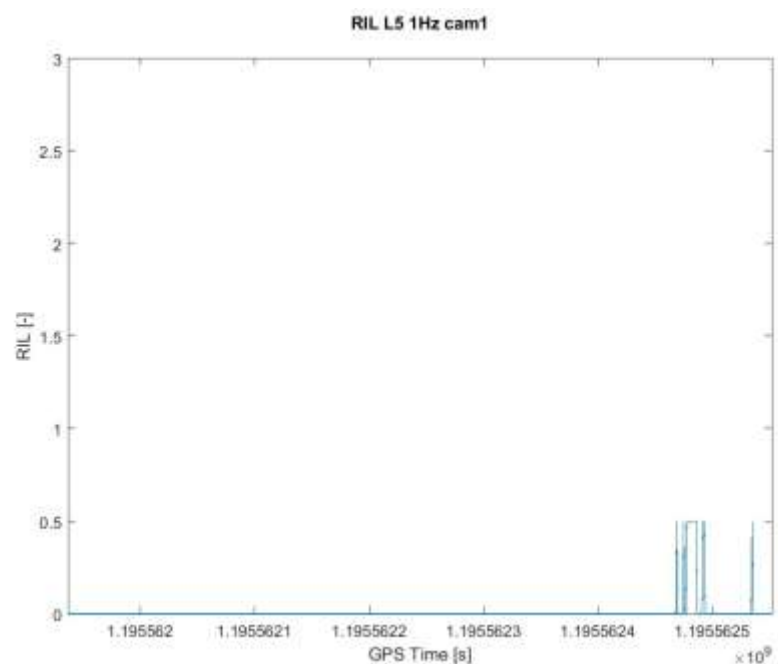


Figure 112: Case of camera measurement 1 – RIL_L5/E5 (1Hz output rate)

4.3.9 Case of panoramic camera measurement 2

The analysis is carried out from data obtained from measurement performed on November 24 (2017), at South Bohemia test track.

Source file of raw data: CVO_4250_1711241102_10H_10Z.SBF

Source file of reference position data: CVO_4250_1711241145_08H_10Z.RPO

Analysis carried out in GPS Time interval: 1195562590 s – 1195562904 s.

The real situation is depicted in Figure 113.

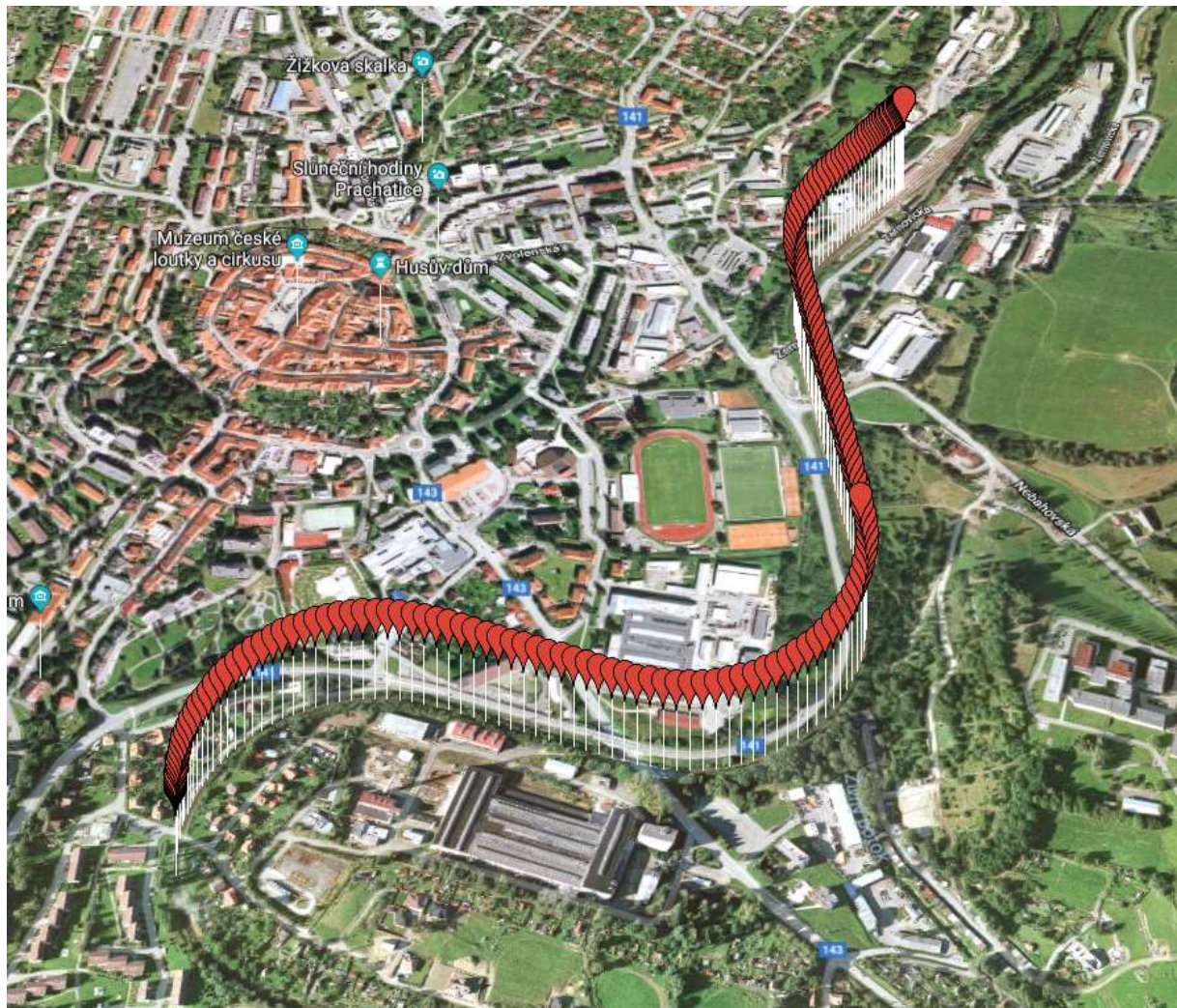


Figure 113: Case of panoramic camera measurement 2 (AZD test track at the South Bohemia)

The HNSE of EGNOS-based solution is presented in Figure 114, HNSE of GPS L1 solution is outlined in Figure 115. Both outputs are provided by composition of PP-SDK and RTKLIB solution outputs. The reference position is provided by ground truth. The HNSE from both position solutions is relatively low. Some increase appears around time epoch 1195562670 s. Outputs of both solutions seem to be correlated. HNSE has some higher values only for EGNOS mode. HNSE from GPS L1 has low values (under 1.6 m) in the full range. Higher values of HNSE come from RTKLIB solution at around time epoch 1195562670 s, PP-SDK is not available here (Error=8: Not enough differential corrections available). As it could be seen from figures below, low multipath is detected in this epoch

and low SVF also correlates in this epoch. Probably limited visibility is the main reason of higher HNSE.

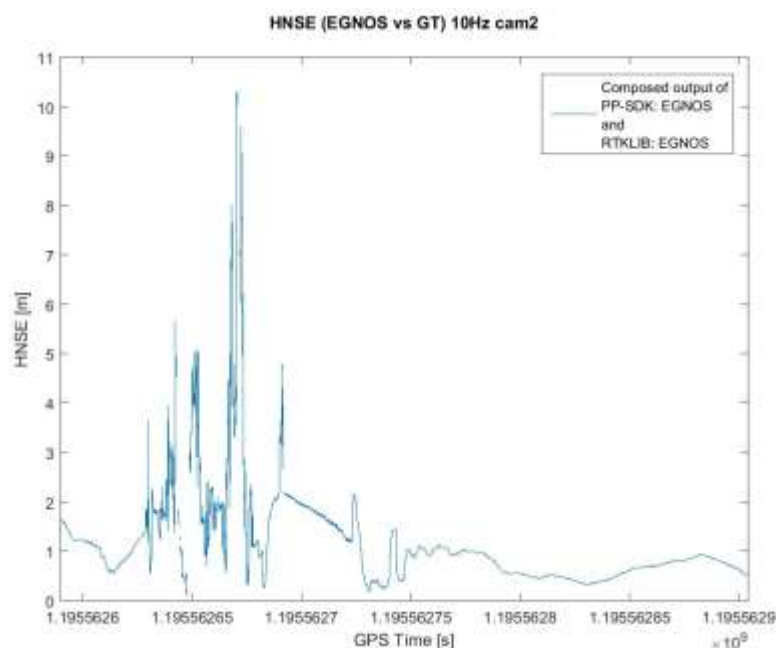


Figure 114: Case of camera measurement 2 – HNSE EGNOS values (10Hz output rate)

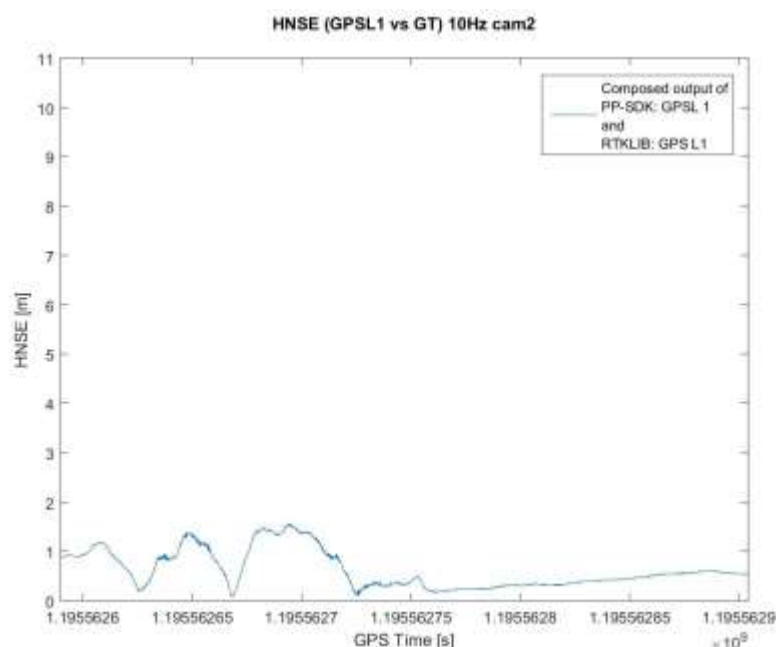


Figure 115: Case of camera measurement 2 – HNSE GPSL1 values (10Hz output rate)

The number of satellites is shown in Figure 116 and Figure 117.

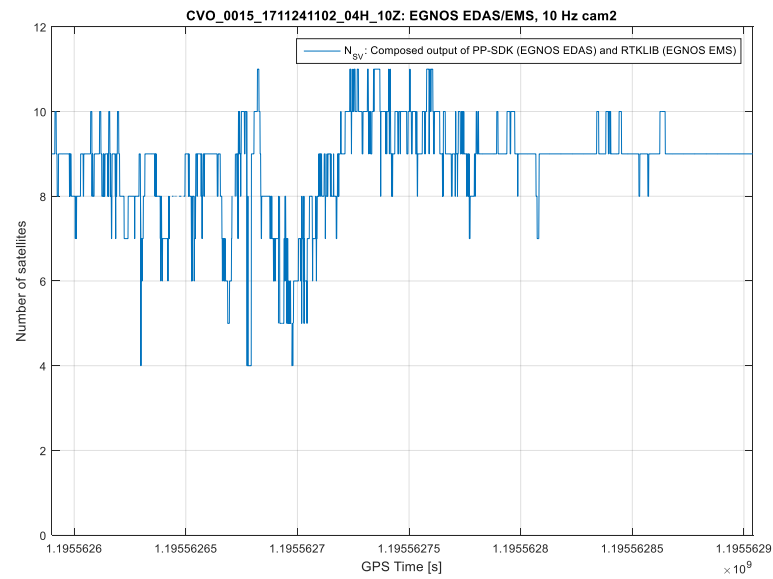


Figure 116: Case of camera measurement 2 – Number of satellites (EGNOS solution)

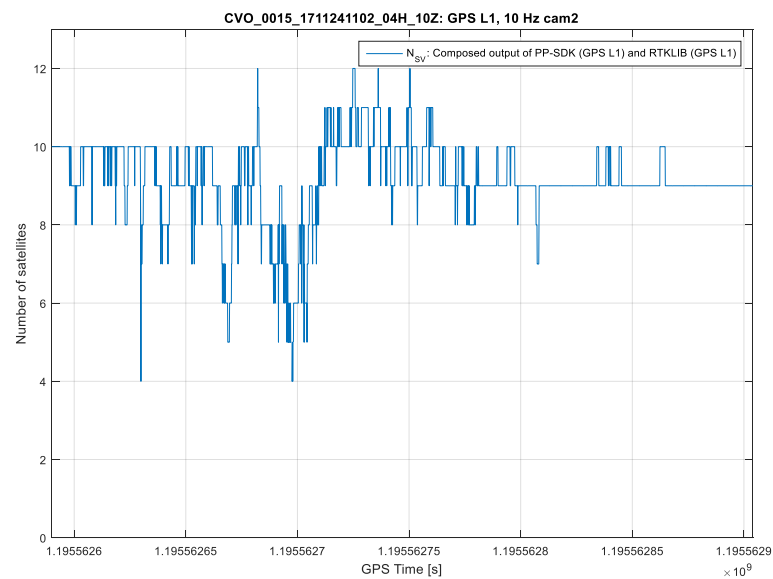


Figure 117: Case of camera measurement 2 – Number of satellites (GPS L1 solution)

The train speed profile is presented in Figure 118. PDOP parameter is depicted in Figure 119.

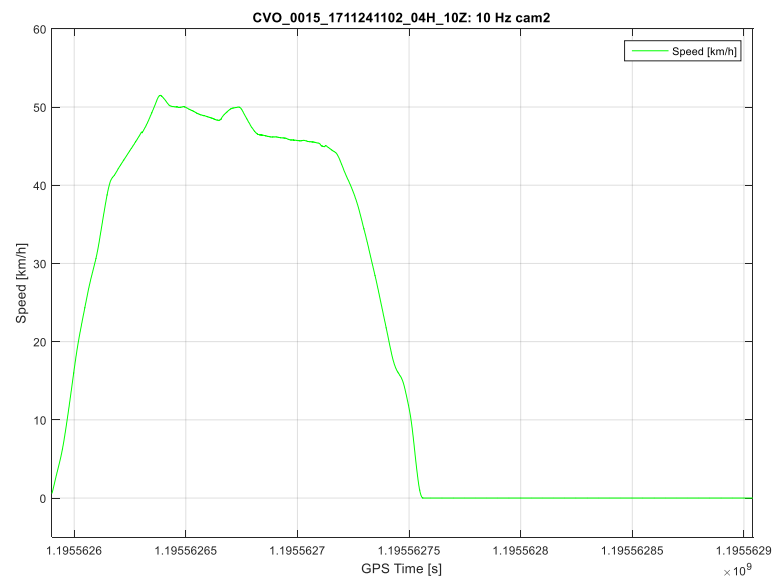


Figure 118: Case of camera measurement 2 – Train speed profile

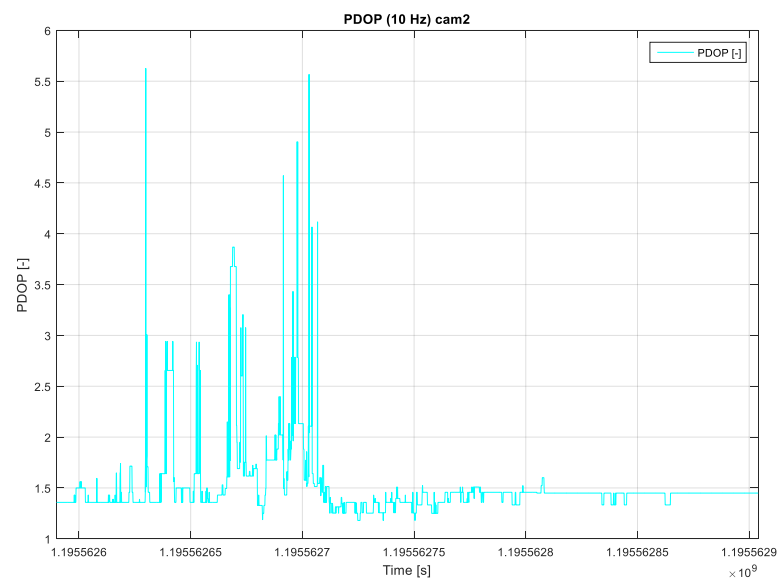


Figure 119: Case of camera measurement 2 – PDOP (10 Hz output rate)

Figure 120 shows MPL parameter values in selected time range of this case for signal GPS L1 and output rate 10Hz. Low multipath is indicated around time epoch 1195562670 s which is correlated with higher value of HNSE from EGNOS position solution. No correlation between HNSE from GPS L1 position solution and MPL L1 is observed, only small values of HNSE from GPS L1 position solution are presented in this time interval.

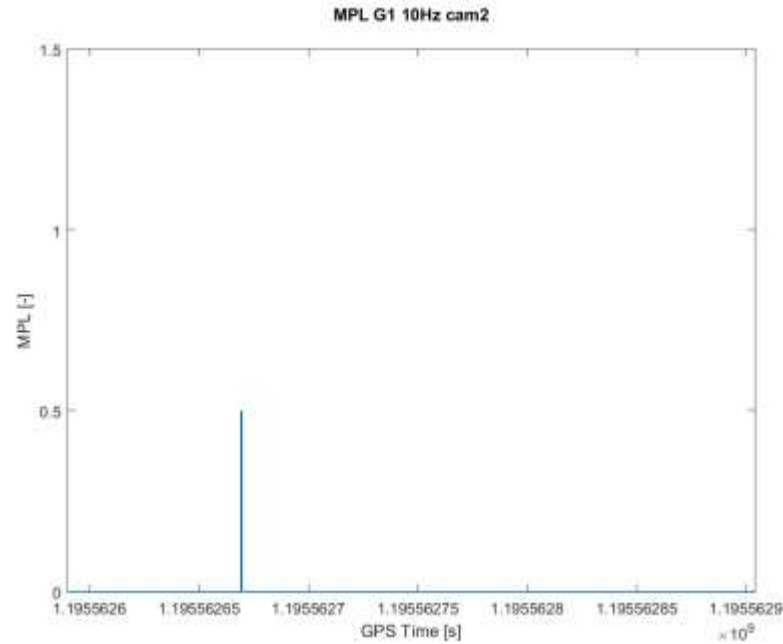


Figure 120: Case of camera measurement 2 – MPL_GPS_L1 (10Hz output rate)

SVF_{APV} parameter values are presented in Figure 121. There is well evident correlation of SVF_{APV} with HNSE derived from EGNOS-based solution in selected time interval of this case, in range of time epochs 1195562670 - 1195562690 s.

SVF_{APV} also indicates standstill in a station roughly from time epoch 1195562750 s in Figure 121. Changes in values of SVF_{APV} are very low from this time epoch.

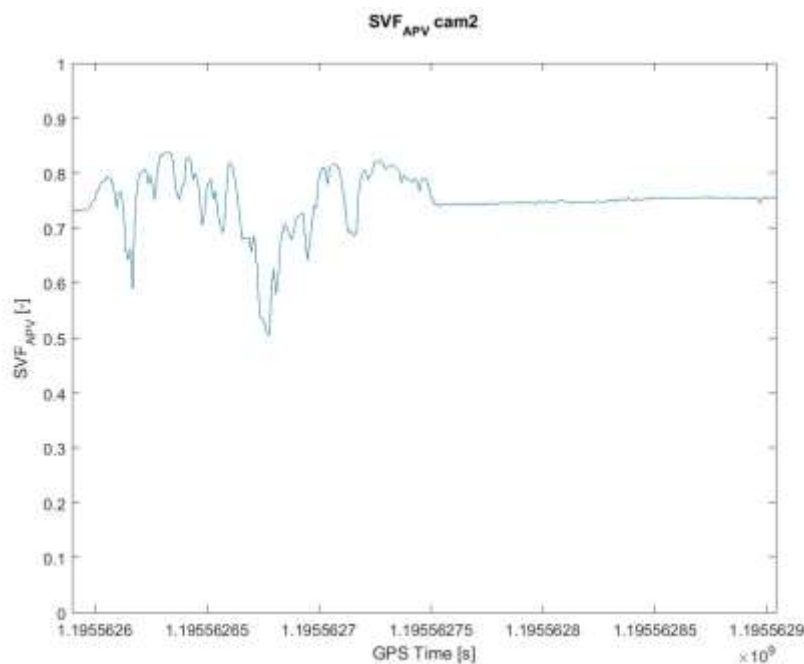


Figure 121: Case of camera measurement 2 – SVF_{APV} (1Hz output rate)

RIL parameter values for L1/E1 and L5/E5 bands are presented in Figure 122 and Figure 123. Occasional stronger RF interference is indicated in L1/E1 bands in selected time interval⁶, but no influence on HNSE is observed. Low level RF interference is also indicated in L5/E5 bands in selected time interval. Similarly to Section 4.3.8, the observed RF interference was detected and probably partially suppressed by the receiver as the output ES = 1 indicates “*RF interference detected and suppressed*” and the output ES = 4 indicates “*RF interference detected*”. Moreover, the nature of RF interference determines a degree of impact on GNSS measurement.

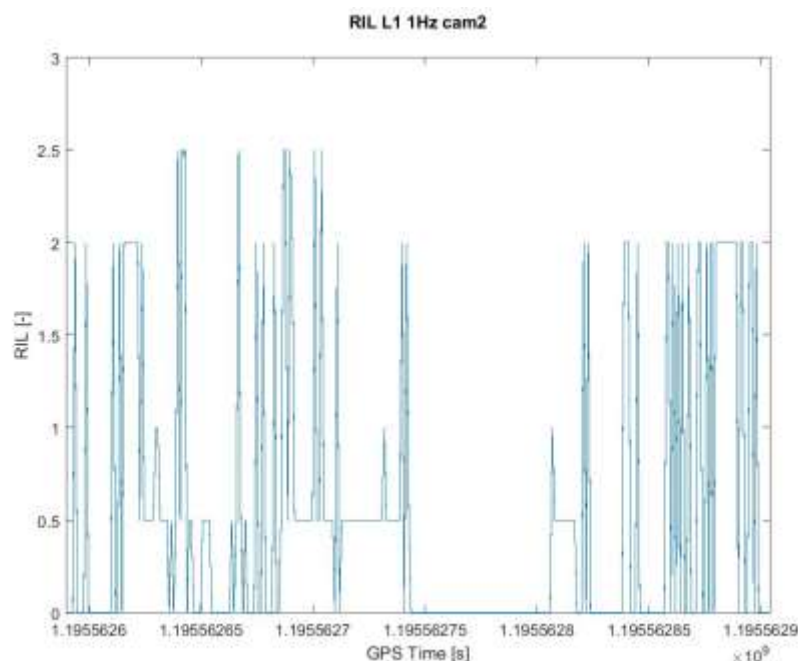


Figure 122: Case of camera measurement 2 – RIL_L1/E1 (1Hz output rate)

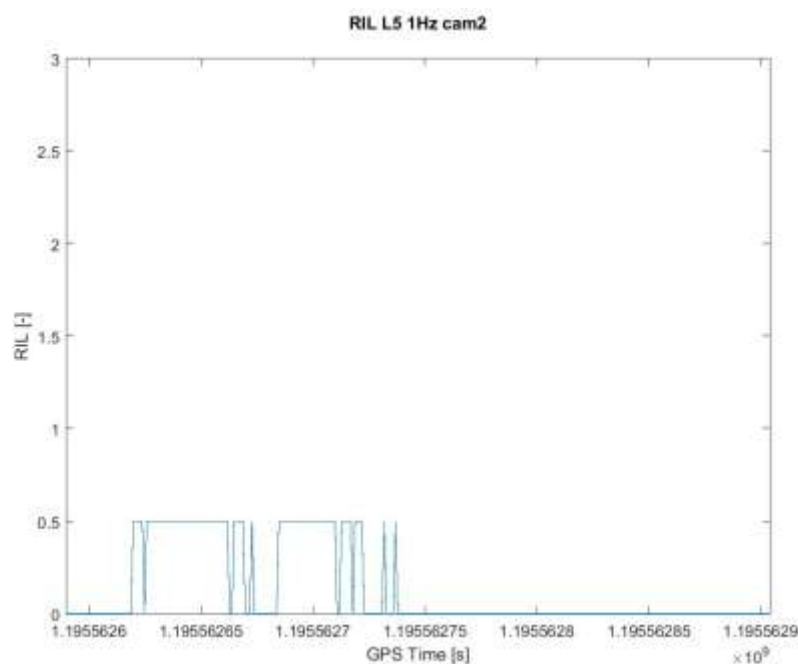


Figure 123: Case of camera measurement 2 – RIL_L5/E5 (1Hz output rate)

4.3.10 Case of panoramic camera measurement 3

The analysis is carried out from data obtained from measurement performed on November 24 (2017), at South Bohemia test track.

Source file of raw data: CVO_4250_1711241102_10H_10Z.SBF

Source file of reference position data: CVO_4250_1711241145_08H_10Z.RPO

Analysis carried out in GPS Time interval: 1195565698 s – 1195567545 s.

The real situation is depicted in Figure 124.



Figure 124: Case of panoramic camera measurement 3 (AZD test track at the South Bohemia)

The HNSE of EGNOS-based solution is presented in Figure 125, HNSE of GPS L1 solution is outlined in Figure 126. Both outputs are provided by composition of PP-SDK and RTKLIB solution outputs. The reference position is provided by ground truth. Increase of HNSE values from both position solutions occurs around time epoch 1195566120 s, between time epochs 1195566900 s - 1195567080 s and between time epochs 1195567350 s - 1195567400 s. Outputs of both solutions look correlated.

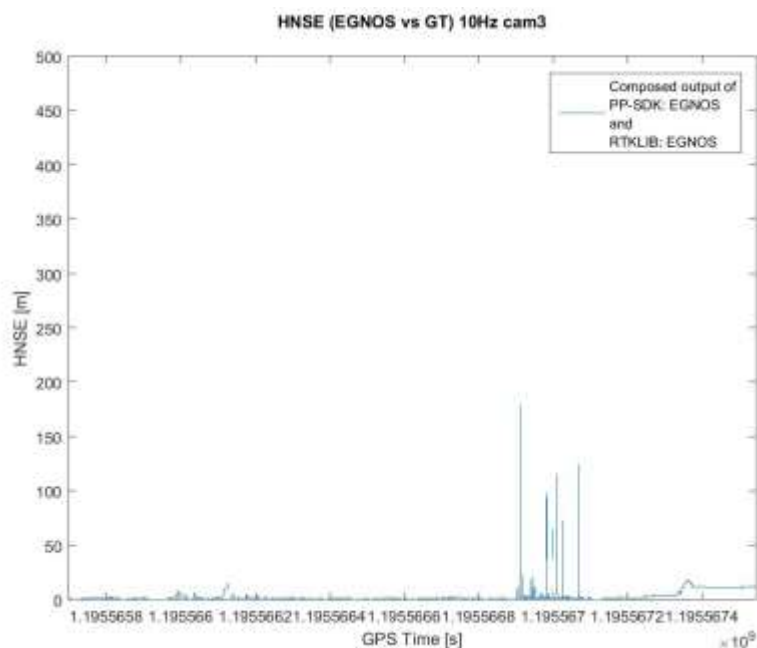


Figure 125: Case of camera measurement 3 – HNSE EGNOS values (10Hz output rate)

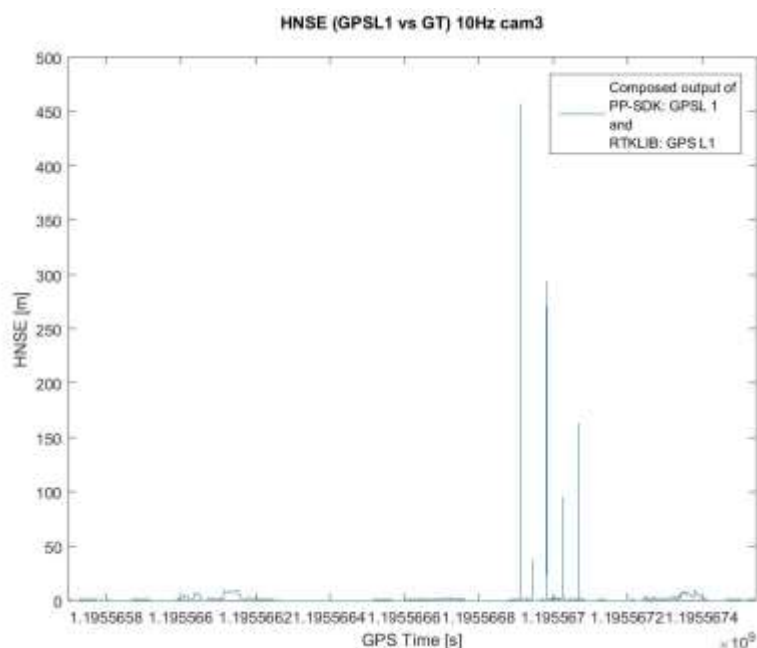


Figure 126: Case of camera measurement 3 – HNSE GPSL1 values (10Hz output rate)

The number of satellites is shown in Figure 127 and Figure 128.

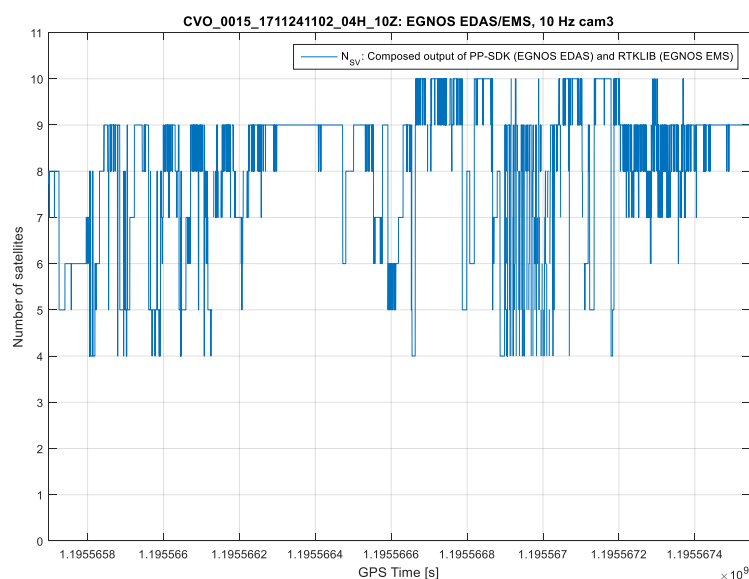


Figure 127: Case of camera measurement 3 – Number of satellites (EGNOS solution)

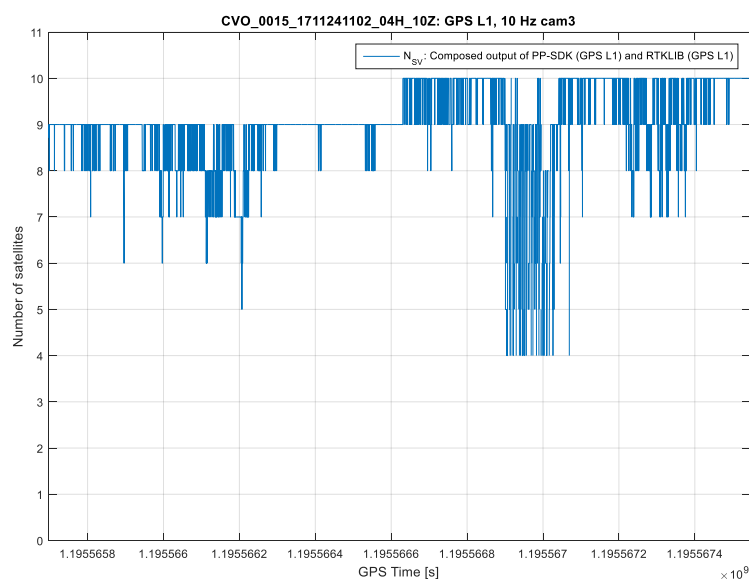


Figure 128: Case of camera measurement 3 – Number of satellites (GPS solution)

The train speed profile is presented in Figure 129. PDOP parameter is depicted in Figure 130.

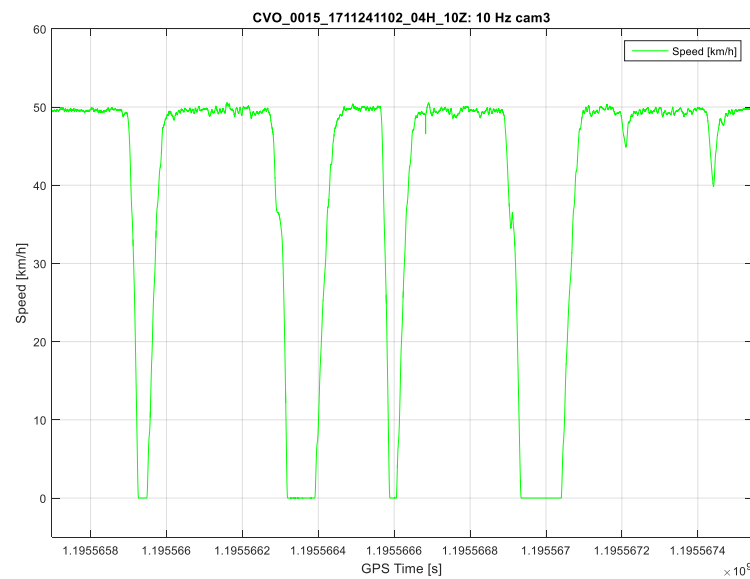


Figure 129: Case of camera measurement 3 – Train speed profile

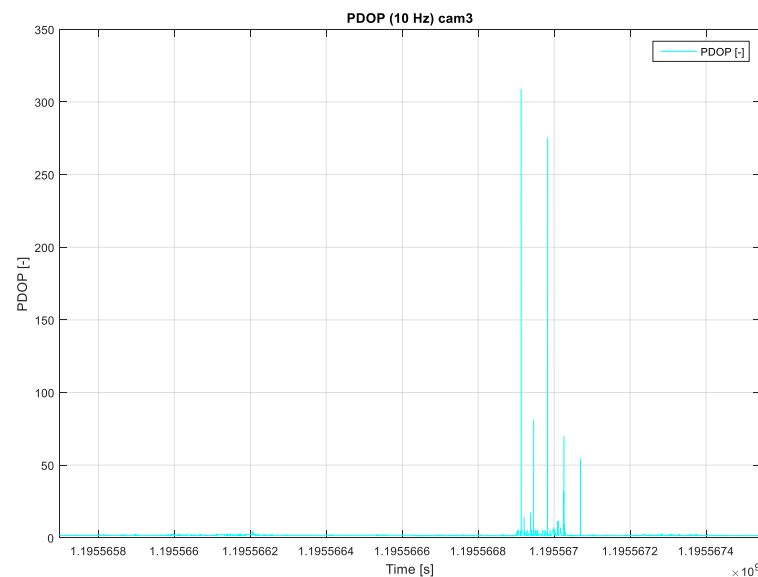


Figure 130: Case of camera measurement 3 – PDOP (10 Hz output rate)

Figure 131 shows MPL parameter values in the selected time range of this case for signal GPS L1 and output rate 10Hz. Stronger multipath is indicated around time epoch 1195566120 s, strong multipath between time epochs 1195566900 s - 1195567080 s, lower multipath between time epochs 1195567350 s - 1195567400 s. High values of multipath indicated by MPL in above time epochs are well correlated with high values of HNSE from both EGNOS and GPL L1 position solution.

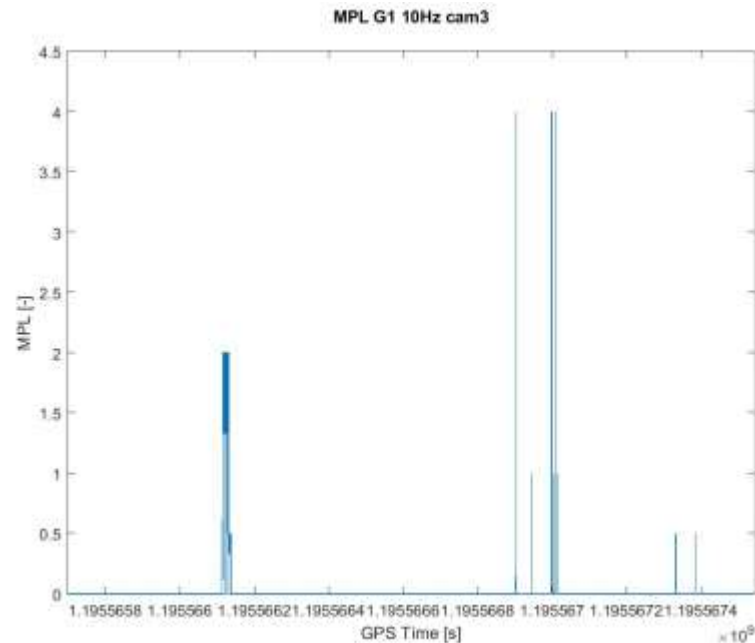


Figure 131: Case of camera measurement 3 – MPL_GPS_L1 (10Hz output rate)

SVF_{APV} parameter values are presented in Figure 132. There is well evident correlation of SVF_{APV} with both HNSE outputs and MPL for signals GPS L1 around time epoch 1195566120 s and in range of time epochs 1195567350 s - 1195567400 s. SVF parameter reaches its minimum values here, therefore unfavorable sky visibility conditions cause a decrease of a number of satellites in position solution, worse DOP and consequently higher values of HNSE.

The strong multipath indicated between time epochs 1195566900 s - 1195567080 s occurs during train standstill in station, when GNSS receiver is more prone to multipath effect. The standstill is indicated by roughly constant values of SVF_{APV} in time epochs 1195566900 s - 1195567100 s. But influence of RF interference cannot be excluded as short time outages in pseudorange measurement for some satellites happened under unchanged LOS conditions.

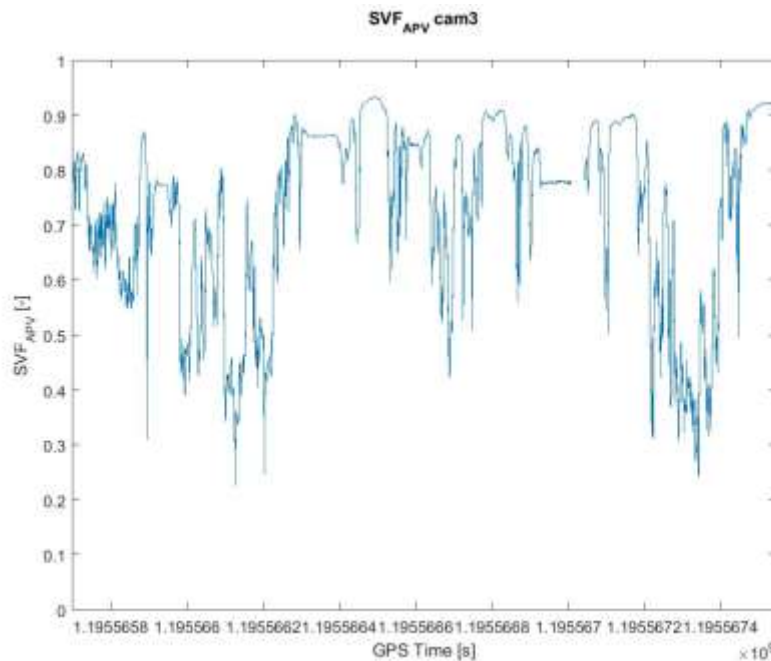


Figure 132: Case of camera measurement 3 – SVF_{APV} (1Hz output rate)

RIL parameter values for L1/E1 and L5/E5 bands are presented in Figure 133 and Figure 134. Often stronger RF interference is indicated in L1/E1 bands in selected time interval⁶. The strongest RF interference between time epochs 1195566900 s - 1195567100 s can contribute to high value of HNSE, but as it was already written in Section 4.3.8, the impact on GNSS measurement depends on a nature of RF interference. Low level RF interference is also indicated in L5/E5 bands in selected time interval.

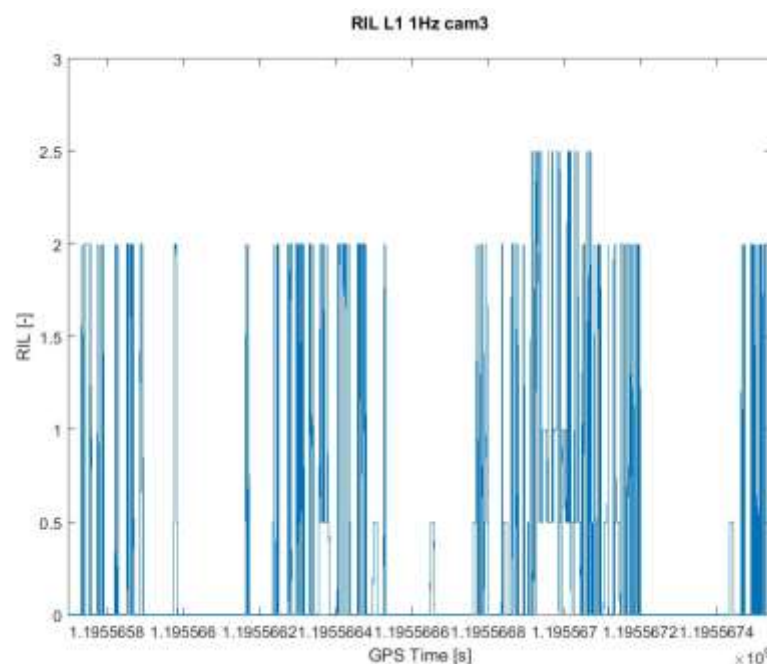


Figure 133: Case of camera measurement 3 – RIL_ L1/E1 (1Hz output rate)

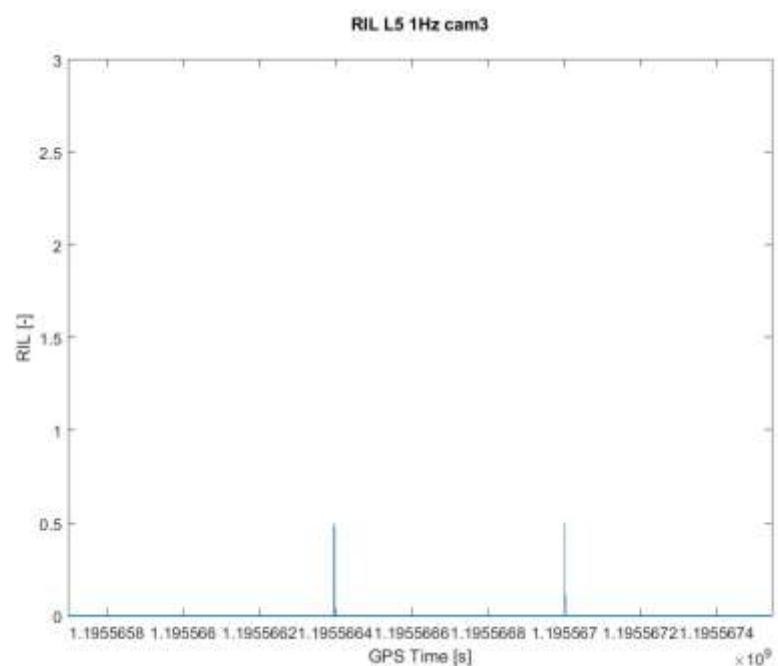


Figure 134: Case of camera measurement 3 – RIL_ L5/E5 (1Hz output rate)

4.3.11 Case of panoramic camera measurement 4

The analysis is carried out from data obtained from measurement performed on November 24 (2017), at South Bohemia test track.

Source file of raw data: CVO_4250_1711241102_10H_10Z.SBF

Source file of reference position data: CVO_4250_1711241145_08H_10Z.RPO

Analysis carried out in GPS Time interval: 1195569947 s – 1195572139 s.

The real situation is depicted in Figure 135.

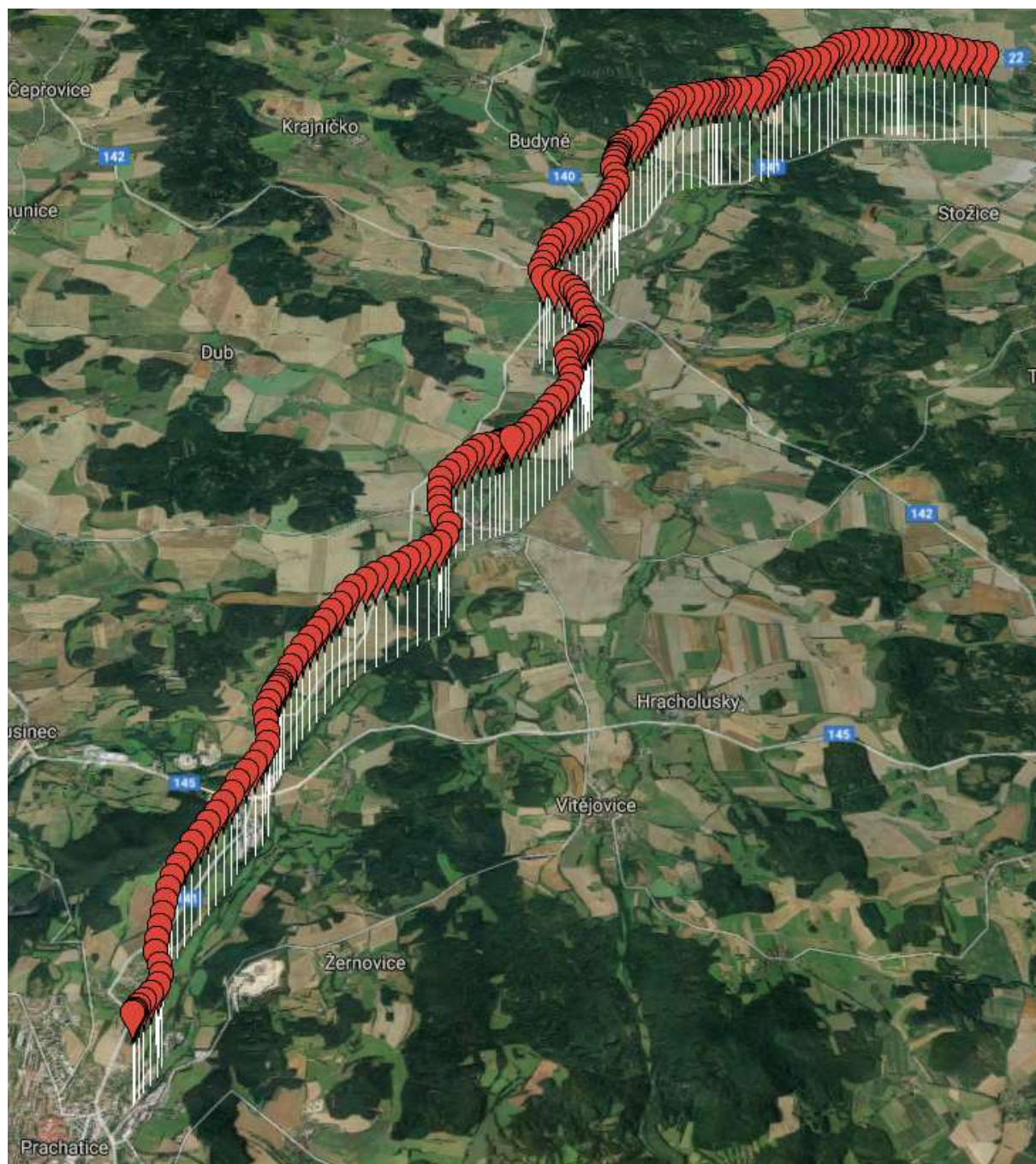


Figure 135: Case of panoramic camera measurement 4 (AZD test track at the South Bohemia)

HNSE of EGNOS position solution is presented in Figure 136, HNSE of GPS L1 position solution is outlined in Figure 137. Both outputs are provided by composition of PP-SDK and RTKLIB solution outputs. The reference position is provided by ground truth. The difference between peak magnitudes of HNSE from EGNOS and HNSE from GPSL1 is caused by above mentioned composed output of the solutions. Increase of HNSE values from both position solutions occurs around time epochs 1195570220 s, 1195570630 s, 1195571090 s and 1195571520 s. Outputs providing both solutions seem to be correlated.

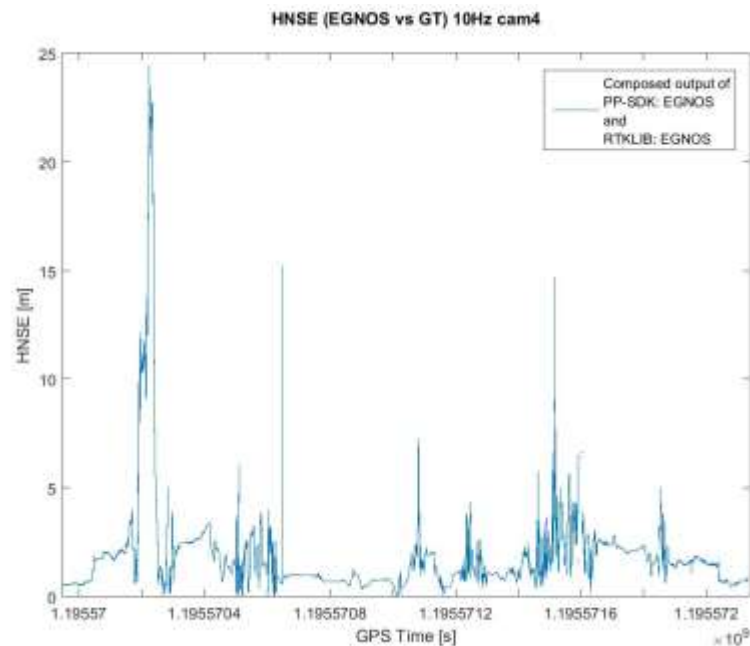


Figure 136: Case of camera measurement 4 - HNSE EGNOS values (10Hz output rate)

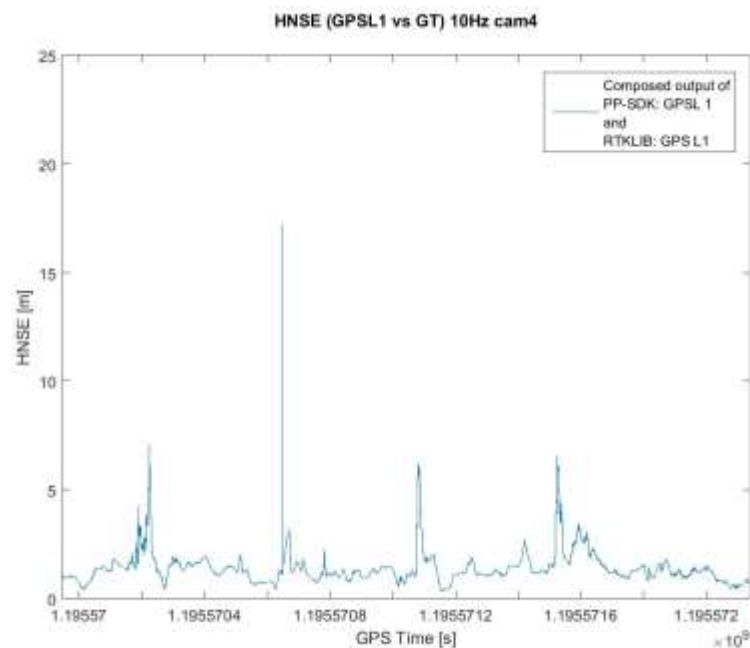


Figure 137: Case of camera measurement 4 - HNSE GPSL1 values (10Hz output rate)

The number of satellites is shown in Figure 138 and Figure 139.

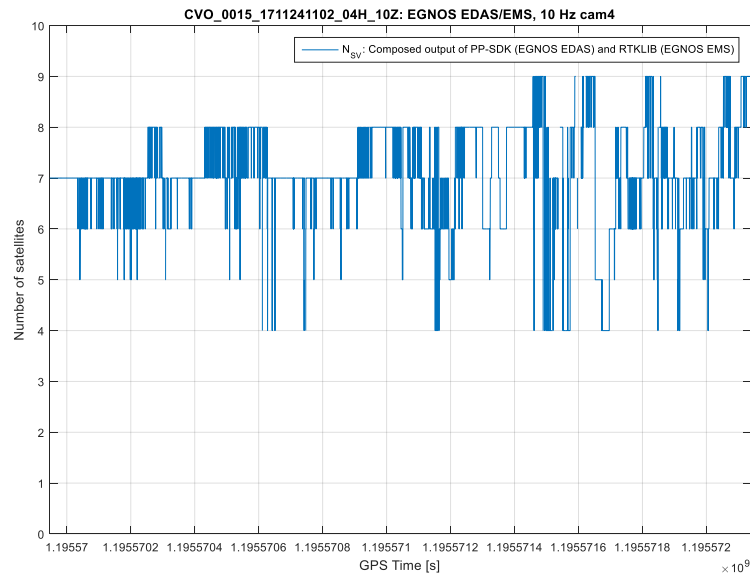


Figure 138: Case of camera measurement 4 – Number of satellites (EGNOS solution)

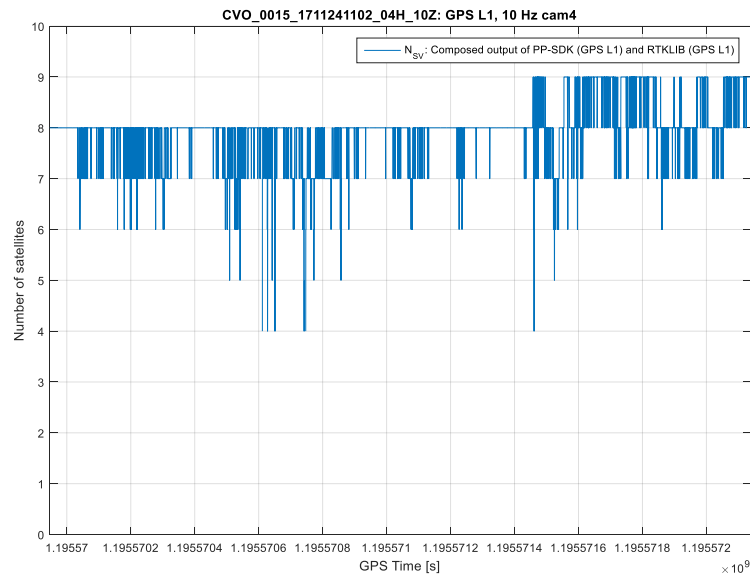


Figure 139: Case of camera measurement 4 – Number of satellites (GPS L1 solution)

The train speed profile is presented in Figure 140. PDOP parameter is depicted in Figure 141.

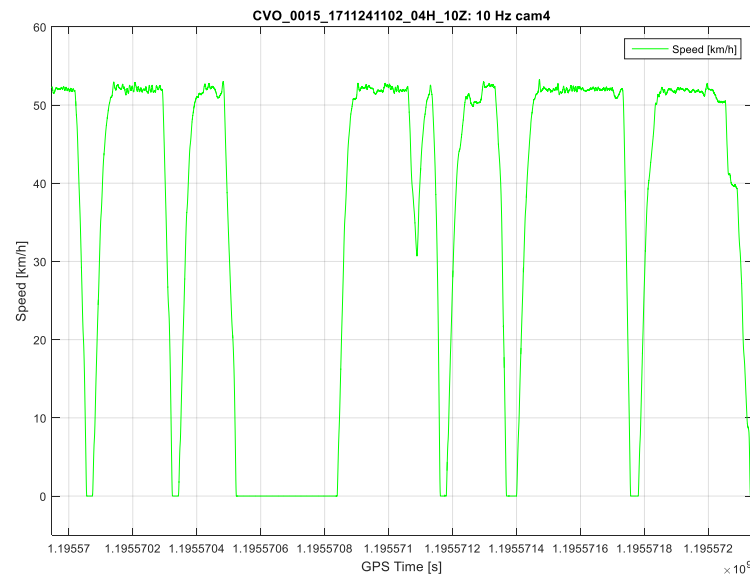


Figure 140: Case of camera measurement 4 – Train speed profile

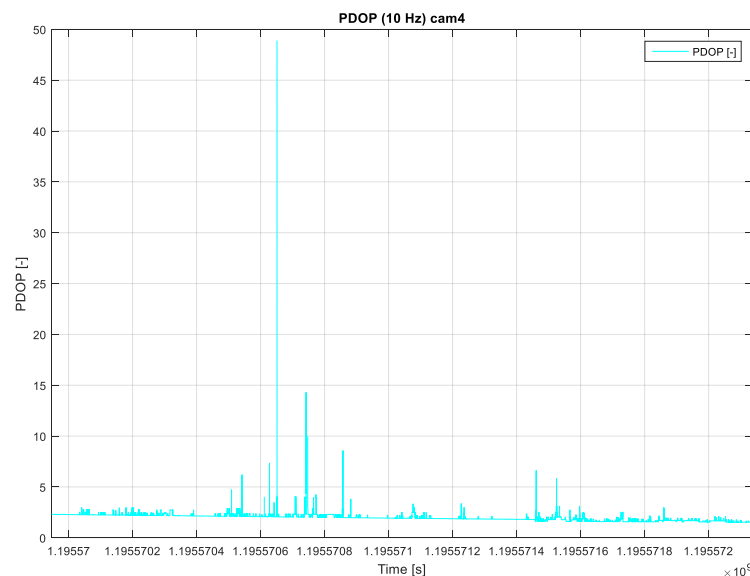


Figure 141: Case of camera measurement 4 – PDOP (10 Hz output rate)

Figure 142 shows MPL parameter values in selected time range of this case for signal GPS L1 and output rate 10Hz. Strong multipath is indicated around time epoch 1195570630 s, lower multipath between time epochs 1195570450 s - 1195571000 s and around time epoch 1195571510 s. High values of multipath indicated by MPL in above time epochs are well correlated with high values of HNSE from both EGNOS and GPL L1 position solution.

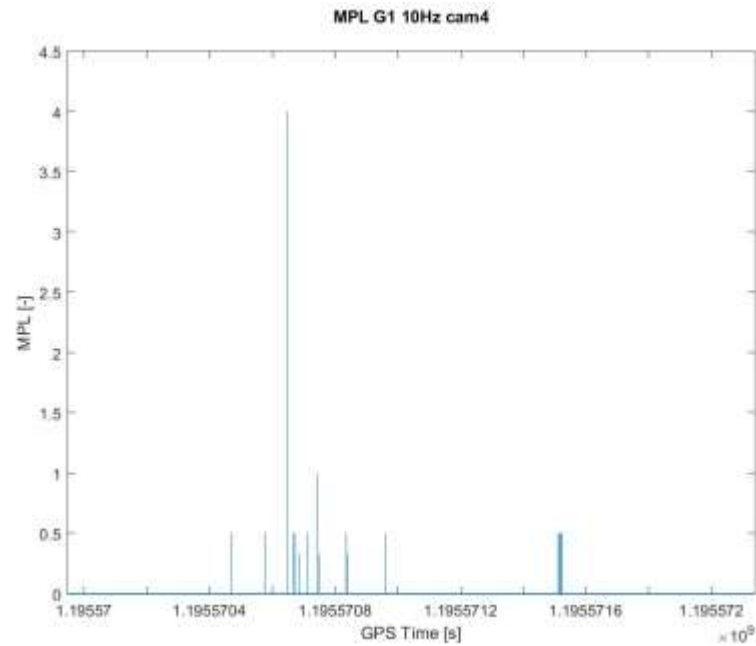


Figure 142: Case of camera measurement 4 – MPL_GPS_L1 (10Hz output rate)

SVF_{APV} parameter values are presented in Figure 143. As could be seen in Figure 136 and Figure 137 there is well evident correlation of SVF_{APV} with both HNSE outputs around time epochs 1195570220 s, 1195571090 s and 1195571520 s. SVF parameter reaches its minimum values around these epochs. Therefore, similarly to the case of camera measurement 3, there are presented unfavorable sky visibility conditions in this track section which cause a decrease of a number of satellites in position solution or worse DOP and consequently higher values of HNSE.

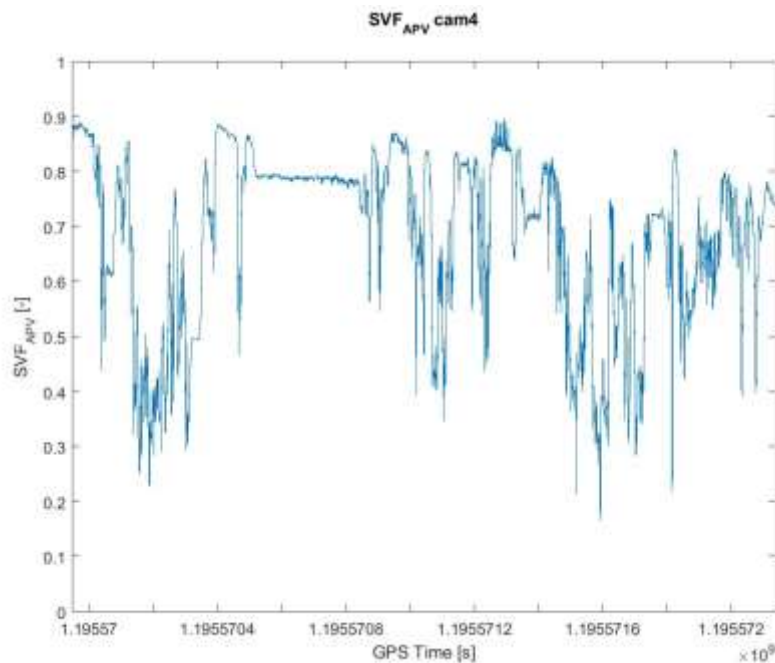


Figure 143: Case of camera measurement 4 – SVF_{APV} (1Hz output rate)

The strong multipath indicated around time epoch 1195570630 s occurs during train standstill in station when receiver is more prone to the multipath effect. The standstill is indicated by roughly constant values of SVF_{APV} in time epochs 1195570450 s - 1195571000 s. RF interference influence cannot be excluded for the reason of short time outages in pseudorange measurements for some satellites under unchanged LOS conditions.

RIL parameter values for L1/E1 and L5/E5 bands are presented in Figure 144 and Figure 145. Similarly to Section 4.3.8, the observed RF interference was mostly detected and probably partially suppressed by the receiver as the output $ES = 1$ indicates “*RF interference detected and suppressed*” and the output $ES = 4$ indicates “*RF interference detected*”. Moreover, the nature of RF interference determines a degree of impact on GNSS measurement.

Stronger RF interference is indicated in L1/E1 bands in selected time interval⁶. The strongest RF interference visible roughly between time epochs 1195570500 s - 1195570850 s can contribute to high value of HNSE, but due to the time limit of the project, the proportion of RF interference in HNSE could not be analyzed. Low level RF interference is also indicated in L5/E5 bands in selected time interval.

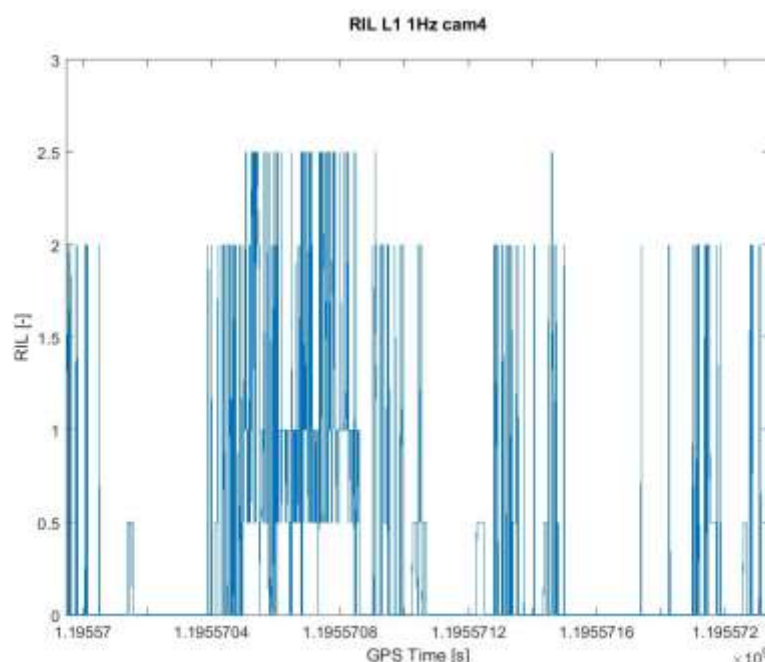


Figure 144: Case of camera measurement 4 – RIL_L1/E1 (1Hz output rate)

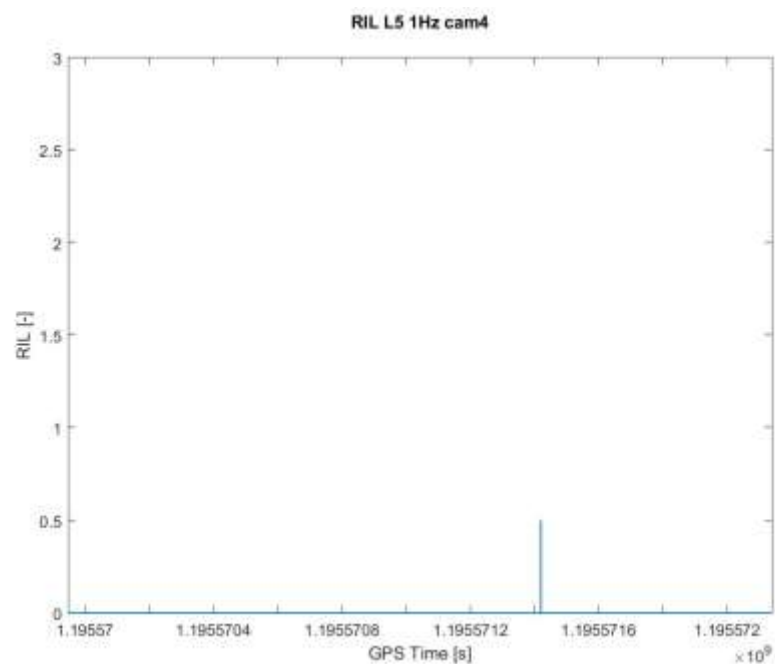


Figure 145: Case of camera measurement 4 – RIL_L5/E5 (1Hz output rate)

4.4 RAILWAY ENVIRONMENT CHARACTERIZATION – EVALUATION OF RESULTS

The main goal of WP4.3 is the characterization of the railway environment from the perspective of its impact on the GNSS signals. Three parameters MPL, RIL and SVF have been proposed for the characterization with supposition of their orthogonality.

The results obtained from the analysis of selected scenarios indicate that the proposed solution for the railway environment characterization, i. e. characterization of the environment by three scalar parameters, is correct and applicable in the future. Even though the outputs of some WP4.3 sub-tasks described in Table 1 were not used in both the analysis and the calculation of MPL and RIL, these parameters are already capable to indicate with a high probability the location where local negative effects can occur. Significant correlation of all the three parameters and HNSE was proven in selected analyzed scenarios. However, it would be desirable to process and analyze all measured data in terms of statistics to find out the real efficiency of the proposed solution.

It was also shown in the analysis that each of the three proposed parameters has an irretrievable role in the characterization and complements each other in the detection of negative local phenomena.

Several important findings have been made in the carried out analysis.

4.4.1 Higher multipath in a forest

The AZD test track in South Bohemia often passes through forest in its southern portion. Presence of a higher level of the multipath was observed (indicated by the MPL parameter) in Section 4.3.6, in a case when the train passes through the forest. Strong correlation of MPL and HNSE confirms multipath as one of sources of HNSE error. The consequence of this finding could be a requirement to develop and implement different error budgets for different railway environments, in which different algorithms for the calculation of the protection level are to be used. The algorithm dedicated for unfavourable conditions of GNSS signal reception will provide higher, but more credible value of the protection level compared to the algorithm for standard conditions. It could be useful if the accuracy requirement of an application is low in the area with such conditions. Apart from that, the implementation of an onboard function for online multipath detection will be desired.

4.4.2 High multipath during standstill in a station

The higher multipath level was observed in several cases in a station, see sections 4.3.2, 4.3.10, 4.3.11. It's known that stationary GNSS receivers can be more affected by multipath than moving GNSS receiver. In future GNSS based railways applications appropriate technique should be included to handle multipath effects during train standstill, e.g. the integration of an optical or a microwave sensor for detection of train standstill.

4.4.3 RF interference

Stronger RF interference mainly in L1 bands was indicated by a significant increase of RIL parameter in Sections 4.3.5, 4.3.10, 4.3.11.

In a case in Switzerland, the RF interference was repeatedly observed during train acceleration after stopping in railway stations. There was a clear correlation between an increase of the RIL parameter and the HNSE. Processing and analyzing data from RF measurements showed increased RF interference during train acceleration. This suggests that the source of RF interference is onboard the train, e.g. the traction system. It should be investigated whether the installation of the GNSS antenna in another location or a different routing of the antenna cable in different position in the train could mitigate such RF interference, or whether the interference created by the train would have to be reduced.

In case of the test track in South Bohemia, the detected RF interference had a different nature. Strong RF interference appeared mainly in stations during train standstill, lower RF interference also

during the train run. Because the RF interference was not detected in the beginning of the measurement campaign with that train, it seems that the source of RF interference could probably be a newly installed device onboard the train.

It's evident that railway vehicles intended for installation of GNSS technology should be tested on EMI, and that the GNSS antenna, receiver and cables should be installed in suitable location and as far as practical from potential sources of RF interference.

4.4.4 Lower value of HNSE from GPS L1 position solution compared to EGNOS position solution

In several cases it was observed that the HNSE provided by GPS L1 solution is lower than HNSE provided by an EGNOS-based solution. The reason is probably PP-SDK/RTKLIB solution. Primarily, PP-SDK is used for HNSE calculation. But occasionally position solution is not provided by PP-SDK for reason of e.g. "Error=1: Not enough measurements" or "Error=8: Not enough differential corrections available". In these cases position solution provided by the RTKLIB is used for HNSE calculation.

4.4.5 High detection efficiency of panoramic camera

Based on results of analyzed cases with panoramic camera, it can be stated that the panoramic camera represents a highly efficient and powerful device for the railway environment characterization.

Analysis carried out in Sections 4.3.8 to 4.3.11 shows strong correlation between higher values of HNSE and minimum values of SVF_{APV} also in locations where MPL is negligible. These events are well visible mainly in Section 4.3.11, in Figure 136, Figure 137 and Figure 143.

The higher values of HNSE are more often caused by insufficient sky visibility conditions compared to multipath in case of such line like the line in the South Bohemia. In a case of the Sardinia test track and analysis in Section 4.3.3, it can be supposed that the cause (a road bridge) of high values HNSE could be successfully detected just by the panoramic camera.

The main advantage of the camera measurement is to provide a data set (images) for the sky visibility mask determination or the detection of the obstacles that could be a potential source of multipath within only one measurement due to nearly stationary nature of the track surroundings.

Preliminary results from the correlation in position domain analysis as described in Section 2.2.2 confirm this advantage of the camera. Strong correlation of SVF was found at the same place in different times. Contrary, smaller correlation of MPL or RIL was observed at the same places in different times as MPL and RIL are time dependent at the least (MPL due to a change of constellation, RIL due to irregular time of occurrence RF interference). The only exception concerning repeated RF interference (and correlation of RIL) was presented by SIE in a case of "Train acceleration from a station". There RF interference is presented every time when train accelerates on departure.

The use of the camera is limited by visibility conditions, night and bad weather conditions represent significant constrains. But terrain profile surrounding a track is almost stationary, so there is a need for only a few train runs under optimal visibility conditions.

4.4.6 HNSE, MPL and RIL dependency

In several analyzed cases (see Sections 4.3.5, 4.3.10, 4.3.11) strong correlation has been found between high values of HNSE, MPL and RIL. As it was already described in Section 4.3.5 in these cases, RF interference seems to be the primary cause of high HNSE, either due to a loss of lock of some satellites or the introduction of additional noise to the pseudorange measurements (in this way it can indirectly contribute to high value of MPL).

The separate analysis of measured data from the campaign in Switzerland, prepared by Siemens [11], describes repeated train runs where HNSE increases during train acceleration after stopping in a station and GNSS receiver switching from the SBAS aided mode to the Stand-Alone mode. The RF interference could be one of causes⁷ of these increases.

The confirmation of this hypothesis requires a deeper analysis of the data from RF measurements and GNSS receiver raw data.

4.4.7 Reference position error

It was considered that the accuracy of the RPO would be sufficient considering how it was generated. But it is evident that the RPO inaccuracy is high in some cases. It was revealed during the analysis [10] that the travelled distance (longitudinal) error of the ground truth reached up to 7 meters. This fact should be taken into account in a case of some future analysis. Such high value of the reference position error can evidently overpass the error of EGNOS position solution. It can result in wrong HNSE determination, which can exceed the protection level and cause false alarm in the analysis. Solution of this problem could be the use of reference position from GNSS carrier-phase solution, which provides one to two order better precision compared to EGNOS position solution, or improvements to the way the RPO is generated.

4.4.8 Software tools for analysis

As described in the origin of Section 4.3, different HNSE values were obtained from different software tools for the same input data from the Septentrio receiver in the first comparisons. Step by step, various causes were discovered and mitigated. But some differences in calculated HNSE still remain. One of the reasons for the difference in results is the impossibility to set all important parameters related to PVT. Various SW tools have also different options for setting of their parameters. Another reason is the inability of SPRING (as well as TEQC) to properly decode data from .SBF files if the data of both antenna inputs of the Septentrio receiver are simultaneously recored. This fact should be considered if re-execution is intended.

It can be seen from all the cases analyzed that SPRING provides the highest availability of position solutions and hence HNSE as compared to RTKLIB and PP-SDK. RTKLIB and PP-SDK exhibit alternately sufficient availability. PP-SDK solution availability is limited by GDOP value equal to 15 and also EGNOS data availability. RTKLIB solution is more sensitive to presence of obstacles and multipath.

Generally, it can be concluded that the software tools developed primarily for purpose of position calculation are less suitable for detection of the negative phenomena (e.g. multipath) than the software tool developed for GNSS data analysis. However, the use of more mutually independent sw tools in analysis is desired to check results provided by these sw tools.

4.4.9 Receivers for railway environment characterization

The Septentrio AsteRx4 receiver was selected for common measurement set used in all three measurement campaigns. Optionally, U-blox Neo M8T and JAVAD TRE-G3T receivers were installed in some measurement sets and connected to the common antenna together with AsteRx4 receiver. An analysis of segment of raw data from all above receivers was investigated for such time epochs, where a significant increase of HNSE was observed during standstill. It has been found that the AsteRx4 receiver loses several satellites in a short time, but the other receivers have been able to track these satellites at the same time epoch. More detailed analysis is not feasible due to the different sampling frequency of the GNSS receivers. This fact opens a question on suitable GNSS receivers for the measurement of reference raw data for the railway environment characterization.

⁷ GNSS raw data analysis by Thales Alenia Space France has shown that the expiration of the EGNOS data may be another cause.

Probably, only some standardized receiver disposing suitable parameters and providing a complete set of raw data without any constraints or filtering should be used.

4.4.10 Necessity of measurement

The classification of the railway environment should be an objective process whose one part has to be a measurement. The reason is that the railway environment can be divided into discrete categories only in some cases where the environment is sufficiently homogenous. In other cases the effort to classify the environment would be an extremely complex and theoretical task, as too many parameters would have to be considered, e.g. how many buildings are in track vicinity, their sizes, shapes, materials, distances and direction vectors from a track, etc., similarly in case of a forest, in case of a transition between environments or a mix of environments. Only measurements as carried out in WP3 of the STARS project can provide the necessary information to characterise of railway environment. The panoramic camera can be effectively used for quick and reliable mapping locations where multipath, lower number of satellites or poor constellation (geometry) can be expected.

It has to be noted however that the railway environment will change over time, measurements might therefore have to be repeated regularly to keep track of these changes.

5 RELATION OF CHARACTERISTICS TO THE POSITION OF MEASUREMENT

5.1 POSITION DEPENDENCY OF ENVIRONMENT CHARACTERISTICS

The proposed set of characteristics (SVF, MPL and RIL) is position dependent. However, in the future it seems practical (from the perspective of foreseen applications) to “defocus” this position dependency. The term “defocus” means to release characteristic dependency on the position. There are two reasons why to do this: a) the process of characteristic determination becomes simpler since position accuracy is not so crucial, b) the approach also matches with one possible way of utilization of GNSS in railway signalling applications (see section below regarding Virtual Balise Placement).

The process of defocusing is explained below.

To evaluate a railway line for the further deploying of GNSS based signalling systems, the environment characteristics (SVF, MPL, RIL) are determined at discrete points uniformly distributed along the track. The term “*determination of characteristics*” covers both a train test run which does appropriate measurement and also successive data processing to estimate these characteristics. The characteristics determined in these discrete points are then grouped into overlapping windows. In each window the resulting characteristic is determined in a conservative manner, meaning that the worst case value from the window is selected as characteristic representing the environment in the position of the window center. The length of the window should be related to the max. train speed. The values in the windows can be weighted before the selection of the worst case due to enabling the potential penalization of values near the window margin.

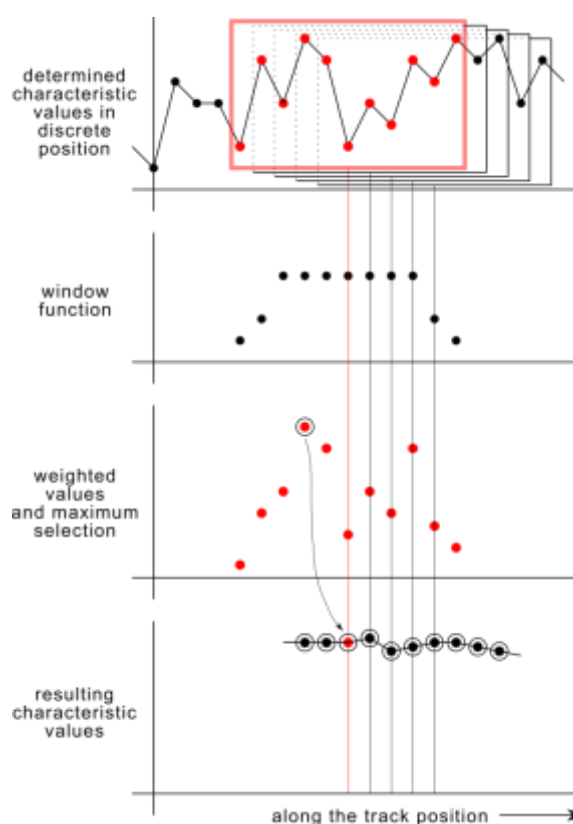


Figure 146: “Defocusing” the characteristic position dependency

The process can be described with the following formula

$$C_i = \max\{W_{-N}C_{p(i-N)}, W_{-N+1}C_{p(i-N+1)}, \dots, W_0C_{pi}, W_1C_{p(i+1)}, \dots, W_NC_{p(i+N)}\},$$

where C_{pi} is a value of determined characteristic at the i -th point on the track. The W means weighting factors of weighted window with the length $2N+1$. The resulting characteristic is denoted as C_i . Symbols C_{pi} and C_i represent one of SVF, MPL, or RIL. Note, the equation with the $\max\{\}$ is applicable for MPL and RIL only, equation for SVF has to have $\min\{\}$.

The process described with the previous equation is depicted in Figure 146.

5.2 VIRTUAL BALISE PLACEMENT

Virtual Balise (VB) is one of the proposed concepts which enable the introduction of GNSS into ETCS. As an advantage of VB concept, a minimum of changes in current ETCS is supposed, this is a reason why VB is analyzed in frame of UNISIG and related projects (NGTC WP7, Shift2Rail).

The section justifies the reason of defocusing of position dependency of characteristics (SVF, MPL, RIL) but here from the application perspective. It is worth noting that this is not strictly related to VB concept but rather to the way of GNSS utilization in an application.

Consider that a Virtual Balise (VB) is “placed” into the specific position on the track. The environment requirements, which guarantee the GNSS performance of this VB, have to be kept not only for this exact position but also in the region before and after this position along the track. The rationale behind this is the fact that the GNSS receiver yields position fixes in the regular time interval (the most common interval is 1 second) and cannot be ensured that the GNSS receiver would yield the position fix exactly in the position of VB. The need of this region was already mentioned in NGTC WP7.3, where the term VB Environment (VBE) is used, see [16].

The length of the VBE should be related to the maximum allowed speed in the track segment and also to the number of position fixes required for Virtual Balise detection.

Besides the VBE, there should be defined another region, which precedes the VBE in the direction of train move. In frame of NGTC WP7.3, the term VB Pre-environment (VBP) is used for this region, see also [16]. While the VBE should have relatively strict requirements due to its role to guarantee the GNSS performance, the VBP should mainly ensure that the GNSS receiver can acquire and track GNSS signals. Note that depending on the concept of how EGNOS is being included, the VBP must also ensure that EGNOS data is received, which requires significantly more time than tracking GPS or Galileo signals.

The length of VBP should be also related to the maximum allowed speed in the track segment and also to the receiver acquisition time.

The situation of both VBE and VBP is depicted in Figure 147.

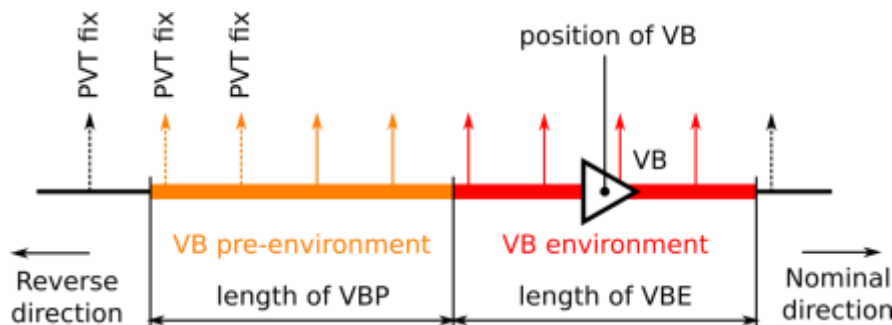


Figure 147: Relation of regions VBE and VBP

6 RECOMMENDED FUTURE ACTIVITIES

The task Railway environment characterization required very complex and time-consuming analysis. Even though extensive analysis has been performed on a significant amount of collected data there are some open issues which are worth to be investigated further in frame of future research projects. The following list contains a number of these issues:

- Different statistics could be elaborated such as a frequency of occurrence of strong multipath or RF interference with significant influence on HNSE, a correlation rate between HNSE and MPL/RIL, a rate of successful detection of multipath or RF interference for individual methods, a rate of undetected cases of high HNSE etc. It could provide better knowledge on the railway environment from GNSS perspective and also information on efficiency of the individual methods employed in the algorithm evaluating the railway environment in Task 4.3.7.0.
- Processing and analysis of additional recorded raw data is required for generating the above mentioned statistics.
- Correlation in position domain could confirm the correctness of the already developed approach for characterizing the railway environment. It could also help to improve the setting of the weights both for the outputs of the individual methods and magnitudes of the output values in the algorithm of Task 4.3.7.0.
- A more detailed analysis of the RF spectrum and detected interferences in measured data could provide knowledge on the nature of the RF interferences.
- General C/N_0 analysis of RHCP signals could bring additional information on the presence of multipath or RF interferences and a justification of HNSE values in interesting cases.
- The integration of the outputs from sub-task groups 4.3.4 and 4.3.5 (not included in present analysis in Task 4.3.7.0 due to limited time for the analysis) into the overall analysis in Task 4.3.7.0 (in matlab script t4370) could improve multipath detection efficiency and provide more information on the nature of RF interferences.
- A complementary analyses of interesting cases could provide explanation of issues, which are currently not understood, e. g. an analysis of the cases where the MPL for L1/E1 is lower than MPL for L5/E5, or could bring better knowledge on the resistance of Galileo signals against multipath and RF interferences, e. g. a comparison and an evaluation of HNSE from different position solutions including Galileo signals E1, E5.

7 SUMMARY

The results from this work package can be summarised as follows:

- Significant distortions of GNSS signals have been observed and documented on all of the analysed lines.
- The distortions are being caused by multipath effects, by limited visibility of satellites and by electromagnetic interferences.
- Many of the techniques applied to detect the presence of interferences show good correlation with the observed position errors.
- The following observations have been made in regards to the environment:
 - Forests seem to generate significant multipath
 - Multipath is also significantly higher at standstill
 - RF interferences have been observed on the electric train during train acceleration
 - The panoramic camera can give an indication where sky visibility is limited

The following observations have been made in regards to the tools and procedures used in the STARS project:

- Producing ground truth based on fixed position markers and odometry is critical, as longitudinal position errors of several meters have been observed.
- Producing ground truth based on PP-SDK is limited to locations with sufficiently good GNSS coverage
- When using different tools to perform identical analysis some differences in the output have been observed.
- Some tools also sporadically produce erroneous outputs, so care has to be taken when interpreting the results
- Receivers used to record raw data show different behavior, especially at standstill, probably due to some internal filtering which can not be disabled

The following remarks are related to the execution of the data analysis in WP4:

- The WP4.3 was a very complex and time consuming task. It required very high effort of all WP4 members as each WP4 member solved one or more particular sub-tasks.
- The output of WP4.3 comprises not only the analysis and its results, but also includes many important specifications/documents, which had to be developed and continuously updated to perform the analysis and reach the calculated results, e. g. the methodology for comparison in position domain [12], the methodology for different modes of position calculation [13], the specification of format of output data for different sub-tasks [5], [9], [12], [14], updating the file naming convention and the directory structure for calculated outputs in STARS repository [3], [4], the document on the discrepancy in HNSE [10], updating of STARS data inventories [17], [18], [19].
- In each sub-task of WP4.3 the particular solution was proposed and described, appropriate scripts were developed, preliminary result analysis carried out and proposed thresholds justified.

8 REFERENCES

- [1] Deliverable 4.1 Data post-processing, STR-WP4-T-SIR-012-01, September 2016
- [2] Deliverable 4.2 Reference Data Set, STR-WP4-D-AZD-092-03, November 2017
- [3] Database Concept Proposal, STR-WP4-T-SIR-012-01, September 2016
- [4] TN Conventions for File Naming Directory Structure and Time Stamps.docx, STR-WP3-T-AZD-018-05, 19th September, 2017
- [5] Specification of output files, STR-WP4-T-AZD-091-02, October 2017
- [6] Minimum Operational Performance Standards for Global Positioning System/Satellite-Based Augmentation System Airborne Equipment, RTCA DO-229, December 13, 2006
- [7] Interim MOPS for Galileo Civil Aviation Receiver, EUROCAE WG 62, July 2005
- [8] Assessment of Radio Frequency Interference Relevant to the GNSS L5/E5A Frequency Band, RTCA DO-292, Sept. 2004
- [9] Output file format of Task 4.3.7.0 – Railway environment characterization, June 2018
- [10] Discrepancy in HNSE between outputs from WP4.3 and WP5.2, STR-WP4-T-AZD-112-01
- [11] Data Analysis - Domino, STR-WP4-T-SIE-095-02, November 2017
- [12] Methodology of comparison in position domain, STR-WP4-T-AZD-082-02, October, 2017
- [13] T423 Post-processing computation of PVT, STR-WP4-T-AZD-059-09, September, 2017
- [14] Specification of reference data format, STR-WP4-T-AZD-080-02, October 2017
- [15] AsteRx4 Reference Guide, February 2016
- [16] D7.3 Definition of a standard process for GNSS signal coverage and accuracy measurement. NGTC deliverable, version 10, 2017-03-06
- [17] STARS Data Inventory_AZD_v9.xlsx, May 2018
- [18] STR-WP4-T-ANS-115-01_-_STARS_Data_Inventory_ANSALDO_v3.xlsx, December 2017
- [19] 20180514 STARS Data Inventory_Siemens.xlsx, May 2018

9 APPENDIX 1 – DESCRIPTION OF SELECTED TECHNIQUES FOR NEGATIVE PHENOMENA EVALUATION

The structured description of each task employing selected technique for the evaluation of negative phenomena in frame of WP4.3 was elaborated by responsible partner and is provided in this Appendix 1.

Note 1

Four similar techniques were selected for evaluation of negative phenomena occurrence by comparison in position domain as presented in Table 1. Due to similarity of these techniques the common methodology [12] for calculations had to be developed in order to reach comparability of results of these techniques.

9.1 ANALYSIS BASED ON COMPARISON OF ANTENNA POSITION FROM PSEUDORANGE SOLUTION AND REFERENCE ANTENNA POSITION BASED ON GT (TASK 4.3.2.1)

RESPONSIBILITY

The task is performed in the responsibility of BT.

OBJECTIVE

The aim is to analyze the train run data recorded and check it for degradation and anomaly events of the position outputs over time. Analyzed parameter value (APV) and Evaluation symptom (ES) should be assigned to the related timestamps for further analysis.

The dedicated task 4.3.2.1 evaluates a subset of the train run data, which have PVT output calculated without differential corrections available. The task scope has to focus on the analysis of position using the post processed non GNSS corrected PVT only, from task 4.2.3.

INPUT

GT based reference position data and PVT data over time is available from the measurement database in the cloud for each train run to be analyzed.

Reference data set stored in Google cloud provides PVT data from activity 4.2.3 and ground truth based reference antenna position data from activity 4.2.5.

The post-processed PVT used will be from the Septentrio receiver only and will be the uncorrected PVT from activity 4.2.3 which are files with suffix (uf) 03 Autonomous GPS L1, 05 autonomous Galileo and 07 GPS + Galileo.

Format of the input data is specified in the document Post-processing computation of PVT [13].

OUTPUTS

Generally, marked data for next analysis task, i.e. for identification of particular harmful factors. The output data format has to be in line with technical note on output format specification [5]. The output of the task will be an ASCII text file with a header part containing the used error threshold **GT_DeviationLimit** serving for evaluation of APV data and setting appropriate value of Evaluation symptom in dependence on analyzed GNSS performance.

Behind the file header valid for all measurements within the file, the data is listed beginning with the GPS time stamp in seconds, Evaluation symptom, ECEF coordinates of reference position of GNSS antenna in ITRF frame and calculated position difference at least.

DESCRIPTION

GNSS receiver PVT output for the reference antenna location on the train is compared to a GNSS independent ground truth position data set over time, calculated with an on-board offset matching to the GNSS reference antenna location on the train.

Compare antenna position of the train runs based pseudorange (GPS) PVT solution from activity 4.2.3 and GT based reference antenna position adjusted from activity 4.2.5 in order to detect presence of negative factors for position determination which contains the antenna offsets.

Propose error threshold for marking of data when GNSS performance decreases.

TOOLS

The tools of the GNSS receiver providers are preferably used for analysis of received satellite signals and GNSS receiver output data associated with its positioning solution.

- Septentrio **RX Tools** version 17.0.0 and former versions:
 - SBF Converter, version: 2.4.1
 - SBF Analyser, version 2.0.1

The Septentrio RX Tools are free for download after identification by an email address. Installation by copy is possible without admin rights on the windows computer.

- Mathworks **Matlab** R2012a / Octave is proposed for analysis after evaluation calculations from the receiver's measurements.
- **Google Earth** Version 7.1.2.2041 to visualize the KML Files generated by the Septentrio Receiver manufacturer conversion tools.

Automation of data processing will be introduced, when the amount of files to be analyzed is big enough, that automation increases overall efficiency of the analysis task.

ALGORITHM

There is a special script in Matlab/Octave performing the comparison of the pseudorange position estimation with the associated ground truth based reference position data.

The distance between the GNSS antenna position estimation and the GT based reference position of GNSS antenna at the same timestamp will be calculated and compared to an adjustable threshold **GT_DeviationLimit** in meters.

Depending on **GT_DeviationLimit** a corresponding value of Evaluation symptom is assigned for given timestamps in the output file.

This allows later to compare all sub-task outputs together and reliably evaluate GNSS signal disturbances in this way.

9.2 ANALYSIS BASED ON COMPARISON OF ANTENNA POSITION FROM PSEUDORANGE SOLUTION AND REFERENCE ANTENNA POSITION FROM PPK (TASK 4.3.2.2)

RESPONSIBILITY

The task is performed in the responsibility of Cetest and CAF I+D.

OBJECTIVE

The objective of subtask 4.3.2.2 is to evaluate the occurrence of negative phenomena causing GNSS degradation by comparison of PPK technique based position solution and estimated position from pseudorange solution.

An evaluation of the absolute error observed together with additional navigation parameters that may help identify PVT solution limitations are studied within this task.

INPUT

PPK aided PVT solution data and PVT standalone solution data over time is available from the measurement database in the cloud for each train run to be analyzed.

Reference data set stored in Google cloud provides PVT data and PPK based reference antenna position data from activity 4.2.3.

The post-processed PVT used will be from the Septentrio receiver only and will be the uncorrected PVT from activity 4.2.3 which are files with suffix (uf) 03 Autonomous GPS L1, 05 Autonomous Galileo and 07 GPS + Galileo.

Format of the input data is specified in the document Post-processing computation of PVT [13].

OUTPUTS

The outputs are presented as text file including the columns as described in the technical note on output format specification [5]. At least GPS time, Evaluation symptom, ECEF coordinates of reference position of GNSS antenna in ITRF frame and APV (analyzed parameter value, i.e. calculated position difference) will be included for identification of the time when GNSS signal may have been subjected to a disturbance. The error threshold value will also be included in a header part contained in the output file.

DESCRIPTION

In order to provide with a meaningful data analysis the following process is proposed. First of all, files containing pseudorange based position estimation and position calculated by PPK techniques are downloaded.

Once the download of the files is completed the comparison of the files using Matlab is performed. For that purpose the following steps are followed:

- The downloaded data will be imported into Matlab's Workspace.
- If necessary, the geodetic coordinates will be translated into ECEF WG84 coordinate system.
- The absolute error in each coordinate will be computed.
- Results will be compared with an absolute error threshold. All coordinate points that show an absolute error above the established limit will be marked through the appointed Evaluation symptom for further analysis.

To set the threshold correctly other interesting navigation parameters are intended to be analyzed. It is considered to download SBF files from the database and check its consistency with SBF

analyzer. These consistency checks consist of obtaining some graphs and corroborating the graphics are actually plotted and results make sense:

- Planimetric plot
- CN0
- Dilution of precision
- Standard deviation and residuals
- Number of satellites in view

These checks can also be supported by observation analysis in a Google Earth map based on PPK output data exported into a .kml file.

TOOLS

Hereafter listed the required tools:

- SBF analyzer
 - Name: Septentrio RxTools package includes SBF analyzer.
 - Supplier: Septentrio
 - License: Proprietary license
 - Version: RxControl 17.0.0
 - Description: RxTools is a combination of applications that work with any of the latest Septentrio GNSS receivers. RxTools includes RxControl, RxLogger, RxUpgrade, Data Link, SBF Converter and SBF Analyzer. Each of these applications has been specially designed in order to allow an easy and productive interaction with Septentrio receivers.
 - Justification: SBF analyzer tool will be used for preliminary data evaluation.
- SBF converter
 - Name: Septentrio RxTools package includes SBF converter.
 - Supplier: Septentrio
 - License: Proprietary license
 - Version: RxControl 17.0.0
 - Description: RxTools is a combination of applications that work with any of the latest Septentrio GNSS receivers. RxTools includes RxControl, RxLogger, RxUpgrade, Data Link, SBF Converter and SBF Analyzer. Each of these applications has been specially designed in order to allow an easy and productive interaction with Septentrio receivers.
 - Justification of use: SBF blocks will be exported into a Matlab for a readable format.
- Matlab
 - Name: Matlab
 - Supplier: Matlab
 - License: Proprietary
 - Version: R2013a
 - Description: Software tool that facilitates multiple calculations and analysis.
 - Justification: Analysis and comparison of given files as stated for this task.

ALGORITHM

Matlab script is used for comparison of the calculated position estimation of GNSS antenna based on pseudoranges and the position estimation obtained from PPK.

The distance between the GNSS antenna position estimation and the PPK based reference position of GNSS antenna at the same timestamp will be calculated compared to an adjustable threshold.

Depending on the threshold a corresponding value of Evaluation symptom is assigned for given timestamps in the output file.

Correct setting of Evaluation symptom value allows later to compare all sub-task outputs together and evaluate properly a nature of GNSS signal disturbances.

9.3 ANALYSIS BASED ON COMPARISON OF ANTENNA POSITION FROM CORRECTED PSEUDORANGE SOLUTION AND REFERENCE ANTENNA POSITION BASED ON GT (Task 4.3.2.3)

RESPONSIBILITY

The task is performed in the responsibility of TTS.

OBJECTIVE

The dedicated task 4.3.2.3 evaluates a subset of the train run data, which have PVT output calculated with differential corrections available. The task scope has to focus on the analysis of position output using EGNOS differential corrections only.

Earlier task description with additional analysis using GLONASS corrections or corrections from ground based reference stations is not performed. The reason is that EGNOS is expected to have higher preference in future railway safety applications than GNSS local ground reference stations.

INPUT

Ground Truth based reference antenna position data and PVT solution data of GNSS antenna position calculated by corrected pseudoranges.

Reference data set stored in Google cloud provides both PVT data from activity 4.2.3 and GT based reference antenna position data from activity 4.2.5.

The post-processed PVT used will be from the Septentrio receiver only and will be the corrected PVT from activity 4.2.3 which are files with suffix (uf) 03 Autonomous GPS L1, 05 autonomous Galileo and 07 GPS + Galileo.

Format of the input data is specified in the document Post-processing computation of PVT [13].

OUTPUTS

The output of the task will be an ASCII text file with a header part containing the used error threshold (**GT_DeviationLimit**) for assignment of Evaluation symptom value.

Behind the file header valid for all measurements within the file, the data is listed beginning with the GPS time stamp in seconds, Evaluation symptom, ECEF coordinates of reference position of GNSS antenna in ITRF frame and APV (analyzed parameter value, i.e. calculated position difference). The output format complies the format specified in the technical note on output format specification [5].

DESCRIPTION

Off-line computed position of the reference antenna on the train is compared to a GNSS independent ground truth position data set over time, calculated with an on-board offset matching to the GNSS reference antenna location on the train.

The evaluation of a subset of train run data is performed by a comparison of position estimation of GNSS receiver antenna calculated from corrected pseudoranges (GPS+EGNOS) and GNSS independent ground truth based reference antenna position.

TOOLS

The tools of the GNSS receiver providers are preferably used for analysis of received satellite signals and GNSS receiver output data associated with its positioning solution.

- Septentrio **RX Tools** version 17.0.0 and former versions:

- SBF Converter, version: 2.4.1
- SBF Analyser, version 2.0.1

The Septentrio RX Tools are free for download after identification by an email address. Installation by copy is possible without admin rights on the windows computer.

- μ Blox **U-center**, version 8.12
- Mathworks **Matlab** R2012a is used for analysis after evaluation calculations from the receiver's measurements.
- **Google Earth** Version 7.1.2.2041 to visualize the KML Files generated by the receiver provider conversion tools.

The tools of the GNSS receiver providers are well described and of common use within STARS WP4 member companies.

Automation of data processing is planned to be introduced, when the amount of files to be analyzed is big enough, that automation increases overall efficiency of the analysis task.

ALGORITHM

In Matlab special scripts perform the comparison of the corrected pseudorange position estimation with the associated ground truth based reference position data.

The distance between the GNSS antenna position estimation and the GT based reference position of GNSS antenna at the same timestamp will be calculated and compared to an adjustable threshold **GT_DeviationLimit** in meters.

Depending on **GT_DeviationLimit** a corresponding value of Evaluation symptom is assigned for given timestamps in the output file.

This allows later to compare all sub-task outputs together and reliably evaluate GNSS signal disturbances in this way.

9.4 ANALYSIS BASED ON COMPARISON OF ANTENNA POSITION FROM CORRECTED PSEUDORANGE SOLUTION AND REFERENCE ANTENNA POSITION FROM PPK (TASK 4.3.2.4)

RESPONSIBILITY

The task is performed in the responsibility of ALS.

OBJECTIVE

The aim of this data analysis is to identify the test track locations where GNSS performances are degraded.

This analysis focuses on the position domain and compares two different positions computed in task 4.2.3, the receiver antenna position estimated from corrected pseudoranges (DPSR) and the receiver antenna position based on post-processing kinematic (PPK). The difference (APV) between these two positions is evaluated against a threshold in order to mark the data (by properly selected ES) where anomalies are detected.

INPUT

Two inputs are required for the task:

- The receiver antenna position estimated from corrected pseudoranges (DPSR)
- The receiver antenna position based on post-processing kinematic (PPK)

These inputs are computed in task 4.2.3; they are associated to the following PVT modes (see Table 6 in [13]):

PVT Mode	Description	Corrections (Type)	Task
EGNOS	SBAS positioning.	YES (EGNOS)	4.3.2.3 4.3.2.4
PPK (RTK)	Carrier-based corrections data usage for PVT.	YES (Local, carrier-phase)	4.3.2.2 4.3.2.4

The position PPK is computed with GPS and GLONASS constellations while the position PSR is computed with GPS constellation as illustrated in Table 9 in [13]:

PVT Mode	Direction	GNSS usage in PVT	Signals enabled in PVT	GNSS SW	GNSS receiver	File suffix (suf)
PPK (RTK)	FWD	GPS+GLONASS	L1+L2	PP-SDK	AsteRx4	S01
	FWD+BWD	GPS+GLONASS	L1+L2	RTKLIB	AsteRx4	S01
EGNOS	FWD	GPS	L1	PP-SDK	AsteRx4	S02

The files generated by PP-SDK tool are in SBF format. These files have to be converted to ASCII files (PosCart) with SBF converter:

- TOW (Time of Week expressed in whole milliseconds),
- WNc (GPS week number – continuous),

- X (m)
- Y (m)
- Z (m)
- PDOP
- MeanCorrAge

Format of the input data is specified in the document Post-processing computation of PVT [13].

OUTPUTS

Generally, marked data for next analysis task, i.e. for identification of particular harmful factors. The output data format has to be in line with technical note on output format specification [5]. The output of the task will be an ASCII text file with a header part containing the used error threshold **GT_DeviationLimit** serving for evaluation of APV data and setting appropriate value of Evaluation symptom in dependence on analyzed GNSS performance.

Behind the file header valid for all measurements within the file, the data is listed beginning with the GPS time stamp in seconds, Evaluation symptom, ECEF coordinates of reference position of GNSS antenna in ITRF frame and calculated position difference at least. PDOP and Correction Age can be included.

DESCRIPTION

Comparison of position estimation of GNSS antenna calculated by corrected pseudoranges (GPS+EGNOS) and reference position data set obtained from PPK is carried out.

Error threshold is properly set for marking data when GNSS performance decreases.

TOOLS

- RxTool
Septentrio free software, version 17.0.0:
 - SBF Analyser
 - SBF Reporter
 - SBF Converter (ASCII, RINEX and KML files)
 - Timeconv.exe

This tool will be used to analyse the data marked with anomalies.

- Google Earth, version 7.1.8.3036 17/01/2017:
Analysis of KML files
This tool will be used to analyze the data marked with anomalies.
- Python environment 3.6.2

ALGORITHM

The algorithm compares DPSR and PPK inputs and implements the following steps:

1. Import PVT files related to corrected pseudoranges (DPSR) and PPK
2. Select GPS Time/XYZ for PPK and EGNOS
3. Capture threshold for XYZ

4. Compute XYZ difference (APV) for each epoch, compare with the threshold and assign proper value of ES
5. Export GPS time, ES, XYZ values, APV (optionally PDOP, correction age etc.).

9.5 DATA ANALYSIS BASED ON COMPARISON OF POSITION SOLUTIONS FROM DIFFERENT SATELLITE SUBSETS (TASK 4.3.2.5)

RESPONSIBILITY

The task is performed in the responsibility of ZCU.

OBJECTIVE

The aim of the analysis is to identify time instants when the GNSS signal might be disturbed beyond the standard specification. The analysis is based on a fault detection and exclusion algorithm used for receiver autonomous integrity monitoring.

INPUT

The analysis starts with raw data provided by the Septentrio receiver

SBF (Septentrio Binary Files) – binary file including blocks of measured and computed data of Septentrio receiver, file format specification is available in [13].

OUTPUTS

The output of the analysis is a text file that contains time-stamps of time instants at which the difference between a full-solution and a sub-solution exceeds a threshold together with the number of satellites that were included in the sub-solution.

Output description:

GPS Time [s]... [wn*604800 + number of seconds]

A list of integers representing identification numbers of the SVs included in the sub-solution which distance from the full-solution exceeded the threshold [n1 n2 n3 n4 ...]

The output format complies the format specified in the technical note on output format specification [5].

DESCRIPTION

The analysis is performed in the position domain by comparing the position estimate obtained using all visible satellites with position estimates obtained by excluding individual satellites. The position estimate obtained using all satellites is called the full-solution while the position estimates obtained by excluding individual satellites are usually called sub-solutions. If the GNSS is not seriously impaired, the computed sub-solutions should be close to the full-solution. Thus, the analysis of the difference between the full-solution and the sub-solutions could reveal situations where the GNSS signals are disturbed in some way. The identified disturbances reflecting a large error between the full-solution and a sub-solution will be detected and identified in the output of the subtask. It should be noted that this analysis can be false negative in some specific situations.

TOOLS

Since the PVT sub-solutions are not computed in the frame of WP4.2, they need to be obtained within this subtask. Tool used to accomplish this are partially based on a modified ready to use SW and own developed SW. The computation of the PVT sub-solutions is performed by the modified RTKLIB

- RTKLIB, (an open source program package for GNSS positioning) , open source, 2.4.3 b26 (modified for the project STARS purpose)
- A set of tools for GNSS signal processing

- The standard conversion tool **convbin** is used to process the raw files of GNSS receivers to obtain RINEX observation, navigation and SBAS files.
- The modified tool **rnx2rtkpSTARS** is used to compute the PVT full-solutions and save them to a text file together with necessary information (corrected pseudoranges, and satellite positions) to compute the sub-solutions. The further processing is performed in Matlab.

The computation of PVT full-solution sub-solutions and their analysis is performed in Matlab.

- Computation of the PVT full-solution and sub-solutions using the standard weighted least squares algorithm, computation their differences and comparison of the differences with a threshold by a MATLAB script and exporting the results to a text file.

ALGORITHM

The whole processing is run by a single batch file involving

- 1) The conversion of GNSS raw files to the RINEX files (**convbin**).
- 2) The computation of the PVT full-solutions with satellite positions and corrected pseudoranges (**rnx2rtkpSTARS**).
- 3) The conversion of entries of the text file provided by the tool rnx2rtkpSTARS to a MATLAB binary file format (a MATLAB script).
- 4) Analysis of the full-solution and sub-solutions by a MATLAB script and export of the results to a text file (a MATLAB script).

9.6 DATA ANALYSIS BASED ON DEVIATION OF PSEUDORANGES IN TIME (TASK 4.3.3.1)

RESPONSIBILITY

The task is performed in the responsibility of ZCU.

OBJECTIVE

The aim of the analysis is to identify time instants when the GNSS signal might be disturbed beyond standard specification. The analysis is based on time evolution of pseudoranges.

INPUT

The analysis starts with raw data provided by the Septentrio receiver

SBF (Septentrio Binary Files) – binary file including blocks of measured and computed data of Septentrio receiver, file format specification is available in [10].

OUTPUTS

The output of the analysis is a text file that contains time-stamps of time instants at which the time-difference of a pseudorange exceeds a threshold together with the number of the corresponding SV.

Output description:

GPS Time [s]... [wn*604800 + number of seconds]

An integer representing identification number of the SV which pseudorange exceeded the threshold [n].

DESCRIPTION

If the GNSS signal is not disturbed, a pseudorange should basically consist of two components. The first component is a slow trend caused by the relative motion of the satellite and the receiver. The second component is more rapidly changing and can be modelled as a correlated noise that accounts for several factors. As the noise level should be within certain bounds in normal conditions any sudden changes in the pseudorange can indicate a potential disturbing factor. The only expected sudden change in pseudoranges that is not considered as disturbance is reset of internal receiver clock to keep it close to the GNSS time. However, these sudden changes should be easily recognized as they should occur at all observed pseudoranges at the same time and with the same size. In case that the analysis is based on the corrected pseudoranges, the second component will not contain the sudden change caused by the reset of internal receiver clock. Hence, once the sudden changes caused by the clock reset are removed, the remaining sudden changes are supposed to reflect a disturbance of the GNSS signal. Such disturbances will be detected and identified in the output of the subtask.

TOOLS

Since the pseudoranges are not provided in the frame of WP4.2, they need to be obtained within this subtask. Tool used to accomplish this are partially based on a modified ready to use SW and own developed SW. The computation of the pseudoranges is performed by the modified RTKLIB

- RTKLIB, (an open source program package for GNSS positioning) , open source, 2.4.3 b26 (modified for the project STARS purpose)
- A set of tools for GNSS signal processing
- The standard conversion tool **convbin** is used to process the raw files of GNSS receivers to obtain RINEX observation, navigation and SBAS files.
- The modified tool **rnx2rtkpSTARS** is used to compute the corrected pseudoranges and save them to a text file. The further processing is performed in Matlab.

The analysis of the pseudoranges is performed in Matlab.

- Computation of time-differences of pseudoranges for each satellite and the analysis of the differences by a MATLAB script and exporting the results to a text file.

ALGORITHM

The whole processing is run by a single batch file involving

- 1) The conversion of GNSS raw files to the RINEX files (**convbin**).
- 2) The computation of the satellite positions and corrected pseudoranges (**rnx2rtkpSTARS**).
- 3) The conversion of entries of the text file provided by the tool rnx2rtkpSTARS to a MATLAB binary file format (a MATLAB script).
- 4) Analysis of the pseudoranges by a MATLAB script and export of the results to a text file (a MATLAB script).

9.7 DATA ANALYSIS BASED ON COMPARISON OF MEASURED PSEUDORANGE AND DISTANCE BETWEEN SV AND REFERENCE ANTENNA POSITION (TASK 4.3.3.2)

RESPONSIBILITY

The task is performed in the responsibility of ZCU.

OBJECTIVE

The aim of the analysis is to identify time instants when the GNSS signal might be disturbed beyond the standard specification. The analysis is based on a comparison of the pseudoranges and the geometric distance between the SV and the reference antenna position.

INPUT

The analysis starts with raw data provided by the Septentrio receiver and the data providing antenna reference positions (these data are provided by the subtask 4.2.5).

SBF (Septentrio Binary Files) – binary file including blocks of measured and computed data of Septentrio receiver, file format specification is available in [15].

A text file containing the antenna reference positions.

OUTPUTS

The output of the analysis is a text file that contains time-stamps of time instants at which the time-difference of a pseudorange exceeds a threshold together with the number of the corresponding SV.

Output description:

GPS Time [s]... [wn*604800 + number of seconds]

An integer representing identification number of the SV whose difference between the pseudorange and the geometrical distance exceeded the threshold [n].

DESCRIPTION

If the GNSS signal is not disturbed, the geometric distance and the pseudorange should be close to each other. A disturbance of the GNSS signal results in a large difference between the pseudorange and the geometric distance. The analysis will detect time instants at which the difference exceeds a threshold.

TOOLS

Since the pseudoranges are not computed in the frame of WP4.2, they need to be obtained within this subtask. Tool used to accomplish this are partially based on a modified ready to use SW and own developed SW. The computation of the pseudoranges is performed by the modified RTKLIB

- RTKLIB, (an open source program package for GNSS positioning) , open source, 2.4.3 b26 (modified for the project STARS purpose)
- A set of tools for GNSS signal processing
- The standard conversion tool **convbin** is used to process the raw files of GNSS receivers to obtain RINEX observation, navigation and SBAS files.
- The modified tool **rnx2rtkpSTARS** is used to compute the corrected pseudoranges and satellite positions and save them to a text file. The further processing is performed in Matlab.

The computation of the geometrical distance, the analysis of the differences of the pseudoranges and the geometrical distance is performed in Matlab.

Computation of the geometrical distance between the antenna and the SV using the antenna reference position and SV positions, calculation of the differences between the geometrical distance and the pseudorange for each satellite, the analysis of the differences by a MATLAB script and exporting the results to a text file.

ALGORITHM

The whole processing is run by a single batch file involving

- 1) The conversion of GNSS raw files to the RINEX files (**convbin**).
- 2) The computation of the satellite positions and corrected pseudoranges (**rnx2rtkpSTARS**).
- 3) The conversion of entries of the text file provided by the tool rnx2rtkpSTARS, the entries of the file containing antenna reference positions to a MATLAB binary file format (a MATLAB script).
- 4) Analysis of the geometrical distance and pseudorange differences by a MATLAB script and export of the results to a text file (a MATLAB script).

9.8 C/N_0 BASED DATA ANALYSIS (TASK 4.3.3.3)

RESPONSIBILITY

The task is performed in the responsibility of AZD.

OBJECTIVE

Main goal is to evaluate occurrence of negative phenomena by analysis of measured C/N_0 parameter.

INPUT

Septentrio receiver provides information on C/N_0 ratio in dedicated SBF blocks of raw data. Thus the files including SBF Measurement blocks "MeasEpoch" are required as inputs of this task.

SBF (Septentrio Binary Files) – binary file including blocks of measured and computed data of Septentrio receiver, file format specification is available in [15].

OUTPUTS

The output files will comply to the specification provided in document [5]. The following columns will be included: GPS time, Evaluation symptom (0 - open sky environment with negligible multipath, 1 – middle multipath level, 2 – strong multipath level, Analyzed Parameter Value which is calculated by means of maximum function for given epoch of C/N_{0_RHCP} and C/N_{0_LHCP} differences of all satellites (received signals), where each difference is normalized by elevation (by $\cdot \sin(\text{elevation})$) of each satellite.

DESCRIPTION

In this task evaluation of C/N_0 (carrier-to-noise density ratio) parameter is carried out. Solution of this task is supported by a use of advanced GNSS receiver Septentrio AsteRx4 equipped by two RF inputs and connected to dual polarization antenna Antcom G8Ant-3A4T21-RL-RoHS_G8. This equipment is capable to provide C/N_0 parameter for both ordinary GNSS RHCP signal and reflected GNSS LHCP signal.

Analysis is based on observation of C/N_0 values in measured data for both polarizations.

In the receivers data such following events are seek for:

- a decrease of both parameters of arbitrary received signal which indicates mainly attenuation in signal path propagation,
- a decrease of both parameters common to all signals which indicates prevailing RF interferences or environment with high multiple multipath,
- concurrently, a decrease of the parameter for RHCP signal of given satellite and an increase of the parameter of LHCP signal of the same satellite which indicate strong single multipath for signal of given satellite (as reflected signal changes its polarization).

It must be considered that this approach is capable to identify mainly strong multipath when single reflection of GNSS signals is presented or indirect signal is only received. If multiple reflection occurs this method may not provide clear result.

The main benefit of this approach is to provide supplementary information on identification of nature of signal disturbance.

Together with other proposed methods this method efficiently helps to identify the locations where GNSS signal reception is disturbed and cause of these disturbances.

TOOLS

- RxTools Septentrio free software, version 17.0.0:
 - Bin2asc.exe
- Matlab R2006a is proposed to be used in analysis in frame of this task.

ALGORITHM

Behavior of C/N_0 parameter is analyzed in different ways:

- comparison of measured C/N_0 and C/N_0 in open sky view conditions for all received GNSS RHCP signals,
- evolution of C/N_0 of each received GNSS RHCP signal in time,
- concurrent evaluation of C/N_0 of both received GNSS RHCP and LHCP signals.

Analyzed Parameter Value is calculated by means of maximum function for given epoch of C/N_{0_RHCP} and C/N_{0_LHCP} differences of all satellites (received signals), where each difference is normalized by elevation (by $\sin(\text{elevation})$) of each satellite

$$APV = \max\{X_1 \sin(El_1), X_2 \sin(El_2), \dots, X_{N_{SV}} \sin(El_{N_{SV}})\},$$

where N_{SV} is the number of satellites in this epoch, X_i denotes the evaluated parameter of the i -th satellite (difference of C/N_{0_RHCP} and C/N_{0_LHCP}) and El_i is the elevation mask of the i -th satellite in radians, $i = 1, \dots, N_{SV}$.

The ES for APV is assigned according to 0dB and 5dB thresholds:

$APV > 5\text{dB}$,	negligible multipath, ES = 0
$0 \text{ dB} \leq APV \leq 5\text{dB}$	middle multipath, ES = 1
$APV < 0\text{dB}$	strong multipath, ES = 2

The thresholds were set according to the results of analysis of data coming from measurements in clear sky view and multipath environment.

9.9 CODE MINUS CARRIER BASED ANALYSIS (TASK 4.3.3.4)

RESPONSIBILITY

The task is performed in the responsibility of ALS.

OBJECTIVE

The aim of this data analysis is to identify the test track locations where GNSS performances are degraded.

This analysis will focus on the raw measurements and specific indicators from GNSS receiver to determine if measurements performed in WP3 are subject to multipath error.

INPUT

The input file name shall be compliant with the convention used for Septentrio receiver binary files <CCC>_<GCCD>_<YYMMDDhhmm>_<DUR>_<FRQ>.sbf. The field <FRQ> is important because it is used for Doppler computation.

SBF (Septentrio Binary Files) have to be converted to ASCII files (MeasEpoch2 and SatVisibility1 options) with SBF converter. The related text files are inputs of the algorithm.

OUTPUTS

All results computed will be exported into four text formatted files with semicolon separator and according to [6]:

- GPS L1-C/A signal: CCC>_4334_<YYMMDDhhmm>_<DUR>_<FRQ>.G1C.TXT
- GPS L5 signal : CCC>_4334_<YYMMDDhhmm>_<DUR>_<FRQ>.G5Q.TXT
- Galileo L1BC signal : CCC>_4334_<YYMMDDhhmm>_<DUR>_<FRQ>.E1C.TXT
- Galileo E5a signal : CCC>_4334_<YYMMDDhhmm>_<DUR>_<FRQ>.E5Q.TXT

For each signal, a header is provided with a summary of the computation and is followed by a table consisted of 7 columns:

Column	#1	#2	#3	#4	#5	#6	#7
Parameter	GPST	CMC indicator	CMC APV	CMC SVs	DR indicator	DR APV	DR SVs
Unit	[s]	[-]	[m]	[-]	[-]	[Hz/s]	[-]
Resolution	0.001 s	[0/1/2]	0.001m	[Gxx/Exx]	[0/1/2]	0.001m	[Gxx/Exx]
Format	xxxxxxx xxx.xxx	x	xxxx.xxx	32*xxx	x	xxxx.xxx	32*xxx

- GPS Time [s] i.e. week*604800 + number of seconds
- Evaluation symptom (CMC indicator and DR indicator): The values “0”, “1”, “2” and “NaN” are proposed for the symptom, where “0” is related to the evaluated negligible effect of negative phenomena on GNSS signals or performance, “1” is related to the middle effect and “2” is related to the strong impact of negative phenomena on GNSS signals or performance. The “NaN” is used for the case when the analysis could not be performed.

- analyzed Parameter Value: CMC APV and DR APV
- Satellite Vehicles possibly impacted (CMC or DR): Gxx for GPS and Exx for Galileo

DESCRIPTION

The analysis focuses on the data of AsteRx4 GNSS receiver from Septentrio. The SBF files were first analyzed with Septentrio Rxtool 17.0.0 free software.

A bottom-up approach was chosen to examine the code and phase measurements and identify specific locations where PVT outliers have been detected by Septentrio receiver.

Rxtool provides following plots for measurements combinations (different combinations are possible according to values of x/y):

- Lx-Ly (iono)
- Px-Py (iono/multipath)
- Px-Lx (iono/multipath)
- TEC (iono/multipath)
- MPx (multipath)

Px-Lx (code minus phase) and MPx were examined in more details. This preliminary analysis has shown the efficiency of Rxtool to analyse the raw data. The Doppler rate could be a good indicator to detect multipath while the Px-Lx value could be used to detect multipath and to provide a rough estimation of multipath error. However, it must be noticed that the detection/identification/rejection of multipath leads to receiver proprietary algorithms. For this reason, the quantitative estimation of the multipath error would be more precise with the GNSS receiver proprietary estimations.

The second analysis was performed under Excel to provide a first implementation of the algorithm to compute Doppler rates and CMC from the raw measurements. This solution was useful to provide a quick feedback however it required to import each MeasEpoch2 file under Excel and to create an Excel sheet for each satellite and for each GNSS signal.

TOOLS

- Septentrio free software, version 17.0.0:
 - SBF Analyser
 - SBF Reporter
 - SBF Converter (RINEX and KML files)
 - Timeconv.exe
 - Bin2asc.exe (not used)
 - Sbf2asc (source code examples to decode SBF file)
- Google Earth Version 7.1.8.3036 17/01/2017:
 - Analysis of KML files
- Python environment 3.6.2

ALGORITHM

An implementation with Matlab (version 2010) was then performed to compute automatically the Doppler rate and CMC values for all satellites and all signals. This algorithm was dedicated to SBF files and implemented the following steps:

1. Import MeasEpoch2 file
2. Select TOW/Week/Sat/Signal/Pseudorange/CN0/Doppler shift/Carrier phase
3. Capture threshold for Doppler rate and threshold for CMC
4. Compute Doppler rate for each satellite signal according to sampling rate (FREQ)⁸ and tag records above threshold
5. Compute CMC for each satellite signal and tag records with “above threshold” or “out of range” (e.g. 1596 for L1, 2048 for L2 and 2137 for L5)
6. Export GPS time, Doppler rate and CMC values with their associated indicator.

This structure was integrated in the final version of the algorithm developed under Python environment 3.6.2 to have a modular approach and to deal with the unified output format specified in [5].

The purpose of this unified output format is to enable and also simplify further evaluation of technique outputs. An output file is organized into columns with three mandatory columns: GPS System Time (GPST), Evaluation Symptom (ES), and Analyzed Parameter Value (APV).

The APV for each epoch (CMC or DR) shall be calculated according to the following formula

$$APV = \max\{X_1 \sin(El_1), X_2 \sin(El_2), \dots, X_{N_{SV}} \sin(El_{N_{SV}})\},$$

where N_{SV} is the number of satellites in this epoch, X_i denotes the evaluated parameter of the i -th satellite (CMC or DR) and El_i is the elevation mask of the i -th satellite in radians, $i = 1, \dots, N_{SV}$.

The ES for CMC is defined according to 1m and 10m thresholds. A value lower than 1m indicates that integer ambiguity is solved and consequently a good precision for the tracking loop. Above this value, there is a potential adverse effect and a threshold of 10m should separate middle impact and strong impact of this effect. The algorithm evaluates each APV CMC and computes the total number of related records in the header file like in the example below:

```
# Number of records with APV CMC <= 1 m ; 14050
# Number of records with 1 < APV CMC <= 10 ; 7563
# Number of records with APV CMC > 10 ; 13492
# Number of records with APV CMC irrelevant ; 0
```

The ES for DR is defined according to 1Hz/s and 10Hz/s thresholds. A value lower than 1Hz/s indicates that the train runs at constant speed and constant direction without perturbations. Above this value, there is a potential adverse effect and a threshold of 10Hz/s should separate possible impacts of the train dynamics from the reflections due to the environment. The algorithm evaluates each APV DR and computes the total number of related records in the header file like in the example below:

⁸ Observed data have a sampling rate of maximum 10Hz i.e. Septentrio CumClkJumps field can be neglected (maximum 1ms between successive samples).

Number of records with $0 < \text{APV DR} \leq 1$; 2862
Number of records with $1 < \text{APV DR} \leq 10$; 31482
Number of records with $\text{APV DR} > 10$; 757
Number of records with APV DR irrelevant; 0

In both cases, the satellites with an ES equal to 1 or 2 are identified like possible faulty signals.

9.10 SSE BASED ANALYSIS (TASK 4.3.3.5)

RESPONSIBILITY

The task is performed in the responsibility of AZD.

OBJECTIVE

This task is aimed at the detection of GNSS Signal-in-Space (SIS) errors. The detection method is based on the determination and evaluation of the Sum of Squared Errors (SSE).

INPUT

For processing in PP-SDK tool:

- SBF files including SBF Measurement blocks “PVT Cartesian” are required as inputs.

For processing in RTKLIB tool:

- RINEX files (observation and navigation files) are required as inputs.

SBF (Septentrio Binary Files) – binary file including blocks of measured and computed data of Septentrio receiver, file format specification is available in [15].

OUTPUTS

Output files comprise following parameters (columns) in text format:

GPS Time [s]... [wn*604800 + number of seconds], where wn is GPS week number

ES [-] ...evaluation symptom

Symptom can take these values:

- 0... No error from SSE evaluation by PP-SDK and RTKLIB
- 1...Indicated error from SSE evaluation from at least one sw tool
- NaN... Not enough data for SSE evaluation.

DESCRIPTION

The SSE, also known as the quadratic form of residuals, is the sum of the squares of residuals. It is a measure of the discrepancy between the measurements and an estimation model. A small SSE indicates a tight fit of the model to the measurements. In evaluating, the SSE is directly compared with a predefined threshold value. If the SSE is less than the threshold, there is no failure assumed. A failure is supposed when the SSE is greater than the threshold. This method is well known and used in Receiver Autonomous Integrity Monitoring (RAIM) techniques.

Analysis of the SSE can be carried out by means of knowledge of residuals and covariance matrix associated with the measurement errors. If residuals and covariance matrix are unknown the analysis can be realized by means of RAIM technique implementation if selected SW tool allows this. For the evaluation of SSE a suitable threshold value must be well defined.

TOOLS

RxTools, PP-SDK and RTKLIB SW tools have been selected for analysis of SSE. These tools don't provide direct information about SSE values. However, PP-SDK and RTKLIB tools include RAIM algorithm which can be used to indicate that the SSE was exceeded at some threshold.

It is assumed that SSE values are not required to be calculated. If it will be decided that the values of SSE should be known, the PP-SDK tool can't be used since residual solution and weighted matrix

can't be obtained in the case when an event of high SSE arises. RTKLIB includes information about residuals and weighted matrix in its optional output files (Output Solution Status and Debug Trace files). These optional output files contain a large amount of data in which the required information is not transparently visible. The best solution in the case of SSE computation is to modify RTKLIB source code by appropriate means to generate the executable application which will provide a suitable output of the required SSE values. Compilation can be done e.g. with Embarcadero C++Builder.

The Matlab tool and own created subroutines are used for data importing, processing and negative phenomena identification.

ALGORITHM

The threshold value is derived from the probability of false alarm. The appropriate value of probability of false alarm should be the same as the default value used in RAIM algorithm of PP-SDK, i.e. $P_{FA} = 10^{-3}$.

9.11 ANALYSIS BASED ON MULTIPATH DETECTION ALGORITHM BUILT-IN RECEIVERS (TASK 4.3.3.6)

RESPONSIBILITY

The task is performed in the responsibility of Cetest and CAF I+D.

OBJECTIVE

The objective of this subtask is to evaluate the impact of using built-in Multipath Mitigation techniques in Septentrio Receivers for PVT solution improvement assessment.

INPUT

The input file format is SBF data file format described in [15].

Data export of the necessary SBF blocks from the raw SBF files follows. Minimum SBF blocks to be used for 4.3.3.6 processing are:

- ReceiverTime: Time related information
- PVTGeodetic2: PVT solution in geodetic coordinate system
- MeasExtra: Multipath correction factor values
- DOP2: Dilution of precision related information

Required data:

- PVT solution: SBF file containing the PVT solution of the tests

The PVT solution may be in Geodetic Coordinate System

OUTPUTS

The outputs are presented as text file and they will include the columns described in document [5].

DESCRIPTION

An evaluation of the Multipath Correction values for the pseudoranges observed together with additional navigation parameters that may help identify PVT solution limitations are studied within this task.

TOOLS

- RxTools Septentrio free software, version 17.0.0
 - SBF Analyzer - for preliminary data evaluation
 - SBF Converter - SBF blocks will be exported into a Matlab for a readable format
- Matlab, version 2013a – for analysis and comparison of given files as stated for this task.

ALGORITHM

In order to provide with a meaningful data analysis the following process is proposed. First of all, SBF files are downloaded from the database and its consistency is checked with SBF analyzer. These consistency checks consist of obtaining some graphs and corroborating the graphics are actually plotted and results make sense:

- Planimetric plot
- CNO
- Dilution of precision
- Multipath Correction values

- Number of satellites in view

If there are no graphical results and/or the results show that there is no PVT solution available then CETEST will contact the data uploader.

If data is available and results seem to be correct, the next step in the procedure is to convert the files. At the time of converting the files, the corresponding SBF blocks related to the analysis of this task need to be selected. Since the aim of this subtask is to evaluate the impact of using built-in Multipath Mitigation Techniques in Septentrio Receivers, the following blocks are selected:

- ReceiverTime: Time related information
- MeasExtra: Multipath Correction factors for each satellite and signal
- PVTGeodetic2: PVT solution in geodetic coordinate system
- DOP2: Dilution of precision related information

Once the conversion of the files is carried out the comparison of the files using Matlab is performed. For that purpose the following steps are followed:

- The exported data will be imported into Matlab's Workspace.
- Geodetic coordinates will be translated into ECEF WG84 coordinate system.
- The Multipath Correction factor for each satellite will be computed for each epoch together with the corresponding PVT solution for that epoch.
- Results will be compared with a MP value threshold. All coordinate points that show MP value above the established limit will be marked by appropriate value of ES for further analysis.

9.12 ANALYSIS BASED ON RF INTERFERENCE DETECTION AND MITIGATION ALGORITHM BUILT-IN RECEIVER (TASK 4.3.3.7)

RESPONSIBILITY

The task is performed in the responsibility of Radiolabs.

OBJECTIVE

The aim of this task is to identify GNSS bands in which the receiver detects the presence of RF interference and/or mitigates it by applying receiver RF interference mitigation algorithm.

INPUT

Input file required for this task is SBF file (i.e. raw data provided by Septentrio receiver). The necessary SBF block will be extracted from the raw SBF files.

OUTPUTS

All computed results will be exported into .csv formatted files in the format specified in [5]. The files will include following parameters for each row:

- GPS time [s]: time information for data included in the file ($wn \cdot 604800 + \text{number of seconds}$).
- Evaluation symptom [-]: the highest value from receiver action values in a frame of one row will be assigned.
- Analyzed parameter value [-]: This parameter is not defined for this task, Nan will be inserted in all time epochs.

and sets consisting of three parameters

- Frequency [Hz]: Center frequency of the RF band in which interference is detected. In case of no interference, no information will be provided.
- Bandwidth [kHz]: RF bandwidth in which interference is detected. In case of no interference, no information will be provided.
- Receiver action [-]: Possible values for “Receiver action” column are:
 - 1 -> in case of “Interference detected and mitigated”
 - 2 -> in case of “Interference detected”

DESCRIPTION

The Septentrio AsteRx4 receiver disposes by in-built algorithm for RF interference detection and mitigation. Information on RF interference is directly provided by this algorithm and together with information on action taken by the receiver is stored in relevant SBF blocks of raw data file.

Data comprising such information are converted into the format including the crucial parameters for next analysis, as specified in document [15].

TOOLS

- RxTools Septentrio free software, version 17.0.0.

The RxTools is a suite of tools for monitoring and configuring receiver operations as well as logging and downloading SBF data files. Furthermore, mainly for our purposes, there are also tools to analyze the SBF data files and convert them to various other formats. The list of the RxTools used to perform data analysis is given below.

- SBF converter - converts SBF log files to readable format.

- SBF analyser - for preliminary analysis of SBF data files.

ALGORITHM

The following process is adopted for data analysis. SBF files downloaded from the database are firstly analyzed with SBF Analyzer tool for a preliminary consistency check. If data are correct, they are converted with SBF Converter tool in ASCII format. The corresponding SBF block needed for this task is RFStatus block. It provides information on the radio-frequency (RF) bands where interferences have been detected and/or mitigated by the receiver.

At the end of the file conversion, data referred to each epoch are analyzed and marked if interference has been detected and/or mitigated by the receiver built-in RFI detection and mitigation algorithms.

Finally, marked data will be exported into a .csv formatted file.

9.13 ANALYSIS BASED ON AGC LEVEL EVALUATION (TASK 4.3.3.8)

RESPONSIBILITY

The task is performed in the responsibility of Radiolabs.

OBJECTIVE

The aim of this task is to perform data analysis based on AGC (Automatic Gain Control) level provided by the receiver in order to evaluate RF interference and attenuation occurrence.

INPUT

Input file required for this task is SBF file (i.e. raw data provided by Septentrio receiver). The required SBF ReceiverStatus block will be extracted from the raw SBF files and taken as input.

OUTPUTS

All computed results will be exported into .csv formatted files in the format specified in [5]. The files will include following parameters for each row:

- GPS time [s]: time information for data included in the file ($wn \times 604800 + \text{number of seconds}$).
- Evaluation symptom [-]: its value will indicate environment without/with RF interference according to RFI Status data contained in SBF ReceiverStatus block.
- Analyzed parameter value [-]: This parameter is not defined for this task, Nan will be inserted in all time epochs.
- Gain [dB]: value of applied gain on received signal

DESCRIPTION

AGC is a key element in a GNSS receiver. The main functionality of an AGC is to adjust the incoming signal power such that the quantization losses are kept as minimum as possible. In case of a GNSS receiver, where the signal power remains below of the thermal noise floor, the AGC is mostly driven by the ambient noise environment rather than the signal power. In case of an unlikely presence of interference, the AGC gain drops sharply in response to increased power in the GNSS band. This sharp immediate change in the AGC gain pattern can be utilized to indicate an interference occurrence.

TOOLS

- RxTools Septentrio free software, version: 17.0.0
 - SBF converter - It converts SBF log files to readable format.
 - SBF analyser - Preliminary analysis of SBF data files.
 - Matlab, version R2013a
- It will be used for analysis of the given data files as stated for this task.

ALGORITHM

The following process is adopted for data analysis. SBF files downloaded from the database are firstly analyzed with SBF Analyzer tool for a preliminary consistency check. If data are correct, they are converted with SBF Converter tool in ASCII format. The corresponding SBF block needed for this task is ReceiverStatus block. It provides general information on the status of the receiver and the values of gain recorded by the receiver.

At the end of the file conversion, data are imported and analyzed in Matlab. A metric, named as *AGC level changing rate*, is used for interference detection. The AGC level changing rate can be calculated as follows:

$$\tau_i = \frac{x_i - x_{i-1}}{t_i - t_{i-1}}; i \geq 1$$

where x_i is the measured AGC level at time t_i . If interference is detected the corresponding output will be marked.

Finally, marked data will be exported into a .csv formatted file.

9.14 DATA ANALYSIS BASED ON SW RECEIVER IMPLEMENTATION (TASK 4.3.4.1)

RESPONSIBILITY

The task is performed in the responsibility of TAS-F.

OBJECTIVE

The objective of this subtask is to evaluate the occurrence and estimate the parameters of multipath in a railway environment. Based on the comparison between a multipath resistant tracking loop and a standard one, the impact on the pseudorange measurements will also be assessed.

INPUT

The inputs of this task are RF I/Q sample files produced in sub-task 4.2.8.

Three different devices were employed in measurement in WP3 – Spirent GSS6450 (AZD), Spirent GSS6425 (ASTS), TeleOrbit EOB (SIE), but data is analyzed only from the Spirent GSS6450 equipment for recording of RF samples in L1 and L5 bands in frame of the STARS project⁹. The original measured data provided by GSS6450 are converted to a new format available to all project partners and described by AZD. The reason of such conversion is a fact that original file format is not generally available and was provide to AZD under NDA (Non-disclosure agreement).

The recorded data consist of 4 bits I&Q samples sampled at 30.69MHz.

OUTPUTS

The outputs are presented as text files complying output format specification [5]. All multipath estimated parameters per service per SV will be exported into a text formatted file. This file will include following columns:

- GPS Time [s] - Time information for data included in the file. number of seconds in current week
- ES [-] - evaluation symptom value is assigned according to APV value
- APV [m] - analyzed parameter value, where resulting multipath is analyzed parameter
- Additional columns, i.e. parameters for three strongest multipaths at each epoch:
 - SV number
 - Signal
 - Column “LOS_Delay(chip)”: LOS code delay with respect to prompt correlator [chip]
 - Column “LOS_Freq(Hz)”: LOS relative Doppler with respect to local carrier [Hz]
 - Column “LOS_Amp” : LOS amplitude [-]
 - Column “LOS_Phase(rad)”: LOS relative phase with respect to local carrier [rad]
 - Column “NLOS_Delay_1(chip)”: first multipath code delay with respect to prompt correlator [chip]
 - Column “NLOS_Freq_1(Hz)”: first multipath relative Doppler with respect to local carrier [Hz]
 - Column “NLOS_Amp_1”: first multipath amplitude [-]
 - Column “NLOS_Phase_1(rad)”: first multipath relative phase with respect to local carrier [rad]
 - Column “NLOS_Delay_2(chip)”: second multipath code delay with respect to prompt correlator [chip]
 - Column “NLOS_Freq_2(Hz)”: second multipath relative Doppler with respect to local carrier [Hz]

⁹ The reason for processing of data only from this device was limited time for solution of this task. There were three different data fomats from three different devices and very time-consuming calculation. The measured data from all the three devices are available on the Google Cloud.

- Column “NLOS_Amp_2”: second multipath amplitude [-]
- Column “NLOS_Phase_2(rad)”: second multipath relative phase with respect to local carrier [rad]

DESCRIPTION

In order to provide with a meaningful data analysis the following process is proposed.

First of all, I/Q sample files are downloaded from the database.

The next step in the procedure is to convert the files into an input format compatible with GEMS.

The data are then processed by GEMS using on the one hand a standard Early - Late Power discriminator with 1 chip spacing and on the other hand the Multicorrelator tracking technique. This technique allows to detect up to two significant multipaths and estimate their parameters. The pseudorange obtained with both tracking schemes will be compared in order to assess the MP impact on the pseudorange measurements.

Using several successive outputs of a bank of correlators, a weighted sum of reference correlation functions is fitted on the measured sampled correlation function. As a result of the optimization process, the multipath parameters (complex amplitude, Doppler and delay relative to the LOS) are obtained and stored in a time stamped output file.

This procedure is repeated for L1/CA; E1 OS; L5; E5a.

TOOLS

- GEMS SW receiver, version 1.0.0, proprietary license

GEMS stands for GNSS Environment Monitoring Station. GEMS is a full software receiver developed by TAS-F.

Based on its embedded Multicorrelator techniques, GEMS enables to detect multipaths and estimate their parameters.

GEMS embeds the entire signal processing functions required to build all the GNSS observables:

- GEMS is able to track in parallel multi-frequency and multi-constellations digitalized signals;
- It integrates signal degradation detection functions with a focus on interference, spoofing, ionosphere scintillation and multipath;
- It hosts SQM (Signal Quality Monitoring) algorithms aiming at characterizing reception conditions;
- It natively embarks Multicorrelation techniques that estimate any correlation function distortions, either due to a Multi path or a spoofing attempt.
- GEA (GNSS Environment Analyzer)

As per its architecture, GEMS is composed of a signal processing module featuring error identification and characterization functions, called GEA (GNSS Environment Analyzer), as well as a complete graphical user interface and database management.

The GEA (GNSS Environment Analyzer) module embeds the entire signal processing functions required to build all the GNSS observables often used for Signal Quality Monitoring (SQM).
- Man Machine Interface (MMI)

The command and control of GEMS is done through the Man Machine Interface (MMI), called eSurvey, as illustrated below in next figure. The MMI displays in real time the 3D autocorrelation function of the processed signals, as well as the 2D waterfall view (left hand-side plot), on which multipath effect can clearly be observed for instance. It offers a large variety of observable to be displayed on screen. In addition to the visualization of GEA outputs, the interface of GEMS allows the data storages and display in database of measurements and analysis results.

As a monitoring tool, GEMS internal or third party analysis functions can be scheduled and monitoring alerts set up to assess the reception conditions performance in real time. Alarms can then be raised on screen, or log file can be filed in, raw samples stored as configured.

- Matlab, version 2013a, proprietary license

Used to convert the input data format to an input format required by GEMS.

ALGORITHM

GEMS is a full software receiver developed in C++/CUDA for windows platforms.

The GEA module is a C/C++ software based on innovative GPU parallel computing allowing the processing of large quantity of data very fast.

9.15 DATA ANALYSIS BASED ON EVALUATION OF RF SAMPLE HISTOGRAM (TASK 4.3.4.2)

RESPONSIBILITY

The task is performed in the responsibility of TUBS.

OBJECTIVE

The aim of this task is to identify interference in the measured RF samples.

INPUT

For this subtask, RF I/Q sample files are required, which are provided by partners of subtask 4.2.8. This task uses RF samples in L1 and L5 bands of the GPS signal with a 4 bit resolution and a sample rate of 30.69 MHz as input data. The original measured RF data provided by different measurement equipment is converted into a new format. This conversion is necessary due to the fact that the original file format is not generally usable for all project partners.

Outputs

The output of this task will consist of two ASCII TXT files respectively for the I and Q component of the RF sample file, which will include the time and the estimated strength of the detected interference.

The content of the header of the text file is described hereafter:

- Line 1: Name of the analyzed RF sample file
- Line 2: Trip date; Name of line
- Line 3: Measurement Company; Measurement system
- Line 4: Min. threshold value, Max. threshold value
- Line 5: Bandwidth
- Line 6: Signal Band, RF component (I or Q)

The content of the columns of the text file is described in table hereafter.

Column	1	2	3	4-19
Parameter	Measurement time (approximation due to the sample frequency)	Interference flag	Mean difference	Sample value x, Sample values of the measured RF histogram
Unit	s	-	-	-
Resolution	0.1	1	0.00000001	0.00000001
Format	xxxxx.x	x	x.xxxxxxxxxx	x.xxxxxxxxxx

Each element is separated by a ‘;’. The interference flag can be between 0 and 2 with the following classification: no interference detected (0), weak interference (1) and strong interference (2). It will be determined by comparing the mean difference, consisting of the sample values and the reference histogram, and the threshold values.

DESCRIPTION

The GNSS signals have a very low signal strength, which is below the general noise floor. This leads to a high vulnerability of the GNSS signals to interferences such as jamming. It is possible to detect such interferences by monitoring the background noise level.

The power spectrum of the measured signal should have a Gaussian distribution, because the influence of the weak GNSS signal can be neglected and the strong background noise can be adopted as white noise. If the signal is disturbed by interference, the distribution will no longer be

Gaussian, because of the much stronger power of the interference signal in comparison to the GNSS signal in this case. The RF sample can be marked as interfered.

TOOLS

- Mathworks Matlab, version 2016b, with Signal Processing Toolbox

is used to analyse the RF histogram of the measured samples.

ALGORITHM

A Matlab script has been developed and used, which computes the RF histogram of the measured I/Q samples and compares the measured histogram to a default histogram without any interference. For this purpose, the RF I/Q samples will be truncated to snapshots of a length of 1 s. The length of the snapshot was chosen to minimize the calculation time.

The I/Q data will then be split in its in-phase data (I) and quadrature data (Q) and will be analysed separately. The RF histogram of the chosen I/Q component is generated by using the 1 s snapshot and the “buffer” function of Matlab with an interval of 0.033 ms and an overlap of 0.016 ms. After that, the histogram of the snapshot will be compared to a reference histogram.

If both the reference and the measured histogram have similar distributions, no interference is detected. If the distribution of the reference and the measured histogram differ significantly from each other, an interference event is detected. The difference between the two histograms provides the information about the intensity of the interference.

With the aforementioned methodology, it is possible to detect interference such as jamming for the I and Q component of the L1 and L5 frequency bands.

To reliably detect interference in RF histograms, it is necessary to determine threshold values. The RF histogram can slightly change due to factors like the gain control of the antenna or noise, which would lead to a false detection of interference. The threshold values are calculated by the evaluation of interference-free RF samples of the used measurement equipment.

9.16 ANALYSIS BASED ON POWER SPECTRAL DENSITY EVALUATION (TASK 4.3.4.3)

RESPONSIBILITY

The task is performed in the responsibility of Radiolabs.

OBJECTIVE

The aim of this task is spectral analysis of RF signal to evaluate the presence of RF interference.

INPUT

Input file required for this task is .dat file containing I and Q sample of RF Spectrum. These file originated by conversion of the files provided by RPS used in measurement campaign in frame of WP3.

OUTPUTS

At the end of the process, all results computed will be exported into a .csv formatted file, in the format specified in [5]. Following parameters will be included:

- GPS Time [s] - Time information for data included in the file; $wn \cdot 604800$ + number of seconds.
- ES [-] - Evaluation Symptom corresponding to RFI Status of Septentrio GNSS receiver
Two values can be provided in this column:
 - "0" if no RF interference is detected,
 - "1" if no RF interferences detected.
- APV - Analyzed Parameter Value; in this task "Nan" is included in all rows.

Additional task specific parameters are added:

- Frequency [Hz] - center frequency of the base band signal in which interferences has been detected.
- PSD [dB] - Power Spectrum Density value

Task specific data columns are repeated in the same row (in the same time) for the five highest RF interference occurrences. If RF interference is not detected no values are included in these columns.

DESCRIPTION

From RF spectrum, it is possible to evaluate if there is RF interference and at which frequencies (peaks in the Spectrum plot).

TOOLS

- MathWorks Matlab, version R2013a, proprietary license
The tool is used for analysis of the given files as stated for this task.

ALGORITHM

The following process is adopted for data analysis. I/Q sample files downloaded from the database are converted with Matlab script to obtain I/Q samples of RF Spectrum. The "pwelch" Matlab function is used to compute RF Spectrum. Data are then analyzed to check if RF interference is present (peaks in the spectrum plot). If interference is detected the corresponding output will be marked by proper value of the Evaluation symptom.

Finally, data will be exported into a .csv formatted file.

9.17 ANALYSIS BASED ON MEASURED POWER SPECTRUM DENSITY (TASK 4.3.4.4)

RESPONSIBILITY

The task is performed in the responsibility of AZD.

OBJECTIVE

The aim of this task is to evaluate RF interference by analysis of data from Aaronia spectrum analyzer.

INPUT

Files of measured data from Aaronia spectrum analyzer Spectran HF-8060 V5 RSA is used for analysis.

OUTPUTS

Output files of this task are .csv formatted files complying with the specification in document [5]. These output files comprises following parameters:

GPS time [s] - GPS time of measurement

Evaluation symptom [-] – it provides information on RF interference occurrence

Analyzed parameter value [W] – APV corresponds to the power of the signal above defined spectral mask.

DESCRIPTION

For characterization of RF interference the RF Interference Level (RIL) is defined. RIL is defined as a power (in [W]) of hypothetical signal which is above of defined spectral mask.

The spectral mask defines ideal non-interfered environment. This spectral mask is not flat (constant) and thus respects different impact of spectral components on different frequencies.

The comparison of the spectral mask and the measured frequency spectrum by a spectrum analyzer provides information about presence of RF interference.

TOOLS

- Mathworks **Matlab** 2016b

ALGORITHM

A script in Matlab is used for loading input data, calculation of power of a signal above the spectral mask and for preparation of output files with the specified data format.

9.18 EVALUATION OF IMPACT OF DIFFERENT CONSTELLATION ON GNSS SIGNAL AVAILABILITY (TASK 4.3.5.0)

RESPONSIBILITY

The task is performed in the responsibility of TUBS.

OBJECTIVE

The aim of this task is to evaluate the impact of the environment on the GNSS signal availability (depending on the constellation) caused by canopy effects due obstacles beside the track.

INPUT

For this task, the measurements of the Septentrio receiver are needed to evaluate the number of receivable satellite signals for the different PVT solutions.

OUTPUTS

The output of this task will consist of several ASCII TXT files (for each receiver) which will include the number of received satellite signals and the resulting PVT solution.

The evaluation symptom (ES) indicates the possible computable PVT solution corresponding to available satellite signals as it is presented in the following table.

Observable satellite signals	PVT Solution	ES
< 4 for each system	No PVT	0
4 GPS L1 C/A	GPS PVT	1
5 GPS L1 C/A	GPS RAIM PVT	2
4 GPS L1 C/A + 4 GPS L5	dual frequency GPS PVT	3
5 GPS L1 C/A + 5 GPS L5	dual frequency GPS RAIM PVT	4
4 GPS L1 C/A + 4 GAL E1	single frequency GPS + GAL PVT	5
5 GPS L1 C/A + 5 GAL E1	single frequency GPS + GAL RAIM PVT	6
4 GPS L1C/A + 4 GPS L5 + 4 GAL E1 + 4 GAL E5a	dual frequency GPS + GAL PVT	7
GPS L1C/A + GPS L5 + Gal E1 + Gal E5a	GPS + GAL RAIM PVT	8

For this subtask, only GPS L1 C/A, GPS L5, GAL E1, GAL E5a are analyzed.

Output files will be generated by a Matlab script according to the following specifications.

The content of the header of the text file is described hereafter:

- Line 1: Name of the analyzed file
- Line 2: Trip date; Name of line
- Line 3: Measurement Company
- Line 4 – 12: ES as in above presented table

The content of the columns of the ASCII files is described in the following table.

Column	Parameter	Unit	Resolution	Format
--------	-----------	------	------------	--------

1	GPS Time	s	0.001s	xxxxxxxxxx.xxx
2	ES	-	1	x
3	number of observable GPS L1 C/A signals		1	xx
4	number of observable GPS L5 signals	-	1	xx
5	number of observable Galileo E1 signals		1	xx
6	number of observable GPS E5a signals	-	1	xx

Each element is separated by a ‘;’.

DESCRIPTION

By solving this task, performance degradation along the track is evaluated. This is possible by analyzing measured SV signals in view, which are received by the used Septentrio GNSS receiver.

TOOLS

The tool

- Septentrio **SBF Converter**, version 17.0.0,

provided by the GNSS receiver manufacturer is used to convert the measurement data into a Matlab readable format. After that, the tool

- Mathworks **Matlab** 2016b

is used for the analysis of the receiver measurements and for further calculations.

ALGORITHM

A Matlab script has been developed and used, which evaluates the information of the Septentrio GNSS receiver. For this purpose, the files from Septentrio receiver are converted into a Matlab readable ASCII file “MeasEpoch2” with the SBF Converter.

After the conversion, the files can be read and evaluated by a Matlab script. This script evaluates the number of received satellite signals and computes the availability of the respective PVT solution (depending on GNSS constellation).

9.19 SKY VISIBILITY MASK EVALUATION (TASK 4.3.A.0)

RESPONSIBILITY

The task is performed in the responsibility of AZD.

OBJECTIVE

The aim of this task is to process data from panoramic camera, to determine sky visibility mask and to provide rating of the railway environment from perspective of the sky visibility.

INPUT

The figures from the panoramic camera located on the roof of a train represent input data for algorithm for terrain contour determination and assessing shading of the sky.

The figure resolution is 512x512 pixels, 1Hz output rate of figures in JPEG format. The camera disposes five levels of image capture quality, the second best quality was selected.

OUTPUTS

Output file includes GPS Time, ES and values of Satellite Visibility Factor calculated for elevation masks 0°, 5°, 10°, 15°.

Output file format is following:

- GPS Time [s]
- Evaluation symptom [-]. Range of values:
 - 0 - "sufficient visibility" - 90% clear sky view over 5° elevation mask
 - 1 - "sufficient visibility" - 90% clear sky view over 10° elevation mask
 - 2 - "sufficient visibility" - 90% clear sky view over 15° elevation mask
 - 3 - "insufficient visibility" - less than 90% clear sky view over 15° elevation mask
- SVF00 [-] without any elevation mask
- SVF05 [-] with 5° elevation mask
- SVF10 [-] with 10° elevation mask
- SVF15 [-] with 15° elevation mask

Note_1: Satellite visibility factor SVF_{xx} is defined as a ratio of clear sky view area and whole area of camera picture, both above elevation mask xx°. SVF range is interval <0,1>.

Note_2: NaN value is used if there is an invalid reference or unknown train direction or unknown azimuth or unsuitable visibility conditions for camera operation.

DESCRIPTION

The figures taken by panoramic camera situated on the roof of a train together and camera coordinates provides valuable information on sky visibility along a track. Image processing of such figure provide terrain contour enabling evaluation of the sky visibility which is important for railway environment characterization.

TOOLS

- C++ with translator mingw32-gcc-g++ 6.3.0

used for image processing, orientation of the sky, calculation of SVF and generating of output files.

- Library openCV, version 3.2.0

used for image processing and terrain contour determination.

ALGORITHM

The algorithm processes data of figures from the panoramic camera. Output of the algorithm is set of pixels with characteristic features the color and the brightness, therefore RGB values and HSV components of the

color space. The values of these parameters serves for training of a classifier, which will determine with high probability a relevance of each pixel to the set of pixels of the sky.

The pixels which the relevance both to the set of pixels of the sky and the set of the pixels outside the sky cannot be determined for the property of the sky consisting in sharp edge of sky-terrain transition can be used. The segmentation algorithm „watershed“ can be employed for this purpose. This algorithm divides image into two sets of pixels, „sky“ and „outside sky“ sets. These sets are represented by binary images. The final correction of binary visibility mask consists in removing very small areas by means of morphological operations.